A Study of Cell Size Homeostasis and Variability in the Fission Yeast *Schizosaccharomyces pombe*

Elizabeth Wood

University College London

and

Cancer Research UK London Research Institute

PhD Supervisor: Sir Paul Nurse

A thesis submitted for the degree of

Doctor of Philosophy

University College London

August 2015

Declaration

I, Elizabeth Wood, confirm that the work presented in this thesis is my own. Where information has been derived from other sources, I confirm that this has been indicated in the thesis.

“Omnis cellula e cellula”

Rudolf Virchow; *Cellularpathologie*, 1858

Abstract

Proliferating cells maintain a near-constant cell size at division within a given population, suggesting the existence of control mechanisms that buffer cell size perturbations. Wild type cells of the fission yeast *Schizosaccharomyces pombe* divide within a narrow range of cell sizes around a mean of 14 μm. A proposed model for size sensing in fission yeast involves polar gradients of the kinase Pom1 inhibiting Cdr1/2 at medial cortical nodes until cells surpass a size threshold. This model has been further investigated using size homeostasis analyses on single cells growing in a microfluidic chamber. The results demonstrate that Pom1 is not essential for cells to maintain size homeostasis and as such cannot be the only major player in the size sensing mechanism in fission yeast. This single-cell method has been further exploited to investigate the roles of other known cell cycle regulators in maintaining size homeostasis. The investigation has included cells with a Cdc2-L-Cdc13 fusion protein, which is able to drive the cell cycle in the absence of much of the canonical regulation.

In order to elucidate new components responsible for the control of cell size homeostasis, a previous screen of 82% of non-essential genes was used to identify genes which when deleted increase size variability at division. Until now only a few mutations have been described that increase variability in size at division, and these have been shown to directly affect the activity of the cyclin-dependent kinase Cdc2. A follow up of the primary hits from this screen identified 15 genes which when deleted lead to greater variability in size at division. Further size homeostasis analysis on single cells identified two genes that when deleted decrease the ability of cells to sense and/or adequately correct for size deviations.

Acknowledgements

First and foremost I'd like to thank Paul, for being such an incredible mentor over the past four years. Thank you for the many, many discussions on cell size that left us brain-dead and questioning the entire basis of cell cycle control! Thank you for giving me the space to develop as a scientist and for providing me with such a solid foundation to begin what will hopefully be a long and successful scientific career. Your faith in me has made me ever more confident in my abilities. Thank you also for knowing exactly what to say and do in my moments of trouble.

Jacky deserves huge thanks for dealing with my (many) daily questions and comments; I have yet to find something you cannot help me with. Your endless *pombe* knowledge and smiling presence in the lab has made it a joy to work here. Thank you for not retiring before I finish!

Francisco Navarro deserves a special mention too since without him this project would not have existed. Thank you for being a super teacher (I will treasure all your protocol illustrations) and a great friend. I would also like to thank all members of the Nurse lab, past and present, both in London and New York. Special thanks go to Helena and Jessica for taking the time to read my thesis, to Louise for being such a wonderful friend, and to Matthew for making it all that much more fun! Thank you also to my thesis committee, Takashi Toda and Michael Way, for some interesting discussions and guidance on my project. Sally Leevers also deserves a mention for running such a well-organised and supportive PhD programme.

Lastly, thank you to my family; Mum, Dad and Kate. As I read somewhere once, thank you for the nature and the nurture. Your unwavering love and support is the only reason I've got this far and am still smiling. Through the ups and the downs you've always been there to spur me on. Thank you also to my many wonderful friends who've been by my side, to commiserate over the failed experiments and to celebrate even the smallest of triumphs. Caroline, my baby buddy, you deserve a special mention for being a truly wonderful friend and housemate. You've stuck by me for 26 years and that probably deserves a medal!

I am grateful to Cancer Research UK for funding and the London Research Institute for providing such a lovely home for the past four years.

Table of Contents

Table of figures

List of tables

Abbreviations

AF	Thr14Ala Tyr15Phe mutation
BL	Birth length
BL/E	Graph of birth length plotted against length extension
BL/CT	Graph of birth length plotted against cycle time
Cdc13-L-Cdc2	Cdc13-Linker-Cdc2
CDK	Cyclin-dependent kinase
CI	Confidence Interval
CT	Cycle time
CV	Coefficient of variation
DAPI	4',6-diamino-2-phenylindole
d.p.	Decimal place
DYRK	Dual-specificity tyrosine phosphorylation-regulated kinase
E	Length extension
EMM	Edinburgh minimal media
EMM4S	Edinburgh minimal media plus supplements
EMM-N	Edinburgh minimal media minus nitrogen
G	Growth rate value, G = E/(BL·CT)
GFP	Green fluorescent protein
G1/S	Transition point between G1 and S phase
G2/M	Transition point between G2 and mitosis
HU	Hydroxyurea
M	Mitotic phase
MAPK	Mitogen-activated protein kinase
N/C	Nucleocytoplasmic
NETO	New-End-Take-Off
S	Synthesis phase
SEM	Standard error of the mean
s.f.	Significant figure
TOR	Target of Rapamycin
ts	Temperature-sensitive
WT	Wild type
YE4S	Yeast extract media plus supplements

Chapter 1. Introduction

1.1 Introduction

The mitotic cell cycle describes the process by which a single cell divides to form two genetically identical daughter cells. The cycle necessitates the timely coordination of growth and division and relies on controls and checkpoints to ensure that the process is carried out in a unidirectional and completely accurate manner. This work aims at addressing a fundamental question surrounding this process of cell division: how does a cell know how big it is and how big it needs to be? It is surprising that this central issue remains unresolved, especially considering the sheer volume of research on cell growth and cell division that has ensued over the past century.

1.1.1 Why is cell size control important?

For a growing cell to successfully replicate itself it must first make adequate amounts of protein, DNA, membranes and organelles, and also have an appropriate volume of cytoplasm to accurately segregate all of these components into two equally sized daughter cells. To achieve this, the cell must coordinate progression through the cell cycle with the accumulation of mass. There are two main approaches which are important when trying to understand this coordination. The first is a more theoretical and abstract approach. This takes us back to the early studies carried out throughout the 1900s, which considered aspects of different size control systems and tried to un-pick the controls by predicting how different systems may behave. The second is a more mechanistic approach aimed at identifying the molecular mechanisms involved. This has been the focus of the majority of the more recent work on cell size control.

The concept of size homeostasis is a particular focus here and describes how cells may sense their size and use this information to make appropriate corrections to ensure that they divide at the correct size. This is different to merely considering the threshold size at which cells are dividing although this distinction is often not clearly made. (The term ‘size threshold’ is used here to describe a certain size that the cell must reach for a cell cycle transition to occur). We will discuss whether or

not a system requires a size sensing mechanism, an argument that depends heavily on the growth pattern of the cells. Cells which are accumulating mass in a linear fashion can maintain size homeostasis by simply controlling the cell cycle with a fixed timer (Brooks, 1981). (The term 'timer' describes a period of the cell cycle which is defined by a fixed amount of time). This will be referred to as 'passive' size control, since the cells are not directly measuring size yet are indirectly able to control it through the timing of cell divisions. The alternative is an 'active' size sensing mechanism which we argue most eukaryotic cells possess. We envisage such a size sensing mechanism to either measure the volume of the cell or a component related to cell volume, or alternatively to monitor an aspect of the cell geometry, and to feed this information into the cell cycle controls.

The question of cell size control is by no means fully answered here but the aim is to shed new light on the problem and to further our knowledge to aid the progression of this field. This will be done both through the investigation of current cell cycle regulators thought to have a role in size control and also through the identification of novel cell cycle genes.

1.2 A brief history

"Long ago it became evident that the key to every biological problem must finally be sought in the cell; for every living organism is, or at some time has been, a cell."
Edmund B. Wilson
The Cell in Development and Heredity, p1, 1925

1.2.1 The cell and cell division

The cell, which is the smallest structural and functional unit of an organism, was a term first coined by Robert Hooke in his book *Micrographica*, published in 1665 (Hooke, 1665). Over a century later, and following many debates as to the nature of these cells, the cell theory was formulated and has since formed the foundation of all aspects of biological research (Harris, 1999, Turner, 1890). In 1838, Matthias Schleiden and Theodor Schwann stated the first two tenets of this theory; one, that all living organisms are composed of one or more cells, and two,

that the cell is the most basic unit of life. The third principle, that all cells arise only from pre-existing cells, was added a few years later in 1855 and was credited to Rudolf Virchow, although it had by this time already been proposed by Robert Remak and others (Harris, 1999, Turner, 1890). It is from this third principle that the idea of cell division was born. Around this time, Leydig and Schultze put forward a simple formula to describe the cell. They defined the cell as a mass of protoplasm containing a nucleus, and stated that both nucleus and cytosome arise by division of the corresponding elements of a pre-existing cell (Baker, 1952, Turner, 1890, Wilson, 1925). Despite the plethora of research that has been carried out over the last 150 years, this description remains remarkably true today.

This third tenet of the cell theory poses a significant requirement of the cell. In addition to carrying out its required function, it must also grow and double its contents in a timely manner and then finely tune the division of its DNA and organelles into two identical daughter cells. We must not neglect to notice the remarkable nature of this self-replicating miniature machine - we as humans, despite our attempts and efforts, have not yet managed to build a self-replicating machine as complicated as the cell.

1.2.2 Cell size studies

The first observations of the quantitative relationships between chromosome number, nucleus size and cell size were documented by Boveri, Hertwig and colleagues in the early 1900s and summarised by EB Wilson (Wilson, 1925). They concluded that this was a complex and incompletely solved problem. This remains essentially true today, nearly 100 years later. Their observations led to the idea of the ‘karyoplasmic ratio’, now referred to as the nucleocytoplasmic ratio. In 1962, Koch and Schaechter, working with bacterial cells, proposed that “cell size at division, or some closely related property, is under close physiological control” (Schaechter et al., 1962). They also noted the small variation of the size of cells at the time of division. Around the same time, Mitchison began working on cell growth using *Schizosaccharomyces pombe* and after his first publication, describing the growth dynamics of single yeast cells (Mitchison, 1957), his lab began to study the controls of the cell cycle, with a particular focus on the control of cell size (Nurse et

al., 1976). By this time, Killander and Zetterberg had published work describing the relationship between cell mass and the initiation of DNA synthesis in mouse fibroblasts (Killander and Zetterberg, 1965a, Killander and Zetterberg, 1965b). Since then there has been a myriad of studies on cell size control in a wide variety of organisms and cell types, but despite this work molecular mechanisms for the coordination of cell growth with cell division have remained elusive.

1.2.3 The coordination of organelle and cell size

"….it is clear that the quantitative relations of chromosomes, nuclei, cytosomes and cell-aggregates offer a complex problem, and one that is incompletely solved."
Edmund B. Wilson
The Cell in Development and Heredity, p101, 1925

In addition to controlling its overall size it is important that a cell is also able to coordinate the size of its organelles in order to ensure viability. Much is known about membrane growth and trafficking within cells (van Meer et al., 2008) yet the mechanisms coordinating the size of membrane-bound organelles remain elusive. The nucleus is a key example of the necessity of this control and also provides a useful tool to study this problem since it generally has a regular shape and is present in a single copy.

In both budding and fission yeast the ratio of nuclear volume to cell volume (the nucleocytoplasmic or N/C ratio) is around 7-8% (Jorgensen et al., 2007, Neumann and Nurse, 2007) and in fission yeast this has been shown to remain constant during the cell cycle (Neumann and Nurse, 2007). Since there is no change in this N/C ratio following DNA replication in S phase of the cell cycle, the once-believed DNA-dependency of the size of the nucleus appears not to be the case. This is supported by evidence demonstrating that the N/C ratio remains constant across a 16-fold DNA content range in fission yeast (Neumann and Nurse, 2007). Studies in murine hepatocytes have shown proportional cellular and nuclear expansion following the overexpression of c-Myc (Kim et al., 2000), and in *C.elegans* embryogenesis a corresponding decrease in nuclear size is seen following blastomere size decrease (Hara and Kimura, 2009) – in both of these cases DNA content remains unchanged. The conclusion from these studies is

therefore that a control is operating to coordinate cell and nuclear size independently of DNA copy number.

This mechanism is currently under investigation in a variety of different systems and it has been suggested that cytoplasmic factors and nucleocytoplasmic transport may be important for this process (Neumann and Nurse, 2007, Levy and Heald, 2010). It seems clear that cell size information is used in a control system to coordinate with nuclear size and it is important to consider this in future size studies.

1.3 The bigger picture

1.3.1 Other influences on cell size

In addition to the fine coordination of cell size with cell cycle progression, the cell is also able to modify its size in response to a number of external influences, including temperature and nutrient availability (Schaechter et al., 1958, Shehata and Marr, 1975). For unicellular organisms such as *S. pombe*, a major influence on cell size and shape is the surrounding environment; cell surface area to volume ratio plays an important role in how efficiently the cell can take up all the nutrients it needs, and therefore cell size is important for fitness (Smith, 1925). Consequently modifying cell size according to external cues is necessary for survival.

For multicellular organisms, it is the surrounding cells and the position of a cell amongst others that will influence its size and shape, as well as the cell's function in that particular tissue (Jorgensen and Tyers, 2004, Marshall et al., 2012). It should be noted that these controls are not only relevant in the case of proliferating cells. In adult animals some postmitotic cells are able to alter their size in response to extracellular growth factors. For example it has been shown that sympathetic neurons in adult rodents increase in size in response to increasing levels of nerve growth factor, indicating that these cells may be able to adjust to the needs of differing environments (Purves et al., 1988). In both proliferating and non-proliferating populations, cell size can therefore be modulated by external factors and cues from the surrounding cells in addition to the controls operating within individual cells.

1.3.2 Scaling up

Does cell size influence the size of an entire animal or plant and the organs within them? The size of an organism will depend on both the number and the size of its component cells and studies have shown that animals/organs seem to know roughly what their total cell mass needs to be, rather than how many cells they contain (Conlon and Raff, 1999). For example, the corresponding organs in a tetraploid versus a diploid salamander are the same size despite the tetraploid cells being twice the size of the diploid cells, since the diploid amphibian has twice the number of cells (Fankhauser, 1952). The question that surrounds animal size control is therefore how total cell mass is determined and this remains unanswered. It is known however that cell number differences make a larger contribution to body size and broadly speaking cell size does not tend to vary greatly between animals (Conlon and Raff, 1999).

1.3.3 Disease

The fine coordination of cell growth and proliferation in multicellular organisms is central to healthy survival. The deregulation of cell growth control leads to loss of this coordination and thus loss of cell size homeostasis (which will be discussed in detail later) and this is likely to result in disease. Too little growth signalling can lead to atrophy, whereas too much signalling can lead to hypertrophy, seen in cardiac and brain disease, hyperactivity, seen in neurodegenerative diseases such as Alzheimer's, and of course hyperproliferation, which leads to cancer (Lloyd, 2013).

Since this thesis focuses on the single cells of fission yeast there is only a brief discussion of cell size control in multicellular organisms. However it is important that this crucial link to human health is not forgotten. For a recent review of this area see (Lloyd, 2013).

1.4 An overview of the mitotic cell cycle

The mitotic cell cycle describes the process by which a cell divides into two daughters. It can be split into two main phases, mitosis and interphase. Interphase can be further subdivided into G1, S phase – during which DNA is replicated – and G2. During this time the cell prepares for mitosis and division by synthesising all the required proteins and by duplicating its DNA and organelle content. Once these stages have been successfully completed, the cell enters mitosis, whereby two genetically identical daughter cells are produced (Moser and Russell, 2000).

Most eukaryotic cells carry out each of these major cell cycle events however the details of the basic scheme can vary between cell types. The human somatic cell cycle takes on the usual form of events, an 18 hour cycle consisting of G1, S, G2 and M followed by cytokinesis (Morgan, 2007). The single-celled budding and fission yeasts have a similar cell cycle (G1-S-G2-M) although they have a shortened G2 and G1 phase, respectively (Turner et al., 2012). In fact fission yeast cells are unusual in that S phase occurs almost immediately after mitosis and before cell separation (Nurse, 1975).

The cell cycles of early embryos are useful examples of how growth and division can be uncoupled to the advantage of the organism. The early cleavage divisions of *Xenopus laevis* embryos are rapid cell cycles with minimal or absent gap phases and no cell growth. The giant fertilised egg is rapidly subdivided into thousands of individual cells enabling the organism to quickly reach a free-living state (Morgan, 2007). The early embryos of *Drosophila melanogaster* demonstrate the dissociation of nuclear and cellular division. The rapid 8-minute cell cycles occur without intervening cytokinesis and result in a syncytium of thousands of nuclei within a shared cytoplasm (Morgan, 2007). Only after around 13 nuclear divisions does a plasma membrane form around each nucleus to form single cells (Farrell and O'Farrell, 2014).

Although cell cycles can take on a variety of forms depending on the role of the divisions and the subsequent cells, the eukaryotic cell cycle is nevertheless a close-to universal process at the single cell level (Nurse, 1997).

1.4.1 Cyclin-dependent kinases

In all eukaryotes, progression through the cell cycle is driven by cyclin-dependent kinases (Cdks) which form complexes with different cyclins (Morgan, 1995, Morgan, 1997). Association with the oscillating regulatory cyclins is thought to result in Cdk activity rising and falling through the cell cycle, leading directly to the cyclical changes in the phosphorylation status of key cell cycle components (Bloom and Cross, 2007, Loog and Morgan, 2005). The association of different kinases and cyclins is proposed to bring about the sequence of cell cycle transitions through the generation of distinct sets of substrate specificities (Bloom and Cross, 2007).

It is crucial for the cell to replicate its genome only once each cell cycle and to subsequently divide its cytoplasm into two distinct cells. The precise alternation of replication and segregation requires checkpoints, to ensure that one stage has been successfully completed before the next stage begins, and also directionality, to ensure that the underlying steps take place in the correct order. It is the fine control and regulation of CDK complexes that brings about this well-ordered and defined set of events (Coudreuse and Nurse, 2010, Morgan, 1997).

1.5 *Schizosaccharomyces pombe*: a model organism

Since the 1950s, the fission yeast *Schizosaccharomyces pombe* has been used as a model organism to study the cell cycle. Described by Murdoch Mitchison in 1957 (Mitchison, 1957), the fission yeast cell cycle is a convenient model system for a number of reasons. Firstly, cells have a rigid cell wall imposing a regular geometry – a 4 μm wide rod-shape – so cell volume can be calculated from length and width measurements (Mitchison, 1957). Since cells grow by tip extension with no significant change in cell width, the increase in cell length is proportional to the increase in volume and is also indicative of cell cycle stage. This growth pattern can affect the shapes that these cells adopt, and thus the possible mechanisms that could operate to measure cell size. Secondly, cells have a rapid generation time (around 2 hours in ideal growth conditions) (Mitchison, 1957) and so consecutive cycles can be observed in real-time under time-lapse microscopy. Thirdly, it has a simple and well-studied cell cycle which only requires a single

cyclin-dependent protein kinase, Cdc2, in complex with the B-type cyclin Cdc13 (Coudreuse and Nurse, 2010, Fisher and Nurse, 1996, Hayles et al., 1994, Nurse and Bissett, 1981). Fourthly, it is normally a haploid organism (though can grow as a diploid) which simplifies genetic studies and together with a gene deletion collection covering over 90% of genes (Kim et al., 2010, Spirek et al., 2010), means that systematic screens for genes affecting cell cycle transitions can be carried out (Hayles et al., 2013, Navarro and Nurse, 2012). Finally, while there will inevitably be some cell to cell variation in growth rate, there is little variability in cell size at division (Fantes, 1977). This suggests that cell size is actively sensed and regulated and makes *S. pombe* a good system to study the coordination of cell size with cell cycle progression.

1.5.1 Fission yeast cell growth

The rod-shaped cells of *S. pombe* grow by tip extension and divide medially when they reach 14 μm in length (Mitchison and Nurse, 1985). On entry into mitosis, growth ceases as actin patches redistribute from the actively growing ends to the centre of the cell to form the cortical ring for cytokinesis (Marks et al., 1986). After division, the two daughter cells initially resume growth from the old end – the previously growing end – until early G2, when growth is initiated at the new end created by the preceding cell division. This transition from monopolar to bipolar growth is termed NETO (New End Take Off) (Mitchison and Nurse, 1985). Both the actin and microtubule cytoskeleton play important roles in the establishment of a polarised axis in order to carry out this characteristic cycle of tip growth followed by medial fission (Hagan and Hyams, 1988, Marks et al., 1986).

Growth and proliferation are terms often used interchangeably yet they have very distinct meanings which must not be confused. Cell growth defines the accumulation of mass, yet cell proliferation denotes an increase in cell number. Progression through the fission yeast cell cycle is dependent upon the attainment of a critical size or mass and therefore proliferation is dependent on cell growth (Fantes and Nurse, 1977, Fantes and Nurse, 1978, Nurse, 1975, Nurse and Thuriaux, 1977). Growth on the other hand is not dependent on cell cycle progression and cell cycle inhibitors are frequently used to block cells in the cell

cycle without affecting growth, thus generating elongated cells (Mitchison and Creanor, 1971).

1.5.2 The fission yeast cell cycle

The orderly progression of cell cycle events is controlled by the single cyclin-dependent protein kinase Cdc2 (Nurse and Bissett, 1981, Nurse and Thuriaux, 1980, Nurse et al., 1976), the activity of which is low in G1 and increases through the cell cycle (Moreno et al., 1989). Cdc2 therefore drives the onset of both S-phase and mitosis, yet the G1/S transition is driven by lower activity levels of this kinase (Coudreuse and Nurse, 2010). Cdc2 associates with the B-type cyclin Cdc13 early in S phase but its activity is kept low by inhibitory phosphorylation on Tyr15, which is carried out by Wee1 and Mik1 (Lundgren et al., 1991, Russell and Nurse, 1987b). In late G2, Cdc25 removes this inhibitory phosphorylation and cells enter mitosis (Gould and Nurse, 1989, Nurse, 1990, Russell and Nurse, 1986). There are two known pathways acting upstream of Wee1 and Cdc25 that link cell growth to the G2/M transition, the Cdr2-Cdr1 and stress response pathways (Breeding et al., 1998, Kanoh and Russell, 1998, Petersen and Hagan, 2005, Petersen and Nurse, 2007, Russell and Nurse, 1987a). The Cdr2-Cdr1 pathway has been described as a cell geometry sensing pathway and includes the protein Pom1, which has been suggested to act as a size sensor (Martin and Berthelot-Grosjean, 2009, Moseley et al., 2009). This is discussed in further detail later in this chapter. The stress response pathway is formed of a MAP kinase pathway which regulates the recruitment of polo kinase to the spindle pole body and mitotic commitment (Figure 1.1). A number of genes have been found to act at the G2/M transition independently of these two pathways and Cdc2-Tyr15 phosphorylation, suggesting the existence of alternative pathways of cell growth input into the G2/M transition (Navarro and Nurse, 2012).

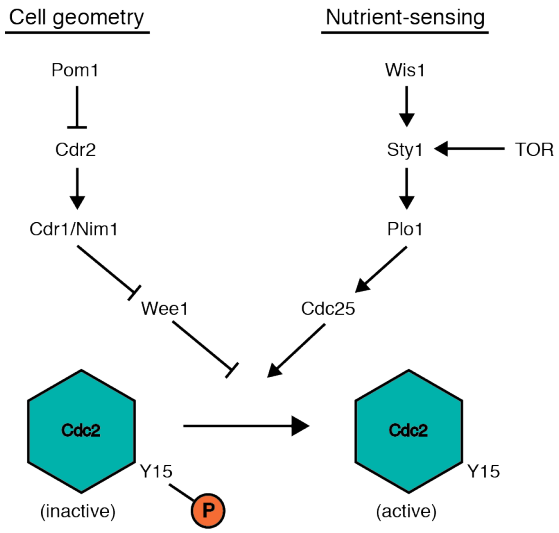

Figure 1.1|Regulation of the G2/M transition

A schematic illustrating the controls operating through Cdc2-Tyr15 phosphorylation at the G2/M transition. The cell geometry and nutrient sensing pathways feed into Wee1 and Cdc25, respectively. The geometry pathway feeds cell size information through Pom1, Cdr2 and Cdr1. The nutrient sensing pathway couples the TOR pathway with recruitment of polo kinase (Plo1) to the spindle pole body. Wee1 and Cdc25 act antagonistically on Cdc2: Wee1 phosphorylates and inactivates the kinase and Cdc25 acts to remove this inhibitory phosphorylation and promote entry into mitosis.

1.5.3 Fission yeast as a model for cell size control

Fission yeast has two size thresholds, one at the G1/S transition and a second at G2/M (Nurse, 1975). In wild type exponentially growing cells only the G2/M threshold is relevant since this results in all G1 cells being large enough to surpass the size threshold to enter S phase (Nurse and Thuriaux, 1977). G1 phase is therefore extremely short in wild type cycling cells. In nutrient-rich conditions, coordination of growth and cell cycle progression happens in G2, which is contracted or extended according to the size of the cell (Fantes and Nurse, 1977) (Figure 1.2). Cells lacking the kinase activity of Wee1 (temperature-sensitive *wee1-50* cells) allowed this so-called cryptic G1/S sizer to be revealed. (The term ‘sizer’ is used here to refer to a period of the cell cycle which is defined by the size of the cell). Since these *wee1-50* cells lack a G2/M size control, G1 cells are smaller than the required size for entry into S phase. These cells have an elongated G1 phase in order to attain the correct size for the G1/S transition, and this is then followed by a timer from S phase to entry into mitosis (often referred to as the minimum

incompressible G2 period) (Fantes and Nurse, 1978, Nurse and Thuriaux, 1977) (Figure 1.2).

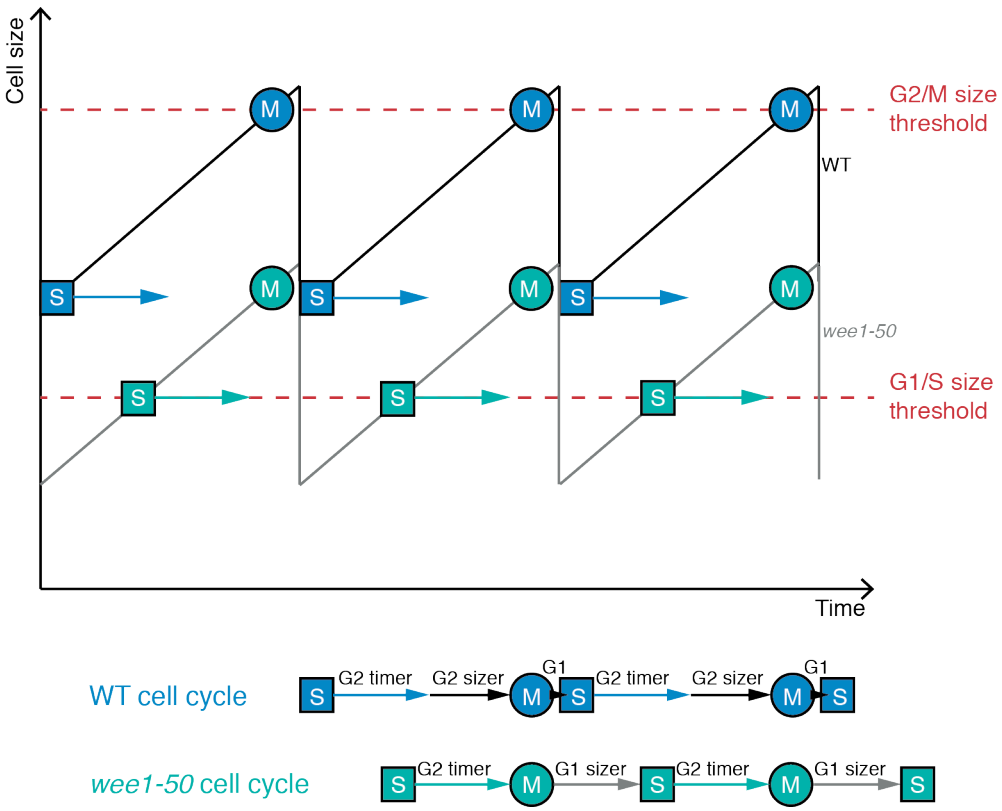

Figure 1.2|The cell cycles of wild type and *wee1-50* cells

Schematic is not to scale, adapted from (Nurse and Thuriaux, 1977). S = S-phase; M = mitosis. For simplicity, linear growth is shown. Wild type cycling cells have a G2/M size threshold which results in G1 cells that already surpass the required size to enter S-phase. G1 is therefore very short. G2 can be contracted or extended depending on the size of the cell. Note the G2 timer is what is sometimes referred to as the incompressible G2, and is the minimum time that a cell must spend in G2. Temperature-sensitive *wee1-50* cells grown at the restrictive temperature do not have a G2/M size threshold. They enter mitosis immediately following the G2 timer period and therefore G1 cells are below the minimum size requirement to enter S-phase. G1 is extended in order for the cell to reach this G1/S size threshold.

In 2012, Navarro and Nurse published the results of a near genome-wide screen for new elements acting at the G2/M transition in fission yeast (Navarro and Nurse, 2012). This screen identified 18 genes that act negatively at mitotic entry, seven of which had not been previously described as having cell cycle regulatory roles. Eleven genes were shown to act through the known stress response and cell

geometry sensing pathways, while the remainder either acted through unknown pathways or were shown to be independent of CDK Tyr15 phosphorylation altogether (Navarro and Nurse, 2012). This work opened up further investigation into as-yet uncharacterised pathways acting on cell size control for entry into mitosis.

The work here focuses on the controls operating at G2/M. However, for many eukaryotic cells, including the budding yeast Saccharomyces cerevisiae, size control is operating earlier in the cell cycle, at the G1/S transition (Johnston et al., 1977, Jorgensen and Tyers, 2004, Turner et al., 2012). Therefore both the G1/S and G2/M controls must contribute to a global cell size sensing mechanism.

1.6 Cell size homeostasis

"Homeostasis: The maintenance of a dynamically stable state within a system by means of internal regulatory processes that tend to counteract any disturbance of the stability by external forces or influences"

The Oxford English Dictionary

A size control system for entry into mitosis has two characteristics: it determines the threshold size at which cells divide, and the variability around this threshold. Cells of a certain type (be it a single-celled organism or cells of a particular tissue within a multicellular organism) will have a critical size at which division takes place. This is evident in the similarity of cell sizes at division within a particular population. The cell may be able to change this threshold size depending on its surroundings, for example the nutrient availability, the temperature, or external cues from surrounding cells. The variability around the size threshold shows how accurately the cells in the population are able to attain this critical cell size. A complete size control system therefore requires the cell to first set a threshold size for entry into mitosis and then sense its size in order to make the appropriate corrections.

These appropriate corrections when cell size deviates from the mean can be thought of as size homeostasis. The definition of homeostasis states that it requires a sensor to detect changes in the condition to be regulated, an effector mechanism that can vary that condition, and a negative feedback connection between the two. In relation to cell size, this can be thought of as a sensor to detect how big the cell

is and how far this is from the required size, a mechanism which allows the cell to delay or promote entry into mitosis accordingly, and finally a continuous feedback mechanism which allows the correction to bring the cell size back to the required threshold without a significant overshoot.

It is important at this stage to distinguish between two possible causes of increased variability in cell size at division within a population. The first possibility is that each individual cell has a different size threshold which is accurately maintained, implying a loss of control at the population level due to clonal variability. The second is that all the cells in the population are trying to attain a common size but there is a problem in the control system, resulting in weak homeostasis at the cellular level (Fantes and Nurse, 1981). When studying the cells of fission yeast we are mostly working with clonal populations of single cells and therefore it is likely that increased variability is due to the second of these two possibilities rather than the first.

1.6.1 The importance of studying size homeostasis

We argue that finding the genes involved in the homeostatic mechanism is key to solving the problem of how cells maintain such accurate size control. We already have a good understanding of the key regulators involved in the decision to enter mitosis in fission yeast. These genes were discovered by mutations which generated a size phenotype, either advancing the cells into mitosis at a smaller size or lengthening G2 so that cells divide at a longer than wild type size (Nurse, 1975, Russell and Nurse, 1986). These genes have a role in relaying some size information into the cell cycle and could be involved in setting the threshold size for entry into mitosis. However, to find the genes involved in sensing cell size, rather than setting or adjusting the threshold, size homeostasis mutants should also be useful. The expectation is that populations of such mutants will display increased variability in cell size at division, since cells will be affected in their ability to correct for deviations in size.

There are two main experimental techniques which allow us to study cell size homeostasis. Firstly, the variation of sizes at division in a population of cells. A tight distribution implies that cells are able to accurately divide at the required threshold

size, while a broader distribution implies 'sloppiness' within this control system (either at the population or the cell level, as discussed above) (Fantes and Nurse, 1981). Secondly, by observing the response of individual cells to natural variations in cell size that occur within a population of exponentially growing cells. If a cell divides to produce a daughter which is smaller than average, an effective homeostatic mechanism will ensure that this small cell elongates more in the subsequent cycle to return to the required size (Fantes, 1977). The reverse would be true for long cells, which will shorten their growth period to divide prematurely at the correct size.

1.7 Mechanisms of cell size control

Before beginning a discussion of size sensing mechanisms, the first consideration is whether or not a size control mechanism is necessary for a population of cells to maintain size homeostasis.

1.7.1 No size control: a 'passive' mechanism

Cell size is something that a cell must control, but does this need to be an active process of sensing and signalling? The answer to this question lies in the growth pattern of the cell, where the term 'growth' strictly refers to the accumulation of mass. Take a population of single cells which are growing in a linear manner, whereby the rate at which they accumulate mass is constant, regardless of their initial mass. If the time between successive divisions is maintained by a fixed timer, all cells will converge towards the population mean regardless of their initial size, since smaller cells will be accumulating more relative mass in comparison to larger cells (Figure 1.3A). The population will therefore maintain size homeostasis in the absence of any size checkpoints, as long as an accurate timer is in place to control the timing between cell divisions (Brooks and Shields, 1985, Conlon and Raff, 2003). If a population of cells are growing exponentially, large cells will grow faster than small cells and thus the population will diverge away from a mean cell size. A fixed cell cycle timer will therefore be unable to maintain size homeostasis within a

population of exponentially growing cells (or cells that are growing in a pseudo-exponential manner, such as a bilinear growth pattern).

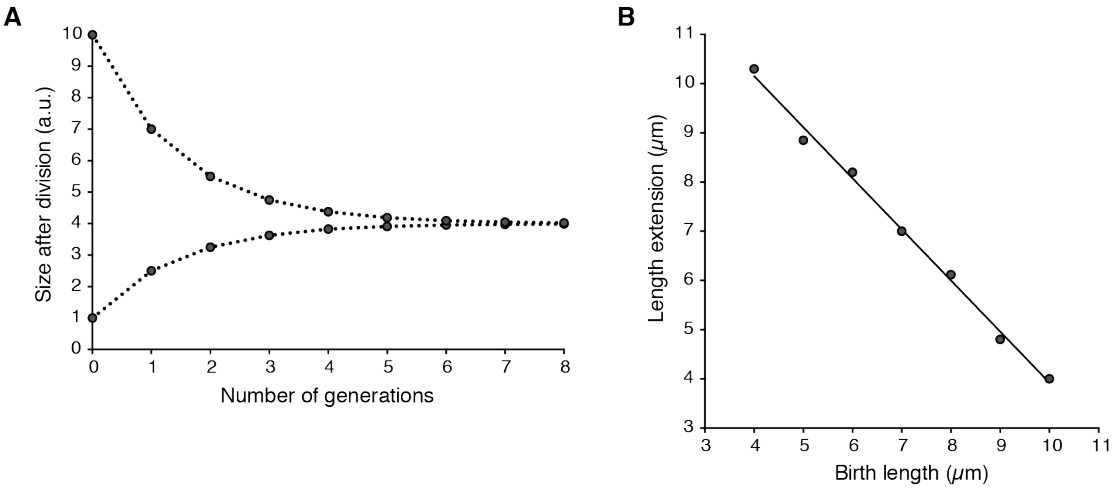

Figure 1.3|Theoretical graphs of 'passive' and 'active' size control mechanisms

(A) A graph showing how linear growth and a fixed timer is able to maintain size homeostasis. If during each cell cycle a cell gains 4 units of mass regardless of its initial size, small cells will add more proportional mass than larger cells and all cells will tend towards the average size of the population (which in this case is 4 units). (**B)** A population of cells showing size control will show a negative relationship between birth length and length extension during the subsequent cycle. For example a cell that is born small will extend more in the next cell cycle in order to attain the correct size (in this case 14 μm).

A major difficulty in testing this model has been the technical limitations in determining linear versus exponential growth. For both budding and fission yeast, it has been established that cells do not accumulate mass in a simple linear fashion for extended periods of time (Baumgartner and Tolic-Norrelykke, 2009, Creanor and Mitchison, 1982, Di Talia et al., 2007, Elliott and McLaughlin, 1978, Godin et al., 2010, Mitchison, 2003, Mitchison and Nurse, 1985). Aside from measurements of several different growth parameters, evidence for this can be taken from the growth of the fission yeast temperature-sensitive size mutants *wee1-50* and *cdc25-22*. At the semi-restrictive temperature these cells have the same generation time as wild type cells, showing that they double their mass in the same time-frame (Thuriaux et al., 1978). Since *cdc25-22* cells are more than three times the size of *wee-50* cells, they are therefore adding more mass per unit time (Nurse and Fantes, 1981). This tells us that fission yeast cells are not growing in a simple linear fashion and therefore cannot rely on a fixed timer to maintain size control.

1.7.2 Multicellular organisms: a challenging debate

The situation has been less clear in cells of multicellular organisms. Cell growth and division must be strictly controlled together with those of the surrounding cells in order to form tissues and organs, and this may mask certain intracellular controls (Jorgensen and Tyers, 2004). After Killander and Zetterberg's pioneering work with mouse fibroblasts (Killander and Zetterberg, 1965a, Killander and Zetterberg, 1965b), many other groups working in a variety of cell types demonstrated that cell size can influence cell cycle timings, particularly at the G1/S transition (Darzynkiewicz et al., 1979, Dolznig et al., 2004, Gao and Raff, 1997, Jorgensen and Tyers, 2004, Kimball et al., 1971, Saucedo and Edgar, 2002, Shields et al., 1978). However, many people have challenged this relationship between cell size and cell cycle timing (Baserga, 1984, Conlon and Raff, 2003, Conlon et al., 2001, Fox and Pardee, 1970), and the question of growth has been at the centre of the long-standing debate as to whether or not mammalian cells require size control (Brooks and Shields, 1985, Sveiczer et al., 2004). Recent studies of mammalian cells using single-cell measurements of fixed steady-state populations and cells in microfluidic chambers have revealed the presence of size regulation at the G1/S transition, supporting those early findings of Killander and Zetterberg (Godin et al., 2010, Kafri et al., 2013, Son et al., 2012). The conclusion is therefore that a size control system feeding in to cell cycle controls, and not simply a fixed timer, acts in most eukaryotic cells to maintain size homeostasis within the population. Of course this conclusion has to be modified in very large cells, such as dividing eggs, which are above the cell size threshold. In these cases progression through the cell cycle is likely to involve timer-like controls.

1.7.3 An 'active' size control system

The alternative to indirect size control through a fixed cell cycle timer is what will be referred to as an 'active' size control system. This describes a mechanism of direct cell size sensing. Further evidence for the existence of an active size control system in fission yeast, rather than simply a fixed timer, is the small variation in cell size at division within a population of cells. These cells divide at 14 μm in length with a coefficient of variation of about 6% (Sveiczer et al., 1996). Single cell studies

carried out in the 1970s showed that cells that are born small are able to correct for this in the subsequent cell cycle, such that a graph of birth length against length extension has a slope of about -0.8 (Fantes, 1977) (Figure 1.3B). This correction is through altered cycle times and not altered growth rates (Fantes, 1977). Cells also show rapid recovery of cell size after perturbation through the altered timing of subsequent cell cycles (Mitchison and Creanor, 1971). Cells arrested in S phase will continue to grow and can reach sizes of 20-25 μm. When the cell cycle block is released, cells undergo rapid synchronous divisions and return to their wild type size within two cell cycles (Wood and Nurse, 2013). Such a rapid recovery suggests that a size control system is acting in these cells. In budding yeast, single cell studies have shown that cells born smaller spend longer in G1 to allow them to grow until a critical size has been reached (Johnston et al., 1977), implying that these too maintain size homeostasis through an active size control system. Therefore the conclusion is that yeast cells have a size sensing mechanism which acts in G1 and G2 for fission yeast, although the G1 control is normally cryptic, and mainly in G1 for budding yeast (Turner et al., 2012).

1.8 Cell size control models

A size sensing and correction mechanism must be able to monitor the size of the cell and use this information to coordinate growth and cell cycle progression so that at the next division the cell is at the average size of the population. When considering the mechanism by which a cell could measure its size we envisage two main possibilities. Firstly, what we will refer to as a volume or concentration model, whereby in the simplest sense the cell is able to measure the volume of the cytoplasm by the concentration of a particular molecule in the cell. Secondly, a geometry model, which will rely on a molecular ruler to measure some aspect of the cell dimensions, for example length or surface area. We refer to this as a geometry model since the cell is probing an aspect of the cell's geometry. These two models will be discussed below, together with the current model for size control in fission yeast which falls into the category of geometry sensing. This Pom1 gradient model, first proposed in 2009 by two independent groups (Martin and Berthelot-Grosjean, 2009, Moseley et al., 2009), has recently been re-visited and

variations of this model have since been proposed (Bhatia et al., 2014, Deng et al., 2014, Pan et al., 2014).

In the context of fission yeast, a model of size control must be able to explain not only how wild type haploid rod-shaped cells are able to measure their size, but also how size control is maintained in a number of other situations. Firstly, cells of differing ploidy, which as will be discussed below, have an almost directly proportional relationship of DNA amount with cell size at division (Gregory, 2001, Nurse, 1985). Secondly, multinucleate cells resulting from the failure or inhibition of cytokinesis, which display synchronous nuclear divisions within a single enlarged cytoplasm (Fantes et al., 1975, Neumann and Nurse, 2007, Nurse et al., 1976). Here, nuclear divisions must either be controlled through a local signal from the surrounding cytoplasm or cortex, or perhaps a diffuse global signal throughout the entire cell. Thirdly, shape mutants, which do not conform to the regular rod-shape seen in wild type cells. In each of these situations, cells are still able to sense their size or volume and coordinate mitosis with cell growth, and therefore must be considered when proposing models for size control in this organism. This is discussed further in sections 1.10 and 1.11.

1.8.1 Volume/Concentration models

In its simplest form we can imagine a size control mechanism whereby a protein acting to drive entry into mitosis accumulates at a rate proportional to cell mass increase. At a certain cell size there is enough of this factor present to initiate division. Since the number of ribosomes in the cell will be proportional to the cell size, protein synthesis rate will correlate with cell size (Elliott and McLaughlin, 1978). As long as this so-called sizer molecule has a high turnover rate, the amount of the factor in the cytoplasm will be a direct reflection of protein synthesis and therefore the size of the cell (Turner et al., 2012). Such models were proposed many years ago to describe the size thresholds for division in bacteria and metazoans, as well as yeast (Brooks, 1977, Donachie, 1968, Fantes et al., 1975, Rossow et al., 1979, Unger and Hartwell, 1976). A problem with this model is that as the cell grows, the increasing volume of the cytoplasm will dilute out the effector molecule, resulting in it being present at a constant concentration. The cell

therefore requires a fixed standard against which to measure the sizing factor, such as a component of the cell itself or a second effector molecule present in a fixed amount against which to titrate the sizer.

This is an issue with the current size control model in budding yeast, whereby the G1 cyclin Cln3, a dose-dependent activator of G1/S, is thought to act as a protein synthesis rate sizer (Cross, 1988, Nash et al., 1988, Turner et al., 2012, Tyers et al., 1992). It has been shown that the concentration of Cln3 does not change as cells grow in G1, supporting the idea that the increase in cell volume acts to dilute out the increasing amounts of this protein (Tyers et al., 1993). One suggestion has been that by importing Cln3 into a nucleus of fixed volume this would allow the cell to measure the absolute amount of the sizer (Futcher, 1996). However it has been shown that in budding and fission yeast, nuclear volume increases with cell volume to maintain a constant nucleocytoplasmic ratio throughout the cell cycle, which means that the nuclear volume does not remain fixed (Jorgensen et al., 2007, Neumann and Nurse, 2007). Other suggestions have involved titrating the sizer against the genome and this will be discussed in more detail in section 1.11 when the focus turns to cell size and ploidy.

1.8.2 Geometry models

An alternative mechanism for measuring cell size is not to measure the amount of a particular protein but rather measure geometrical parameters of the cell. Here the word ‘geometry’ is used to describe any property of cell shape which can be measured, for example length, width or surface area (Moseley and Nurse, 2010). In this case we envisage a molecular ruler measuring an aspect of the cell dimensions.

The Pom1 gradient model proposed for fission yeast size control is an example of such a mechanism, with Pom1 acting as a molecular ruler through its concentration gradient emanating from the cell tips (Martin and Berthelot-Grosjean, 2009, Moseley et al., 2009). More recently, alternative more complex models have been proposed which build on this original model (Bhatia et al., 2014, Deng et al., 2014, Pan et al., 2014). One of these suggests that cell surface area may be being measured (Pan et al., 2014), but we can also imagine other structures in the cell,

for example internal membranes or microtubules, being probed by sizer molecules to feed size-related information into the cell cycle controls.

1.9 The Pom1 model

1.9.1 The Pom1 gradient

Pom1 is a dual-specificity tyrosine-phosphorylation regulated kinase (DYRK) (Bahler and Pringle, 1998) that in fission yeast forms polar cortical gradients along the cell, peaking at the cell tips (Padte et al., 2006). It was first described as providing positional information for both polarised growth and the site of septum formation (Bahler and Pringle, 1998, Celton-Morizur et al., 2006, Padte et al., 2006). Pom1 has also been proposed to play a role in length sensing and the control of mitotic entry (Martin and Berthelot-Grosjean, 2009, Moseley et al., 2009).

The Pom1 gradient is shaped by a combination of lateral diffusion through the cell cortex and autophosphorylation-dependent detachment (Hachet et al., 2011). Pom1 plasma membrane binding is triggered by Tea4-dependent dephosphorylation by the phosphatase Dis2 (Hachet et al., 2011). Since Tea4 is delivered to the cell ends by microtubules, Pom1 binding occurs at the cell tips. Pom1 then moves along the plasma membrane towards the cell middle and undergoes autophosphorylation to lower its lipid affinity, thus promoting release of Pom1 from the membrane (Hachet et al., 2011). Pom1 molecules diffusing at the plasma membrane also associate and disassociate into and from clusters (Saunders et al., 2012). A two-state gradient involving these Pom1 clusters on the membrane has been suggested to serve as a mechanism to buffer against fluctuations in concentration levels. Along with time averaging, cluster formation could act to reduce the effects of inevitable fluctuations in gradient formation and might enable Pom1 to convey more precise spatial information (Saunders et al., 2012).

1.9.2 Pom1 as a molecular ruler

Evidence for the role of Pom1 in the control of cell size and mitotic entry was initially provided by two independent studies (Martin and Berthelot-Grosjean, 2009,

Moseley et al., 2009). Martin and Berthelot-Grosjean and Moseley et al. both showed that Pom1 acts as a dose-dependent inhibitor of the G2/M transition through the Cdr2-Cdr1-Wee1 pathway. Cdr2, Cdr1 and Wee1 are localised to a medial band of cortical nodes in interphase cells and this localisation is driven by Cdr2. Since Pom1 is found at the cell ends, it was hypothesized that Pom1 may be providing spatial cues to the cortical nodes in the middle of the cell containing these cell cycle regulators. This was supported by data showing that Cdr2 spreads from its tight band of cortical dots in *pom1Δ* cells, and that Cdr2 is phosphorylated in a Pom1-dependent manner *in vivo*. Ectopic localisation of Pom1 to the middle of the cell results in a delay in mitotic entry equivalent to the *cdr2Δ* phenotype, and this is dependent on an active Pom1 kinase domain (Martin and Berthelot-Grosjean, 2009, Moseley et al., 2009). Quantification of the distribution of Pom1 and Cdr2 at the time showed that as cells progressed through G2, Pom1 levels in the middle of the cell decreased, such that the proteins overlapped in short but not in long cells (Martin and Berthelot-Grosjean, 2009, Moseley et al., 2009). These data will be discussed in more detail below. The original model proposed was as follows. In short cells, the Pom1 gradient from the cell ends overlaps with mitotic activators in the cortical nodes in the centre of the cell. Pom1 phosphorylates and inactivates Cdr2. As cells increase in length through G2, Pom1 concentration at the medial site becomes progressively lower, reaching a level at which it can no longer inhibit Cdr2. Wee1 is therefore inhibited and active CDK drives the cell into mitosis (Martin and Berthelot-Grosjean, 2009, Moseley et al., 2009) (Figure 1.4). Nif1, a SEL1 repeat protein, was also implicated in this model due to its tip localisation and the small cell phenotype of *nif1Δ* cells (Martin and Berthelot-Grosjean, 2009, Wu and Russell, 1997).

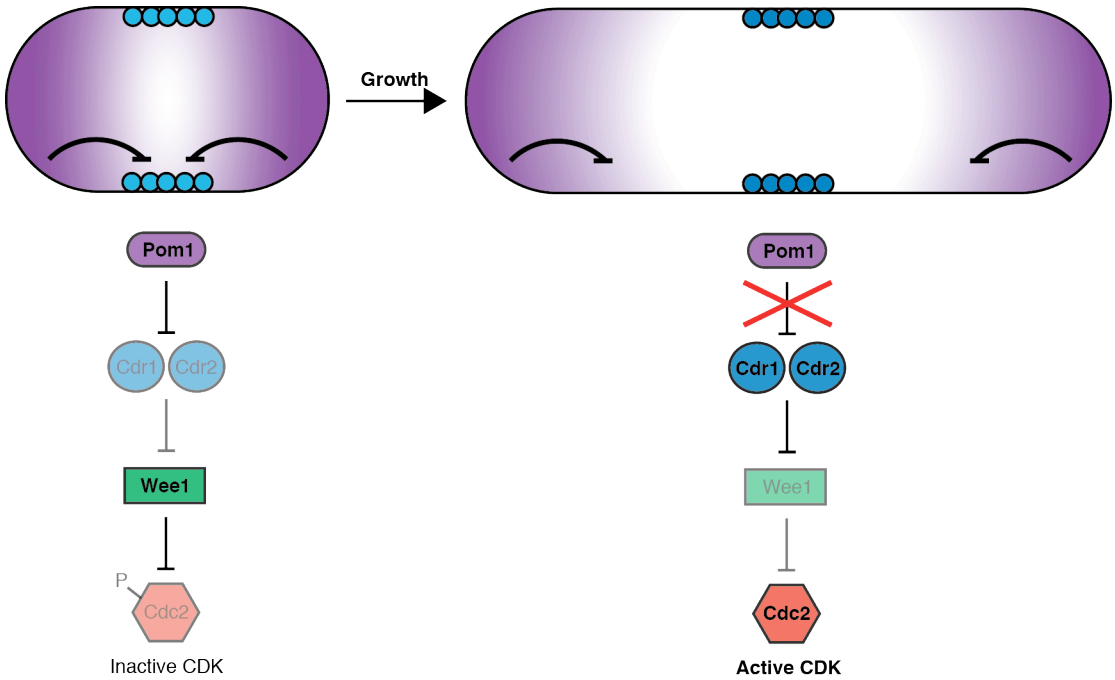

Figure 1.4|The original Pom1 gradient model for length sensing in fission yeast

An early G2 cell (left): Pom1 protein emanating from the cell tips (purple) inhibits Cdr1/Cdr2 in the cortical nodes (light blue circles). Wee1 is therefore active and carries out inhibitory phosphorylation of Cdc2. A late G2 cell (right): Pom1 concentration at the medial site is decreased. At a critical threshold, Cdr1/Cdr2 are no longer inhibited (dark blue circles) and so the Wee1 inhibition of Cdc2 is lifted. The active CDK drives mitotic entry. Figure is from (Marshall et al., 2012).

More recently, Deng et al. have implicated another protein kinase, Ssp1, in this length sensing model (Deng et al., 2014). They propose that Ssp1 phosphorylates and activates Cdr2 to promote mitotic entry, but that this activation is inhibited in small G2 cells by Pom1. Thus it is suggested that Cdr2 integrates the input signals from both the activating kinase, Ssp1, and the inhibitory Pom1 gradient (Deng et al., 2014).

1.9.3 The Pom1 model, past and present

Despite these data supporting a gradient model, whereby Pom1 and possibly Nif1 act as a molecular ruler to measure cell size, there are outstanding questions which need addressing.

A quantitative analysis of the Pom1 protein, published after the initial model was proposed, shows a short decay length of the Pom1 gradient at the cell tips in

relation to the length of the cell (Saunders et al., 2012). This study also found large cell-to-cell variability in both the intensity and distribution of the protein, as well as fluctuations in the cortical gradient over time on a single cell level (Saunders et al., 2012). This means that changes in the protein gradient according to cell length may be less consistent than originally proposed and leads to questions regarding whether or not Pom1 could act as a reliable molecular ruler.

The Pom1 gradient model is also unable to explain size control in the three situations mentioned earlier: namely ploidy, multinucleate cells and shape-mutants. The model could be modified to take account of ploidy if perhaps one of the components of the network was determined by gene copy number, however so far no such component has been identified (Marshall et al., 2012, J. Hayles, personal communication). With regards to multinucleate cells, the synchronous nuclear divisions suggest a global control mechanism throughout the continuous cytoplasm which is able to coordinate mitosis in each nucleus simultaneously (Fantes et al., 1975). Whether it is overall cell size or local nuclear cytoplasmic mass which is monitored has yet to be determined, and further insight into how this fits with the Pom1 gradient model requires further investigation. Lastly, cell shape mutants which do not conform to the regular rod-shape of wild type cells cannot measure cell length through the Pom1 gradient alone, since these mutant cells have been shown to divide at a constant surface area rather than a constant length (Pan et al., 2014).

Finally, in this work we show that cells deleted for *pom1* demonstrate cell size homeostasis (Wood and Nurse, 2013). The role of Pom1 and Nif1 in size homeostasis was implied with the initial model but never directly tested. The studies described in Chapter 2 suggest that neither Pom1 or Nif1 are critical players in cell size homeostasis, although both are clearly involved in setting the cell size threshold.

1.9.4 Alternative Pom1 models

Further evidence supporting an alternative mechanism for cell size control was published after the work detailed in this thesis was carried out but nevertheless will be discussed briefly here. The evidence came with new data showing that with

improved cortical measurements of Pom1 there is no detectable difference in medial Pom1 concentration between short and long cells (Bhatia et al., 2014, Pan et al., 2014), as had been previously reported. It has been suggested that the difference in the interpretation of the data could be due to the fact that the previous measurements of Pom1 had been derived from total cellular fluorescence, which did not account for the exclusion of Pom1 from the nucleus (Bhatia et al., 2014, Pan et al., 2014, Saunders et al., 2012).

Despite the amount of Pom1 in the very middle of the cell being similar in all cells regardless of their size, the medial region of basal Pom1 widens linearly with increasing cell length. The Cdr2 domain also varies in width, node number and intensity over the cell cycle (Bhatia et al., 2014, Pan et al., 2014), though the width increase of the Cdr2 domain is less than that of the basal Pom1 region (Bhatia et al., 2014). The result is that the degree of overlap between Pom1 and Cdr2, although very small, diminishes with increasing cell length (Bhatia et al., 2014). These data have led to a number of alternative length sensing models.

The first model, most similar to the original one, states that Pom1 inhibits Cdr2 activity at the edges of the node domain (Bhatia et al., 2014). Since the region of overlap between Crd2 and Pom1 decreases with increasing cell length, this provides a mechanism for length-dependent activation of Cdr2 and thus mitotic entry. This model would be inherently noisy due to the very small overlap of Cdr2 and Pom1 and also does not explain size control in diploids, in which the Pom1/Cdr2 overlapping region correlates poorly with cell length (Bhatia et al., 2014). Like the original model, this one also describes a length sensing mechanism. The model is therefore, in its simplest form, unable to explain the behaviour observed in multinucleate cells or mutant haploid cells of varying shapes. For this, the cell must be able to measure something other than merely its total length.

The second model postulates that cell size could be measured through the ratio of polar Pom1-bound cortex to total cortex, a ratio that diminishes as the cell elongates (Bhatia et al., 2014). Cdr2 will be inhibited close to the cell poles where Pom1 concentration is highest. If the turnover of this inhibitory phosphorylation is slow compared with the dynamics of Cdr2 on the cortex (also regulated by Pom1), inhibited Cdr2 will accumulate in the middle of the cell. At a certain threshold, dependent on cell length, too little of the cortex will have Pom1 bound and therefore there will be sufficient active Cdr2 to drive mitotic entry (Bhatia et al.,

2014). It is possible that this system could measure the surface area of the cortex rather than the length of the cell *per se*, and therefore this model could perhaps be fitted to describe the behaviour of both multinucleate cells and shape mutants which cannot rely on a length sensing mechanism alone. Another recent publication has proposed a surface area model that doesn't involve the Pom1 gradient directly but instead places more focus on the medial cortical nodes (Pan et al., 2014). The model proposes that cells sense their size using Cdr2 to probe the entire surface area of the cell and relay this information to the medial cortex. Whilst both of these surface area-based models may be able to explain size control in cells of varying shapes and with more than one nucleus, they are still insufficient to explain the relationship between cell size and ploidy, since no component of these models has been linked to gene copy number.

A final possibility is that Pom1 is not acting as a direct size-sensor at all (Bhatia et al., 2014, Pan et al., 2014, Wood and Nurse, 2013). The low levels of this kinase in the cell centre may be enough to keep Cdr2 inactive and act as a constitutive buffer against mitotic commitment in response to other stimuli, such as the adaptation of cell length under stress (Bhatia et al., 2014). The higher levels of Pom1 at the cell tips could simply be acting to prevent nuclear division occurring too near to the cell ends, where there may not be sufficient space to allow complete separation of the two daughter nuclei (Wood and Nurse, 2013). This is consistent with the data shown here which suggests that Pom1 is not the major size-sensor and that another mechanism acts to coordinate cell size with progression through the cell cycle (Wood and Nurse, 2013).

1.10 Testing size control models

A major part of the challenge in identifying mechanisms of cell size control has been the experimental limitations associated with measuring cell size and separating the pleiotropic effects that many cell cycle regulators have. It is therefore crucial to isolate different tools and systems that can be used to test predicted size control models. Here we discuss two ways that are being used by us and others to investigate more closely the size sensing model for fission yeast.

1.10.1 Multinucleate cells

Wild type fission yeast cells are haploid and proliferate through repeated cycles of nuclear division followed by cell separation (Mitchison, 1957). However, these cells can be forced to undergo rounds of nuclear division without intervening cytokinesis through the inactivation of genes required for cell separation. Cdc11 is a septation initiation network scaffold protein and is essential for the onset of septum formation (Krapp et al., 2004, Nurse et al., 1976). A temperature-sensitive allele has been isolated (*cdc11-119*) which at the restrictive temperature blocks the onset of cytokinesis and results in multinucleated cells (Nurse et al., 1976). These cells enable the investigation of multiple nuclei within a continuous cytoplasm and allow us to ask questions regarding the nuclear or cytoplasmic autonomy of certain cell cycle controls.

When using these multinucleate cells to investigate the controls operating over nuclear division it is important to consider other multinucleate systems such as the cells of the multinucleate fungus *Ashbya gossypii*. In this system asynchronous nuclear divisions are observed and this has been suggested to be due to nuclei using microtubules to establish individual cytoplasmic territories to insulate their division cycles from one another (Anderson et al., 2013, Lee et al., 2013). Since these cells are naturally occurring syncytia in contrast with the experimentally-induced syncytia created by the *cdc11-119* mutation in the fission yeast cells the mechanisms involved may be different. Nevertheless we may be able to glean additional information from *A.gossypii* to aid with our understanding of the mechanistic controls operating on nuclear division in *S.pombe*.

1.10.2 Cell shape mutants

The originally proposed Pom1 model for cell size control in fission yeast (Figure 1.4) heavily relied on the regular geometry of these cells (Martin and Berthelot-Grosjean, 2009, Moseley et al., 2009). The Pom1 gradient can only act as a reliable ruler if the cells maintain a constant width during the cycle and elongate only in the direction of the protein gradient. This also means that the gradient sensing model cannot be extended to any cell type with a different shape or with a flexible form which changes over the course of a cell cycle. There is as yet

no evidence that the size control mechanism in fission yeast is conserved and so it is possible that a Pom1 gradient is unique to this organism in feeding size information into the cell cycle controls.

However an important tool to study this size sensing mechanism in *S.pombe* is cells which do not conform to the regular rod shape. These shape mutants allow us to study what aspect of the cell geometry, if any, the cell is measuring. It was originally proposed that fission yeast cells are measuring their length (Martin and Berthelot-Grosjean, 2009, Moseley et al., 2009) however more recent work using cell shape mutants has suggested that this may not be the case (Pan et al., 2014). These mutants are therefore a useful system to use when testing any proposed model of cell size control in this organism. In addition to shape mutants it is also necessary to link our findings to cells of other single-celled yeasts such as those of the budding yeast *Saccharomyces cerevisiae*, which do not have such a regular geometry. Whether these distantly-related organisms share core components of a size sensing system has yet to be determined, however if findings in fission yeast are to bear any importance for a more global mechanisms it is crucial that proposed models are tested in other systems.

1.11 The ploidy problem

An important consideration in the understanding of cell size control for fission yeast is that of ploidy. Observations regarding the almost direct proportionality between cell size at division and ploidy were made as early as the 1950s and it is considered an almost universal property of cell size in many cell types (Gregory, 2001, Nurse, 1985). Ploidy series in yeast have allowed us to observe this relationship directly (Mortimer, 1958, Mundkur, 1953) and conclude that ploidy determines cell size at division, which in turn determines the size of the daughter cells and their nuclei (Neumann and Nurse, 2007). Cells are therefore able to feed information regarding their ploidy into the size sensing mechanism and this is more difficult to imagine in the setting of the current geometric size models described above.

1.11.1 Volume-based models involving ploidy

This is less of an issue if we turn to volume-based models for cell size control. We can predict two variations which would allow the cell to integrate information about DNA content into the size control system. Either the cell produces a factor according to ploidy, or it measures a factor against ploidy (Marshall et al., 2012).

Making a factor according to ploidy could involve producing a transcript as a single pulse at a particular stage in the cell cycle. The amount of this transcript will be a direct function of DNA copy number. If the product of this critical transcript is stable and acts as a mitotic inhibitor, we can imagine that the fixed amount of protein produced from the pulse will be diluted as the cell grows. Below a critical protein concentration, and thus a critical cell size, entry into mitosis will be permitted (Fantes et al., 1975). As the ploidy of the cell increases, the amount of this protein produced will increase with ploidy and thus the cell will have to grow proportionally more before this critical concentration is reached. A prediction of this model is that a heterozygous diploid with only one copy of such a gene would be the size of a haploid. No such gene has yet been described (Marshall et al., 2012, J. Hayles, personal communication), however this may indicate redundancy within the system. In fact we can imagine a more robust size sensing mechanism involving multiple interacting factors acting together in a redundant manner.

The second volume-based model, measuring a factor against ploidy, could involve genomic titration (Donachie, 1968, Fantes et al., 1975, Sompayrac and Maaloe, 1973). Here, a protein is made at a constant concentration and said protein binds sites within the genome. As the cell grows, the absolute amount of protein increases and thus more genomic sites are bound (independent of protein concentration which may remain constant due to the increasing volume of the cell during the cycle). The binding itself could drive division so that as more sites are bound the probability of entering mitosis increases. Alternatively the protein in question may only be active in its free form and therefore only once all the genomic sites are occupied will there be enough unbound protein to drive division. In both of these cases, an increase in ploidy would mean more sites on the DNA to bind. The cell would thus have to grow to a larger size before division is permitted. The first of these two possibilities has been suggested for budding yeast, in which the

synthesis rate sizer model involving Cln3 requires a fixed standard within the cell against which to titrate the G1 cyclin. It has been shown that Cln3 binds SBF binding sites across the genome and so it is possible that division is permitted only when a certain number of these sites are occupied (Wang et al., 2009). This would allow the cell to measure the amount of the cyclin, eliminating the problem of the constant concentration of Cln3 as the cell grows and also allowing for an input of ploidy into this size sensing mechanism.

A third possibility can be envisaged which is a combination of these two models. A factor produced according to ploidy could be used to titrate out the synthesis rate sizer protein which is present at a constant concentration. This would allow the cell to measure the comparative amounts of these two factors, a ratio which will change in a cell volume-dependent manner (Fantes et al., 1975).

1.11.2 The Pom1 model and ploidy

Turning to the Pom1 model in fission yeast it is important that we consider ploidy when proposing further adaptations of this size control mechanism. Pom1 is haploinsufficient for cell size (Bhatia et al., 2014), showing that dosage of this protein is important for mitotic size control. However, heterozygous diploids are not reduced to the size of haploid cells and therefore we conclude that Pom1 alone is not acting to measure ploidy directly. It could however be working in concert with other proteins involved in the proposed model.

1.12 Aims of this work

Despite being an excellent system in which to study such a problem, the question of cell size control in fission yeast is one that is incompletely solved. The work detailed in this thesis aims to further our knowledge of the controls operating to regulate the timing of mitotic entry and to coordinate this cell cycle decision with cell growth. Chapter 2 probes the Pom1 gradient model for cell size control. When this work began the current understanding was that a Pom1 gradient acted to measure the length of the cell and feed this information into the activation of Cdk. The work described in this thesis challenges this model since population variability

studies and single cell size homeostasis experiments show that Pom1 is not essential for the sensing and correction of cell size at division. Over the course of this work new studies were published which supported this finding.

The single cell size homeostasis studies were able to provide additional information regarding the proposed size control model, which previous population cell size studies had not revealed. To this end, size homeostasis was used as a tool to investigate other known cell cycle regulators. Chapter 3 details the findings of these studies and provides a new outlook on the control and regulation of cell size at division and the mechanisms used by the cell to correct for deviations in size that arise in a population.

Finally, Chapter 4 describes the continuation of a near genome-wide screen. The original screen was carried out in the lab to identify gene deletions that advance cells prematurely into mitosis at a small cell size. The data from this screen was used here to reveal new elements acting at the G2/M transition by identifying genes which when deleted lead to increased variability in cell size at division. This investigation revealed two genes, which had not been previously identified as size mutants, which may have a role in the size sensing mechanism acting to control entry into mitosis.

Parts of this Introduction have been published in an Annual Reviews article (Wood and Nurse, 2015).

Chapter 2. An analysis of the Pom1 model for cell size sensing

2.1 Introduction

Despite many years of investigations into how cells sense and regulate their size, molecular mechanisms remain elusive. The most well studied system in this field is the fission yeast *Schizosaccharomyces pombe* due to its regular size and shape and tractable genetics. A model has been suggested in this organism which involves the mitotic inhibitor, Pom1, which has been proposed to measure cell length through its polar cortical gradient acting on medial nodes containing the mitotic activators Cdr1 and Cdr2 (Martin and Berthelot-Grosjean, 2009, Moseley et al., 2009). The aim was to further test this model with particular emphasis on size homeostasis.

When work for this chapter began, the cell size sensing model was as follows. Pom1 is enriched at the cell tips (Bahler and Pringle, 1998, Padte et al., 2006) and forms a gradient along the length of the cell. Cells deleted for *pom1* divide at a shorter size compared with wild type cells and this inhibitory effect is dose-dependent, supporting its role as a mitotic inhibitor (Martin and Berthelot-Grosjean, 2009, Moseley et al., 2009). Cdr1 and Cdr2 are mitotic activators localised to cortical nodes organised into a medial band and both proteins inhibit the kinase Wee1. Pom1 phosphorylates and inhibits Cdr2, implicating Pom1 as part of the mechanism sensing size at mitotic entry (Martin and Berthelot-Grosjean, 2009, Moseley et al., 2009). Initial findings found the concentration of Pom1 in the middle of the cell to be length-dependent, and as cells grow during G2 Pom1 concentration around the cortical nodes was found to decrease. The model suggested that below a critical Pom1 threshold Cdr2 is no longer inhibited, Wee1 inhibition of Cdc2 is lifted and CDK is activated driving mitotic entry (see Figure 1.4). Pom1 was therefore suggested as the key sensor component of a gradient mechanism for cell size control at mitotic entry (Martin and Berthelot-Grosjean, 2009, Moseley et al., 2009). Nif1 was also implicated in this mechanism due to its tip localisation and small cell phenotype (Martin and Berthelot-Grosjean, 2009).

This chapter describes further investigations into this proposed model, which aim at identifying whether Pom1 behaves like a size sensor. Data supporting the model show that Pom1 (and Nif1) have a role in setting a threshold size for mitotic entry but the purpose was to test whether these proteins are acting as direct sensors of cell size. The experiments here suggest that Pom1 and Nif1 do not have major roles in sensing cell size. During this investigation further work was published by other groups which supported this finding (Bhatia et al., 2014, Pan et al., 2014) and this will be discussed at the end of this chapter as well as in the General Discussion.

2.2 Results

2.2.1 Pom1 and Nif1 both localise to the cell tips and division site

Pom1 and Nif1 were tagged at the endogenous locus with GFP. As has been shown previously, both Pom1-GFP and Nif1-GFP are enriched at the ends of the cell and are excluded from the nucleus (Figure 2.1A). This tip localisation persists through G2 as the cells lengthen, and just prior to division both proteins localise to the division site (Figure 2.1A). While Pom1 is always seen at both cell tips (albeit often enriched at the non-growing end (Bahler and Pringle, 1998)), Nif1 is enriched at one, both, or neither of the cell tips (Figure 2.1A and B).

In order to examine whether a gradient of Nif1 protein could act alongside Pom1 in late G2 as a length-sensor for mitotic entry, the localisation of Nif1 was investigated further. The majority of early G2 cells, shorter than 10 μm and presumed to be prior to NETO, are enriched for Nif1 at one end only (Figure 2.1B). On staining with calcofluor it was confirmed that Nif1 is at the growing tip (Figure 2.1C). As the cells grow and undergo NETO, an increasing proportion of cells have Nif1 present at both ends. Just prior to septation (12-14 μm) the majority of cells have Nif1 present at both tips (Figure 2.1B). This is consistent with data showing that Nif1 localisation is dependent on actin (Martin and Berthelot-Grosjean, 2009). It is only in a small proportion of cells, around 20% of small G2 cells and 10% of larger G2 cells, that no enrichment of Nif1, at either of the cell tips, is seen (Figure 2.1B). For the majority of cells therefore Nif1 could be working with Pom1 cooperatively in late G2 to form a gradient sensor of cell size.

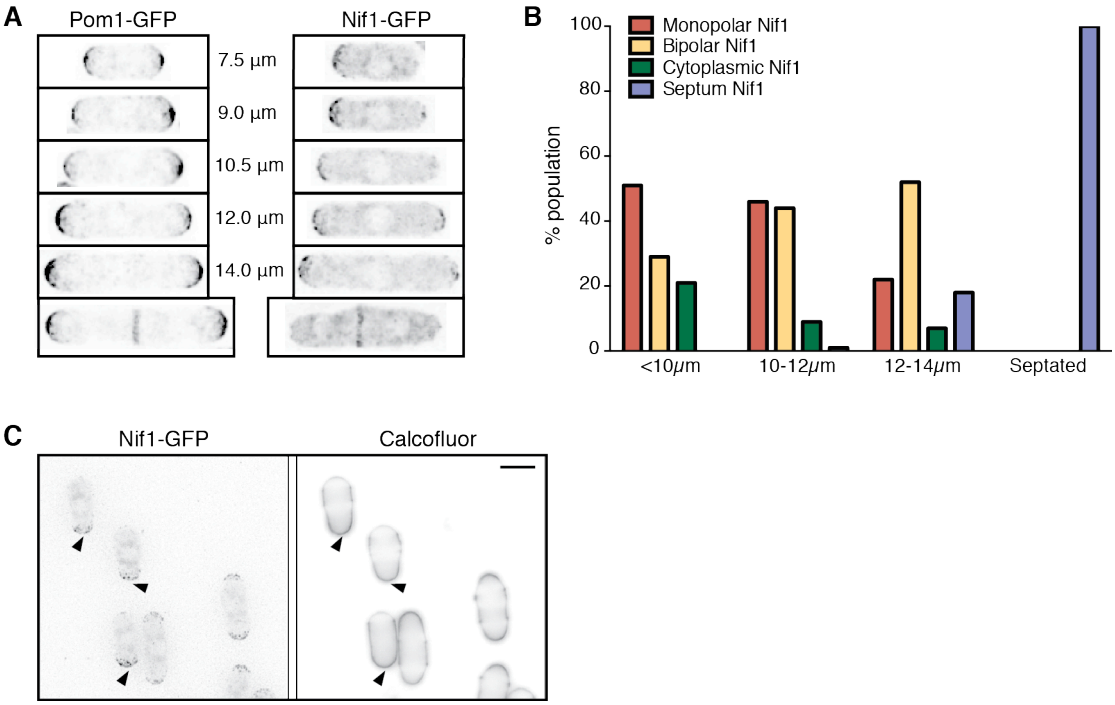

Figure 2.1|Pom1 and Nif1 localise to the cell tips and division site

(A) Localisation of GFP-tagged protein in cells of indicated size. Inverted maximum intensity projections of deconvolved images (Z stacks through entire cell). **(B)** Quantification of Nif1 localisation in cells of indicated size. Cytoplasmic Nif1 refers to cells with no visible protein enrichment. All septated cells were 12-14 µm in length. n=444. **(C)** Calcofluor staining of the newly incorporated cell wall distinguishes growing from non-growing ends. Arrows indicate the growing end where staining is darker. Nif1-GFP image is inverted maximum intensity projection of deconvolved image (Z stacks through entire cell). Calcofluor image is inverted image, medial single focal plane. Scale bar represents 5 µm.

2.2.2 Cdr2 localises to a ring of medial cortical nodes that widens with increasing cell length

These mitotic inhibitors, Pom1 and Nif1, have been shown to inhibit the mitotic activator Cdr2 (Martin and Berthelot-Grosjean, 2009, Moseley et al., 2009). Cdr2 tagged with GFP localises to a band of medial nodes, as previously reported (Martin and Berthelot-Grosjean, 2009, Moseley et al., 2009) (Figure 2.2A). It was confirmed that these nodes are restricted to the cortex of the cell and are not present throughout the medial cytoplasm. Images taken in Z slices through the width of the cell and reconstructed into a 3D image show the medial nodes as a ring around the cell cortex (Figure 2.2B). This localisation is consistent with a

model whereby Pom1 and Nif1 at the cell ends may overlap with Cdr2 in short but not in long cells, acting as a read-out of cell size to control mitotic entry. Further investigation of these cortical nodes suggests that the length of the Cdr2 node domain increases somewhat with increasing cell length (slope is significantly non-zero, $p<0.0001$) (Figure 2.2C). Since this work was carried out, additional publications have reported this increasing Cdr2 domain width and have integrated this new finding into the model (Bhatia et al., 2014, Pan et al., 2014).

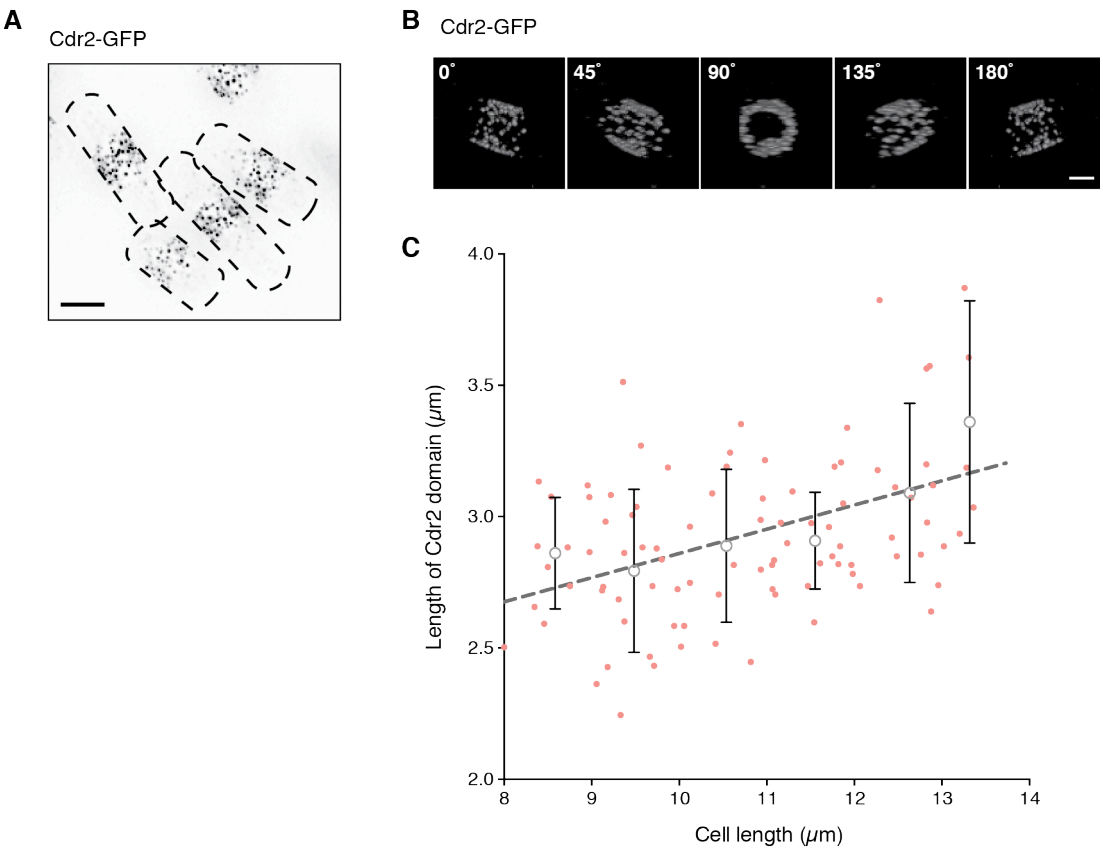

Figure 2.2|The medial band of cortical Cdr2 nodes increases with cell length

(A) Cdr2-GFP tagged cells showing protein localisation to medial nodes. Inverted maximum intensity projection of deconvolved image. Black dotted line indicates cell perimeter (from brightfield image). Scale bar represents 4 μm. **(B)** 3D projection of a cell tagged with Cdr2-GFP shows the medial band of nodes is only in the cell cortex. Cdr2 is absent from the cytoplasm. Images are taken from a deconvolved image. Z section spacing is 0.25 μm. Scale bar represents 2 μm. **(C)** Graph showing cell length plotted against length of the Cdr2 node domain. Red dots show individual measurements. White circles show mean of cohorted data, bars represent standard deviation. Dotted line shows linear regression of individual data points, $r^2=0.19$. n=94.

2.2.3 Pom1 and Nif1 have an additive effect on cell length at division

If Pom1 and Nif1 act as gradient sensors of cell size, it is expected that cells deleted for these mitotic inhibitors will affect cell length at division. Cell length analyses were carried out on populations of wild type, *pom1*Δ, *nif1*Δ and *pom1*Δ*nif1*Δ cells. Cells were first stained with calcofluor in order to clearly visualise the septum and cell wall (Figure 2.3A). Images were taken and the length and width of around 100 septating cells was measured using ImageJ. Due to the redistribution of actin patches from the cell ends to the site of septum formation at mitosis, cells cease to elongate between mitotic entry and cytokinesis (Marks et al., 1986). This is known as the constant length period and enables us to use cell length at septation as a proxy for cell length at mitotic entry (septated cells can be more easily identified and measured) (Mitchison, 1957).

In accordance with previous data, it was found that cells deleted for *pom1* or *nif1* enter mitosis at a significantly smaller size compared with wild type cells, dividing on average at around 90% of the wild type cell length (Figure 2.3B). Their effect on cell size at division is additive, the double *pom1Δnif1Δ* mutant dividing at around 11 μm, significantly shorter than either single mutant (Figure 2.3B). Wild type cells have very little variation around the mean and cells deleted for *nif1* have a similar distribution. Single *pom1Δ* mutants and the double *pom1Δnif1Δ* cells on the other hand both have increased variation in size at division (Figure 2.3B).

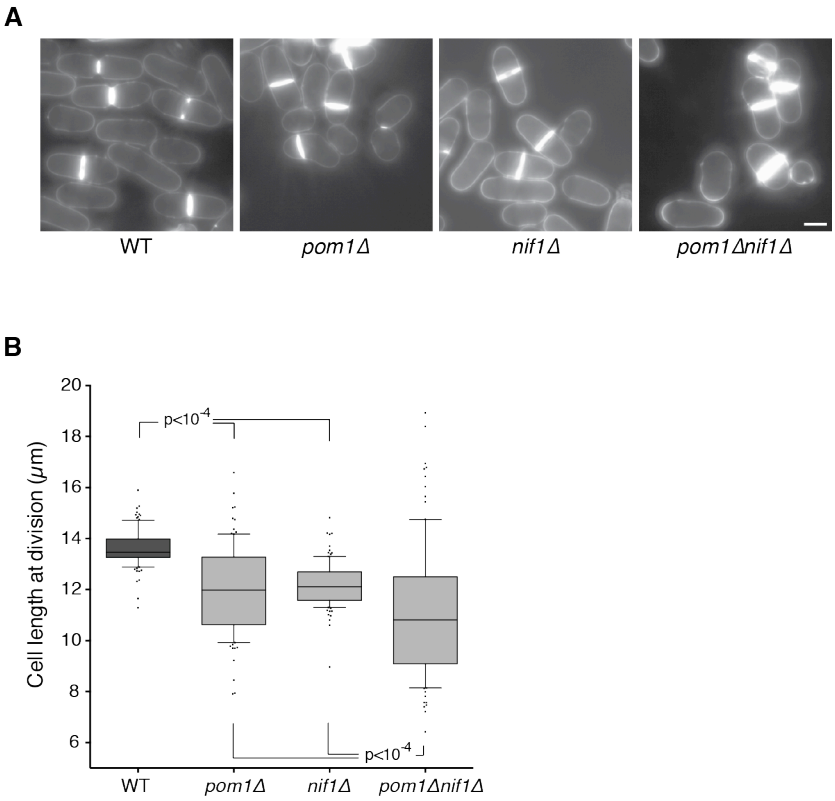

Figure 2.3|Pom1 and Nif1 have an additive effect on cell length at division

(A) Cells of indicated strain stained with calcofluor. Images taken at medial focal plane. Scale bar represents 4 μm. **(B)** Box plots showing cell length at division of WT, *pom1*Δ, *nif1*Δ and *pom1*Δ*nif1*Δ calcofluor-stained cells. Boxes delimited by first quartile, median and third quartile and whiskers mark maximum and minimum values within a 10-90% range. Values outside this range displayed as single points. P values calculated using two-tailed unpaired Student's *t*-test. 100 cells of each strain measured in exponential growth in YE4S at 32°C.

2.2.4 Cells deleted for *pom1* show asymmetric septation

A reason for this increased variation in cell size at division of the *pom1Δ* mutant is the asymmetry of division (Bahler and Pringle, 1998), and this was investigated further. The position of the septum was investigated on a single cell level by measuring the absolute distance between the septum and the cell middle. Since the Pom1 protein has a role in septum positioning in addition to the timing of mitotic entry, *pom1Δ* cells often divide asymmetrically, placing the septum at an average distance of 2 μm from the cell centre (Figure 2.4A). This phenotype is also seen in the double *pom1Δnif1Δ* mutant (Figure 2.4A). The septum displacement is independent of cell length in WT, *pom1*Δ and *pom1*Δ*nif1*Δ cells (Figures 2.4B-D).

Together with data showing that the central position of the nucleus within the cell is unaffected in *pom1*Δ cells (Figure 2.4E), this observation suggests that the septum may slide from the middle of the cell, where its position is first established, to an off-centre position resulting in an asymmetric division.

Mid1 is required to restrict septum formation to the middle of the cell and is therefore essential for correct positioning of the division site (Sohrmann et al., 1996). It has been previously shown that in *pom1Δ* cells the medial band of Cdr2 cortical nodes spreads to the entire non-growing half of the cell (Martin and Berthelot-Grosjean, 2009, Moseley et al., 2009). Cdr2 is required for the assembly of multiple interacting proteins to the cortical nodes, including Mid1 (Moseley et al., 2009). It is unknown why the cortical nodes spread only to the non-growing half of the cell in *pom1Δ* mutants. One possibility is the presence of another inhibitor of Cdr2 enriched at the opposite growing end of the cell. Nif1 is an obvious candidate for this. However *nif1Δ* cells do not show any septation defect (Figure 2.4A) and Cdr2 localisation shows a wild type band of cortical nodes placed in the cell middle (Figure 2.5).

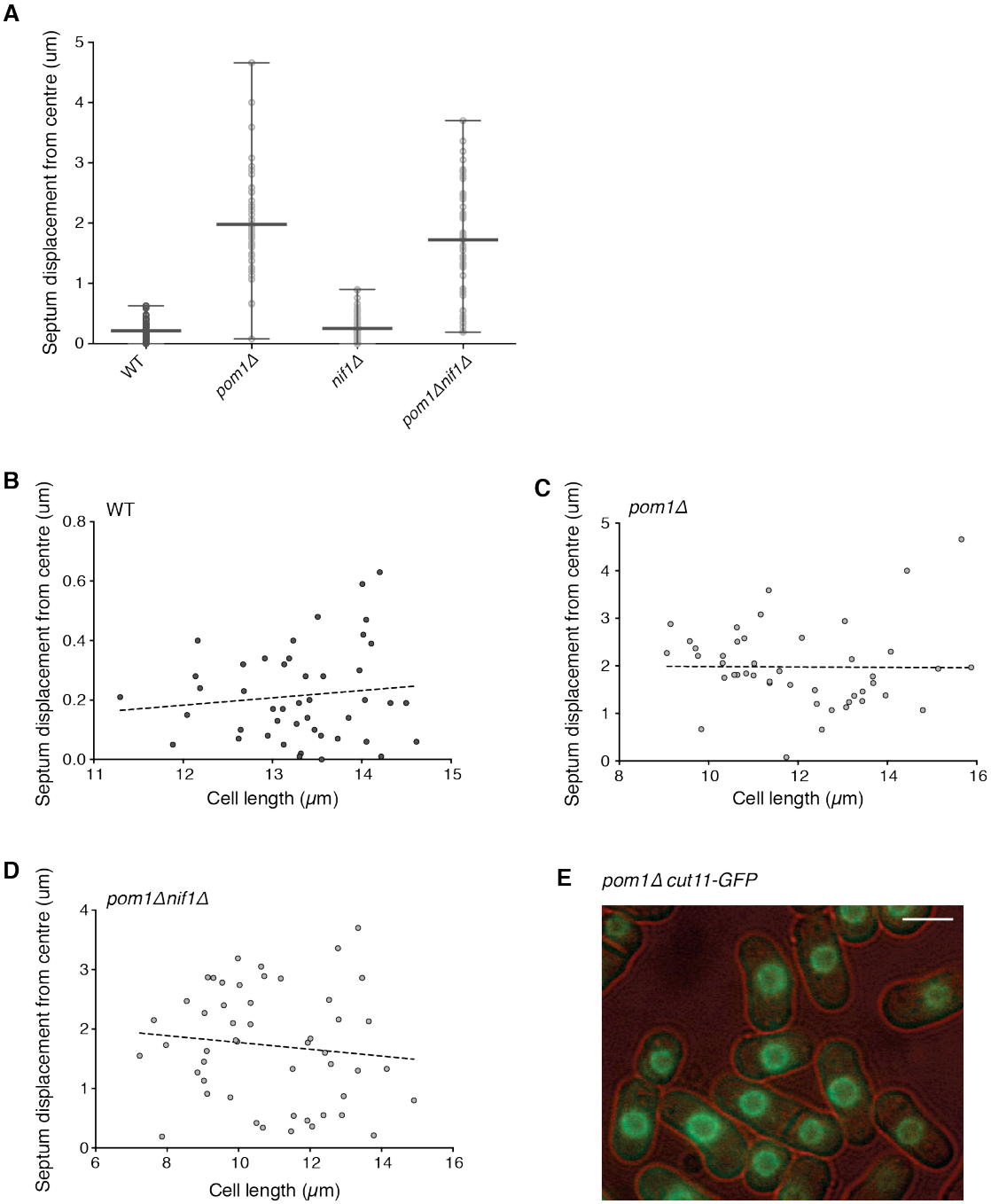

Figure 2.4|Pom1, but not Nif1, has an effect on septum positioning

(A) Septum displacement from the centre of the cell. Lines at lower range, median and upper range. Each measurement shown as an individual point. n=50-100 cells. Cells grown in YE4S at 32°C. **(B)** Cell length plotted against septum displacement for WT cells. n= 45, r^2=0.01. **(C)** Same as **B** for *pom1*Δ cells. n= 45, r^2=<0.0001. **(D)** Same as **B** for *pom1*Δ*nif1*Δ cells. n= 50, r^2=0.01. **(E)** Brightfield image of *pom1*Δ cells (false-coloured red) overlaid with fluorescent image showing cut11-GFP around the nucleus. Image taken at medial focal plane. Scale bar represents 5 μm.

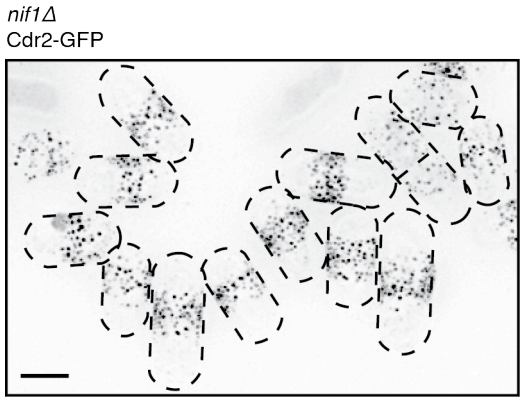

Figure 2.5|Nif1 has no role in Cdr2 localisation

Image of *nif1*Δ cells tagged with Cdr2-GFP. Inverted maximum intensity projection of deconvolved image. Black dotted lines indicate cell perimeter (from brightfield image). Scale bar represents 4 μm.

Despite *nif1*Δ having no apparent septation phenotype, the septation defect observed in *pom1*Δ*nif1*Δ mutants is slightly more severe compared to a population of *pom1Δ* single mutants. In addition to placing the septum very close to one of the cell ends, in the double mutant there is a higher proportion of cells with angled septa, which can result in a delay or complete arrest in septation (Figure 2.6A). This is possibly due to a checkpoint or the inability of the cell to cleave such a misplaced septum. Successive cell divisions were observed by growing cells in a microfluidic chamber and taking brightfield images every 10 minutes over 12 hours. A particularly striking phenotype seen in a small proportion (around 0.1%) of these *pom1*Δ*nif1*Δ cells is the placing of the septum along the long axis of the cell (Figure 2.6A and B). The cell is able to successfully undergo cytokinesis, although the time taken to complete cell separation is longer than a wild type division. In the following cell cycle both daughter cells place their septum along the correct axis, albeit asymmetrically (Figure 2.6B). This second cell cycle is shorter, around 1 hour, and as will be discussed later, this suggests that these cells are running on a timer due to already having exceeded the G2/M size threshold. No significant change in the distribution of microtubules was observed in these cells, although the actin patches could be seen around the entire cell periphery as opposed to just the cell tips as in wild type cells (Figure 2.6C). Nif1 therefore seems to be additive to Pom1 both in terms of cell length at mitosis and the septation defect.

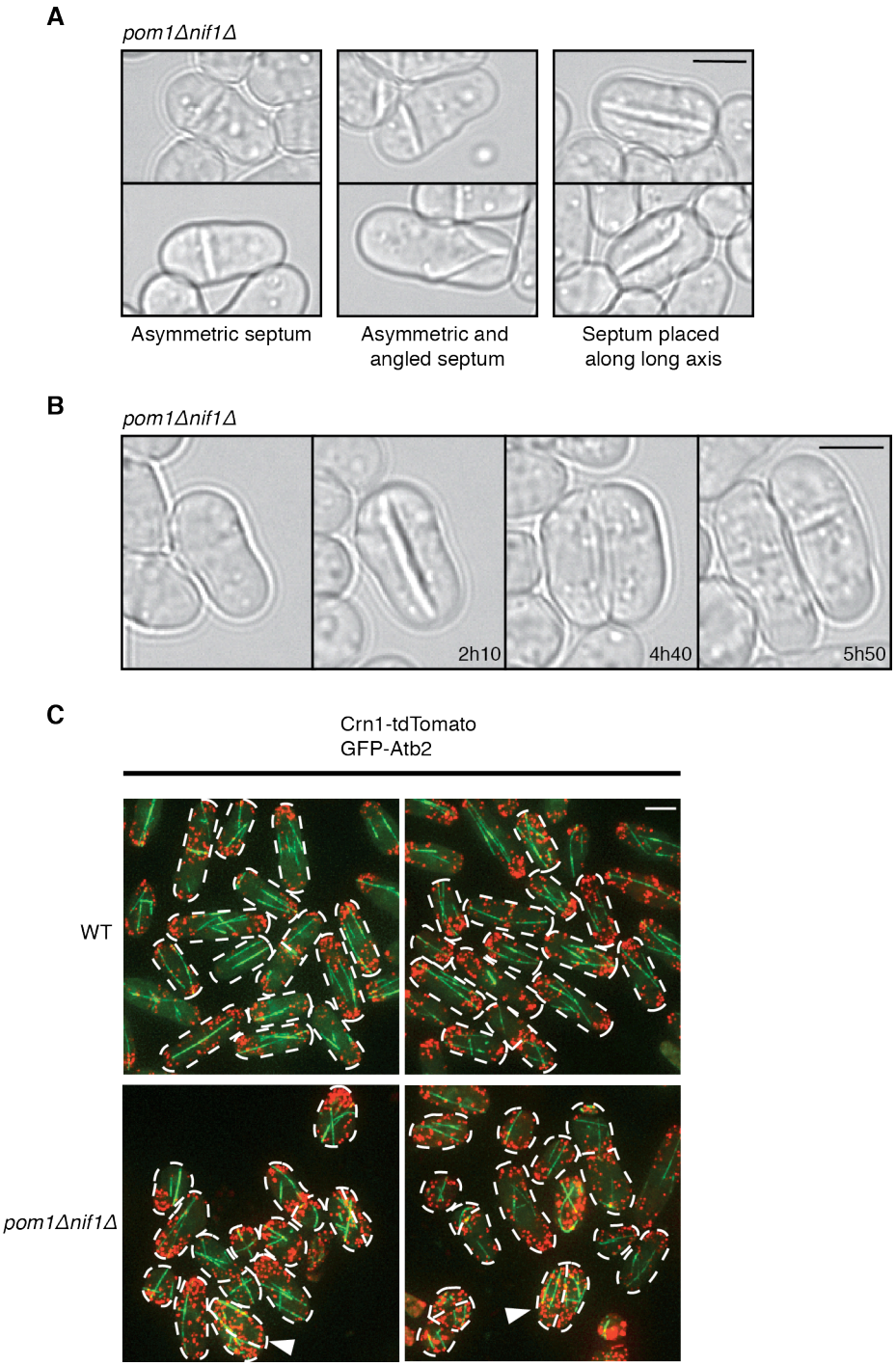

Figure 2.6|Septation defect seen in *pom1Δnif1Δ* cells

(A) Brightfield images of *pom1Δnif1Δ* cells representative of the septation defects observed in the population. Scale bar represents 4 µm. **(B)** Still images captured from a time-lapse movie of *pom1Δnif1Δ* cells growing in a CellASIC plate. Scale bar represents 4 µm. **(C)** WT and *pom1Δnif1Δ* cells tagged with Crn1-tdTomato (marks actin) and Atb2-GFP (marks microtubules). White dotted lines indicate cell perimeter (from brightfield image). Arrows indicate septation defect. Scale bar represents 4 µm. All cells grown in YE4S at 32°C.

2.2.5 Epistasis analysis suggests Nif1 acts upstream of both Cdr2 and Sty1

In order to investigate where Nif1 might be acting in the coordination of cell size with mitotic entry, genetic interaction studies were carried out with two known components of the cell cycle regulation upstream of Cdc25 and Wee1, namely Sty1 and Cdr1. Sty1 is a component of the nutrient sensing pathway and acts upstream of Polo kinase and Cdc25 (Petersen and Hagan, 2005, Petersen and Nurse, 2007). Cdr1 is a known inhibitor of Wee1 and is a component of what we refer to as the geometry sensing pathway (Breeding et al., 1998, Kanoh and Russell, 1998, Russell and Nurse, 1987a). For these genetic interaction studies, cell length at division analyses were carried out on single, double and triple mutants of our genes of interest with the known cell cycle regulators. From these data it can be determined provisionally whether a gene is acting upstream, downstream or independently of another gene, since the cell length phenotype observed will be that of the most downstream component. It is already known, and was confirmed in this study, that *pom1Δ* reduces the length at division of *sty1Δ* cells and not *cdr1Δ* cells, suggesting that Pom1 acts upstream of Cdr1 but independently of Sty1 (it is not known why *cdr1*Δ*pom1*Δ cells are in fact slightly longer than *cdr1*Δ cells) (Navarro and Nurse, 2012) (Figure 2.7). This is the basis of the current model for cell size control which states that Pom1 inhibits Cdr2, which, together with Cdr1, inhibits Wee1. It was found that *nif1Δ* reduces the length at division of both *sty1Δ* and *cdr1Δ* single mutants, suggesting that Nif1 may act independently of both pathways upstream of Wee1 and Cdc25 (Navarro and Nurse, 2012) (Figure 2.7). However, *nif1Δ* does not reduce the length of the double *sty1Δcdr1Δ* mutant, suggesting that Nif1 could be acting upstream of both the geometry sensing and nutrient sensing pathways (Figure 2.7).

There is therefore evidence to support a model whereby the gradients of both Pom1 and Nif1 are acting as cell size sensors coordinating cell size and mitotic entry through Wee1 and Cdc25. However, despite the protein localisation and the cell length data supporting this, there are some remaining questions surrounding this cell size sensing model which need addressing.

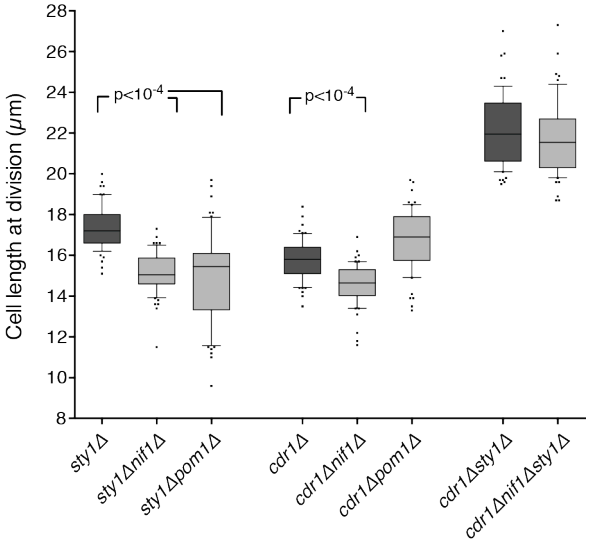

Figure 2.7|Genetic interaction studies of *nif1*Δ and *pom1*Δ with *cdr1*Δ and *sty1*Δ

Cell length at division of single, double and triple mutants indicated. Boxes delimited by first quartile, median and third quartile and whiskers mark maximum and minimum values within a 10-90% range. Values outside this range displayed as single points. P values calculated using two-tailed unpaired Student's *t*-test. 60 cells of each strain measured in exponential growth in YE4S at 32°C (cells stained with calcofluor).

2.2.6 Multinucleate cells show synchronous nuclear divisions

A quantitative analysis of the Pom1 protein, published after the initial model was proposed, shows a short decay length of the Pom1 gradient at the cell tips in relation to the length of the cell (Saunders et al., 2012). This poses a problem for the Pom1 model, which relies on this protein being detected in a length-dependent manner in the cell middle by the cortical nodes overlaying the nucleus. This issue was interrogated further using multinucleate cells.

Multinucleate cells can be induced through the inhibition of cytokinesis using the temperature-sensitive mutant *cdc11-119* (Nurse et al., 1976). At the restrictive temperature these cells show successive rounds of nuclear division without cytokinesis, giving rise to elongated cells containing multiple nuclei. Pom1-GFP and Nif1-GFP localisation was observed in these multinucleate cells and both proteins were found to localise to the cell tips (Figure 2.8A and B). The nuclei in these cells were visualised using an ER marker, SPAC1B2.03c-mCherry (SPAC1B2.03c is involved in lipid metabolism and is an integral component of the endoplasmic reticulum membrane). Cdr2 was found to be located in cortical nodes

overlaying the whole region occupied by the nuclei (Figure 2.8C). Imposing the Pom1 model for size sensing onto these cells, it could be suggested that the outer nuclei, and the Cdr2 cortical nodes surrounding them, could input information regarding the Pom1 and Nif1 gradient into the decision to enter mitosis. However the cortical nodes surrounding the inner nuclei are further from the Pom1 and Nif1 proteins and therefore are detecting a lower mitotic inhibitor protein concentration. The hypothesis is that if the current size sensing model is imposed onto these cells, the inner nuclei should enter mitosis earlier than the outer nuclei due to the lower concentration of Pom1 and Nif1. To test this, the synchrony of nuclear divisions was investigated in these *cdc11-119* cells. If the nuclei in a tetranucleate cell divide synchronously it generates a cell with eight nuclei. However, if the inner nuclei divide earlier than the outer nuclei, this will generate intermediates with six nuclei.

Cells were grown at the restrictive temperature for up to 6 hours and photographs were taken at 3, 4, 5 and 6 hours. The numbers of nuclei in each cell were quantified at each time point. Pictures of the cells with varying numbers of nuclei can be seen in Figure 2.9A. After 3 hours at the restrictive temperature, the majority of the cells were binucleate, with a small proportion of cells having undergone one fewer or one more division (Figure 2.9B). After 4 hours most cells have either 2 or 4 nuclei, the majority being tetranucleate (Figure 2.9C). A very small proportion of cells have three nuclei, but in all of these cells one of the nuclei is extended and about to undergo division (Figure 2.9A). After 5 and 6 hours at 36°C the majority of cells have 4 and 8 nuclei, respectively, with a very small proportion of cells having 3, 6 and 7 nuclei (Figure 2.9D and E).

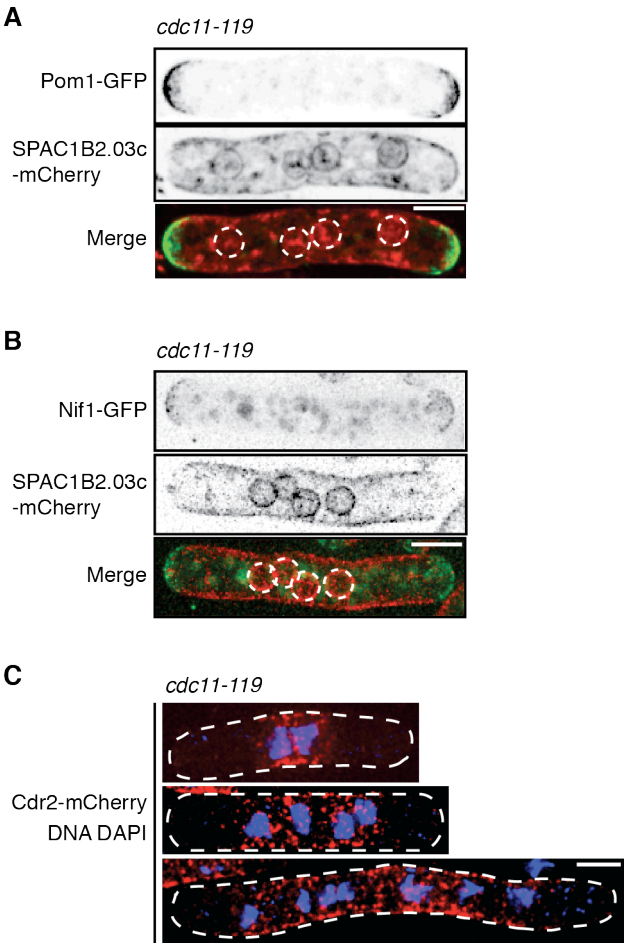

Figure 2.8|Pom1, Nif1 and Cdr2 show wild type localisation in multinucleate cells

(A) Representative *cdc11-119* cell tagged with Pom1-GFP and SPAC1B2.03c-mCherry to mark the ER and show nuclear position. Cells incubated at 36°C for 4 hours. Top two images are inverted maximum intensity projections of deconvolved images. Lower image shows overlay of upper two images with nuclei outlined by white dotted lines for clarity. Scale bar represents 4 µm. **(B)** Same as **A** but showing Nif1-GFP. **(C)** *cdc11-119* cells tagged with Cdr2-mCherry and DNA stained with DAPI. Maximum intensity projections of deconvolved images overlaid with medial focal plane image of DAPI signal. Cells outlined in white for clarity. Different incubation times at 36°C to give varying numbers of nuclei. Scale bar represents 4 µm.

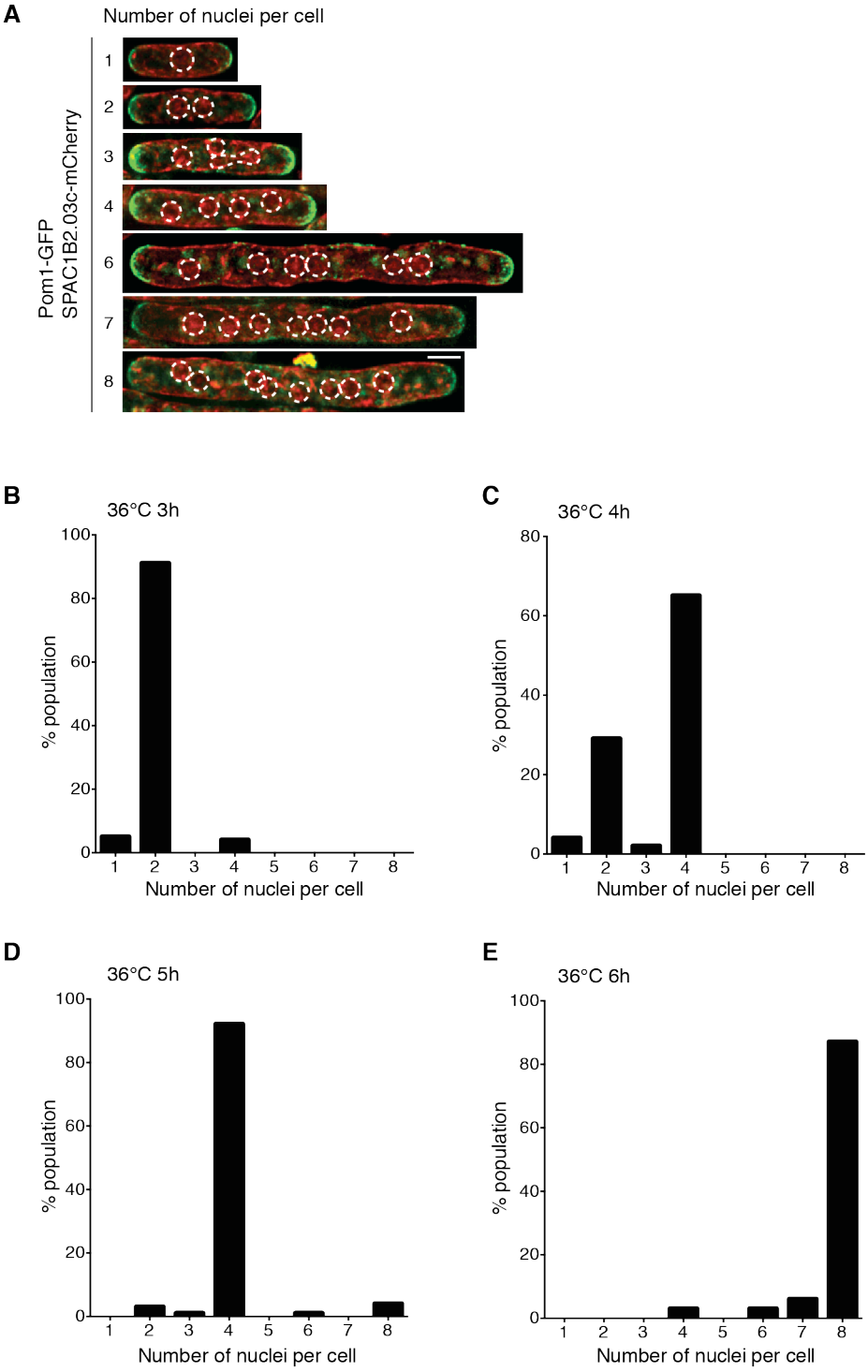

Figure 2.9|Quantification of nuclei indicates synchronous divisions

(A) *cdc11-119* cells incubated at 36°C for varying amounts of time to demonstrate differing numbers of nuclei. Cells tagged with Pom1-GFP and SPAC1B2.03c-mCherry. Nuclei outlined in white for clarity. Maximum intensity projections of deconvolved images. Scale bar represents 4 µm. **(B)-(E)** Quantification of numbers of nuclei per cell in *cdc11-119* cells incubated at 36°C for the times indicated. Total n=1000 cells across all time points.

These data indicate that nuclear division in a single cytoplasm are mostly synchronous. The inner nuclei, hypothesised to be detecting lower levels of Pom1 and Nif1, are therefore not dividing earlier than the outer nuclei. There are two possible explanations for this observation. Either this mitotic synchrony is due to synchrony in local signals received by each nucleus from the surrounding cytoplasm, thus suggesting that Pom1 and Nif1 are not the major components of this mechanism. Alternatively, the synchrony may result from a diffuse global signal which propagates throughout the cell. The outer nuclei could be receiving division timing information through the Pom1 and Nif1 protein gradients and propagating this signal to the inner nuclei so that mitosis is synchronous across the entire cell.

2.2.7 Pom1 and Nif1 are not required for cell size homeostasis: I. Population studies of size variability

The data from the experiments on the multinucleate cells is an indication that the role of Pom1 and Nif1 in a length sensing mechanism may be more complicated than once believed. The next aim was to further probe the roles of these two mitotic inhibitors in cell size sensing and the coordination of cell size with mitotic entry. Size homeostasis studies were used to investigate how well populations of cells are able to attain the critical size for division, and how rapidly cells are able to correct for any deviations in cell size. There are two main experimental techniques which allow us to study this: size variation at division in a population of cells, and observing the response of single cells to natural deviations in cell size.

The first approach involves studying the variation of sizes in a population of cells. The variation in sizes at division can tell us how accurately a population of cells is able to attain the critical size for mitotic entry, where a broad distribution suggests ‘sloppiness’ within the control system. Due to the role of Pom1 in septum positioning causing asymmetric cell divisions (Bahler and Pringle, 1998), it is first important to assess the contribution of this asymmetry to any increase in size variability observed in the *pom1*Δ populations. For this reason it is critical to look at both size at birth and size at division.

Cells were grown in microfluidic chambers and brightfield images were taken every 10 minutes for 12 hours. From these time-lapse films, cell length at birth and division plus cycle time data were collected. Wild type and *nif1*Δ cells grown in this manner have a low coefficient of variation in size at division, both 8%, implying that cells are able to accurately attain the mean cell size of the population (Figure 2.10 and Table 2.1). As can be seen from the histogram distribution of cell size, *pom1*Δ and *pom1*Δ*nif1*Δ cells have greater size dispersion at mitosis (Figure 2.10), with a coefficient of variation of 15% and 14%, respectively (Table 2.1). This is expected due to the asymmetric divisions but it is important to ascertain whether any size correction occurs during the cell cycle. If these cells are able to sense and correct for the variation produced by the preceding division, it is expected that the size at division will have reduced variability compared to that at birth. The coefficient of variation in size at birth of *pom1*Δ and *pom1*Δ*nif1*Δ cells is 22% and 21%, respectively (Table 2.1). This is greater than the variability observed at division and suggests that some of the variation that is caused by the asymmetric cell divisions is sensed and corrected for within one cycle. Wild type and *nif1*Δ single mutants have similar size distributions at birth compared with division, as would be expected for symmetrically dividing cells which have size homeostasis (Table 2.1).

	Number of cells	**Length at birth**		**Length at division**		**BL v E slope value**
		Mean (μm)	CV (%)	Mean (μm)	CV (%)	**(1 s.f.)**
WT	895	8.7	10	14.7	8	-0.8
***pom1*Δ**	840	7.8	22	12.5	15	-0.7
***nif1*Δ**	872	8.0	8	13.2	8	-0.7
***pom1*Δ*nif1*Δ**	834	7.4	21	11.5	14	-0.8

Table 2.1|Cell length and coefficient of variation for strains under investigation

Average cell length at birth and division measurements plus coefficient of variation (CV) values for the strains indicated. All cells grown in YE4S at 32 °C. Final column shows degree of relationship between birth length and length extension (linear regressions calculated from Figure 2.12).

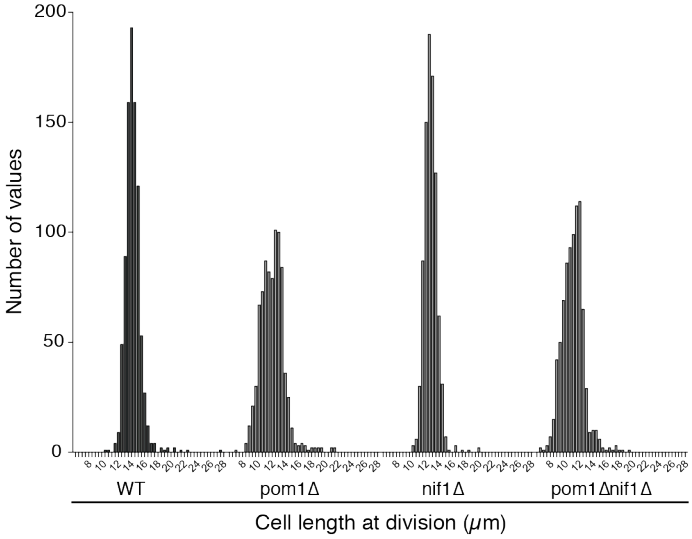

Figure 2.10|Cells deleted for *pom1* show increased variability in length at division

Histogram distribution of cell length at division of wild type, *pom1*Δ, *nif1*Δ and *pom1*Δ*nif1*Δ cells. For each strain 800-900 cells were measured in a microfluidic chamber using brightfield images. Cells grown in YE4S at 32°C. Bin size 0.5 μm.

These data indicate that in the absence of Nif1 the cell size variability at division is not greatly increased, and that in the absence of Pom1 and both Pom1 and Nif1, although there is increased cell size variability due to asymmetric septation, the cell size variability is lower at division than at birth. This suggests that cells of all three strains are reasonably homeostatic. This behaviour would not be expected if either Pom1 or Nif1 acted as a direct sensor in the mechanism for detecting cell size.

2.2.8 Pom1 and Nif1 are not required for cell size homeostasis: II. Single cell studies of natural size variation

In order to address this on a single cell level the focus turns to single cell size homeostasis studies. Using the time-lapse films, complete cell cycles of around 800 cells could be followed for each strain investigated and the natural variability in cell size at division was exploited to assess how cells lacking Pom1 and/or Nif1 are able to correct for deviations in size. Cell length at birth (BL) plotted against length extension during the cycle (E, division length minus birth length) for

the wild type population shows the documented relationship: small cells extend more during the cell cycle than long cells to maintain a constant average size at division (Fantes, 1977) (Figure 2.11A). This relationship is due to altered cycle times rather than altered growth rates since birth length plotted against cycle time (CT) shows the same relationship (Figure 2.11C). This homeostatic mechanism must use information regarding the size of the cell to extend or compress the time spent in G2 accordingly. This allows the cell to increase or reduce the growth period of any particular cell cycle to correct for any deviations that arise. A perfect homeostatic cell size mechanism would result in the BL/E ratio being close to -1, implying that all deviations in size are corrected within one cell cycle. Due to the incompressible period of G2, when the cell must carry out the required processes to prepare for mitosis, cells are not able to achieve such an effective size correction over the entire range of birth lengths that arise. In the case of very long cells, correction will be slower and will take more than once cycle due to this minimum G2 period. This is seen at the inflection points where the BL/E and BL/CT ratio changes and is observed in wild type cells recovering from treatment with hydroxyurea (HU), which imposes a cell cycle block without affecting cell growth, thus leading to elongated cells (Figure 2.11B and D).

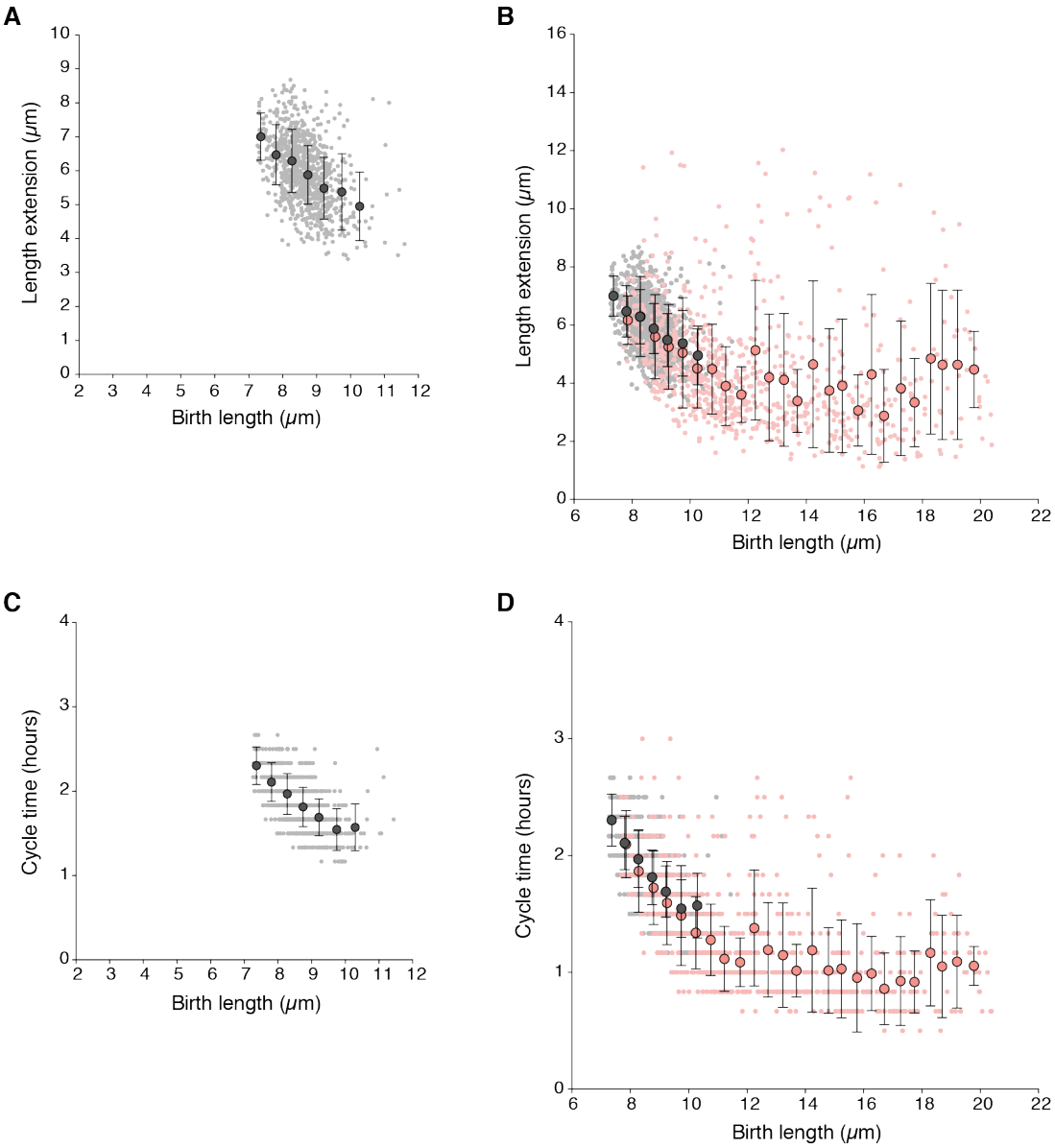

Figure 2.11|Size homeostasis analysis of wild type cells

(A) Cell length at birth plotted against length extension of wild type cells from brightfield time-lapse images of around 800 cells. Length extension calculated from birth and division length measurements. Data shown excludes the outer 2% of birth length and length extension values. Small light grey dots show individual cells. Larger dark grey points show mean values of cohorted data. Bars represent standard deviation. **(B)** Length at birth against length extension. Grey data is replicated from **(A)**. Red data is from wild type cells recovering from HU block and release. **(C)** and **(D)** Data from the same cells as **(A)** and **(B)** but birth length is plotted against cycle time. Cycle time is the time between birth and septation measurements. All cells grown in YE4S at 32°C in a microfluidic chamber.

The slope of the BL/E plot for wild type cells is -0.8 (prior to the inflection point showing the incompressible G2 period) (Figure 2.11A and B). This is similar to the previously reported slopes of Fantes (Fantes, 1977) and Sveiczer et al. (Sveiczer et al., 1996), although the technique used in this study allowed a greater number of cells to be measured. Both *pom1*Δ and *nif1*Δ cells show a wild type relationship between birth length and length extension with a slope of -0.7 (Figure 2.12B and C). This indicates that neither of these genes is essential for size homeostasis. Due to the asymmetric divisions of the *pom1*Δ cells, a greater distribution of birth lengths was analysed for this strain. This enabled the observation of the incompressible G2 period for *pom1*Δ cells with birth lengths greater than 7.5 μm (this break point was selected by eye, based on both the BL/E and BL/CT plots). For these cells the slope of -0.25 shows that size deviations will take longer than one cell cycle to be corrected (Figure 2.12B), as with the long wild type cells recovering from the HU block and release for which this inflection occurs at birth lengths greater than 10 μm (Figure 2.11B). The double *pom1*Δ*nif1*Δ also shows a wild type BL/E ratio (-0.8) and similar to the *pom1*Δ population, the double mutant also shows a loss of this rapid correction above birth lengths of 7 μm, displaying the incompressible G2 period (Figure 2.12D). Birth length was also plotted against cycle time for all four of these strains, confirming that the BL/E relationships are a result of altered cycle times rather than altered growth rates (Figure 2.13).

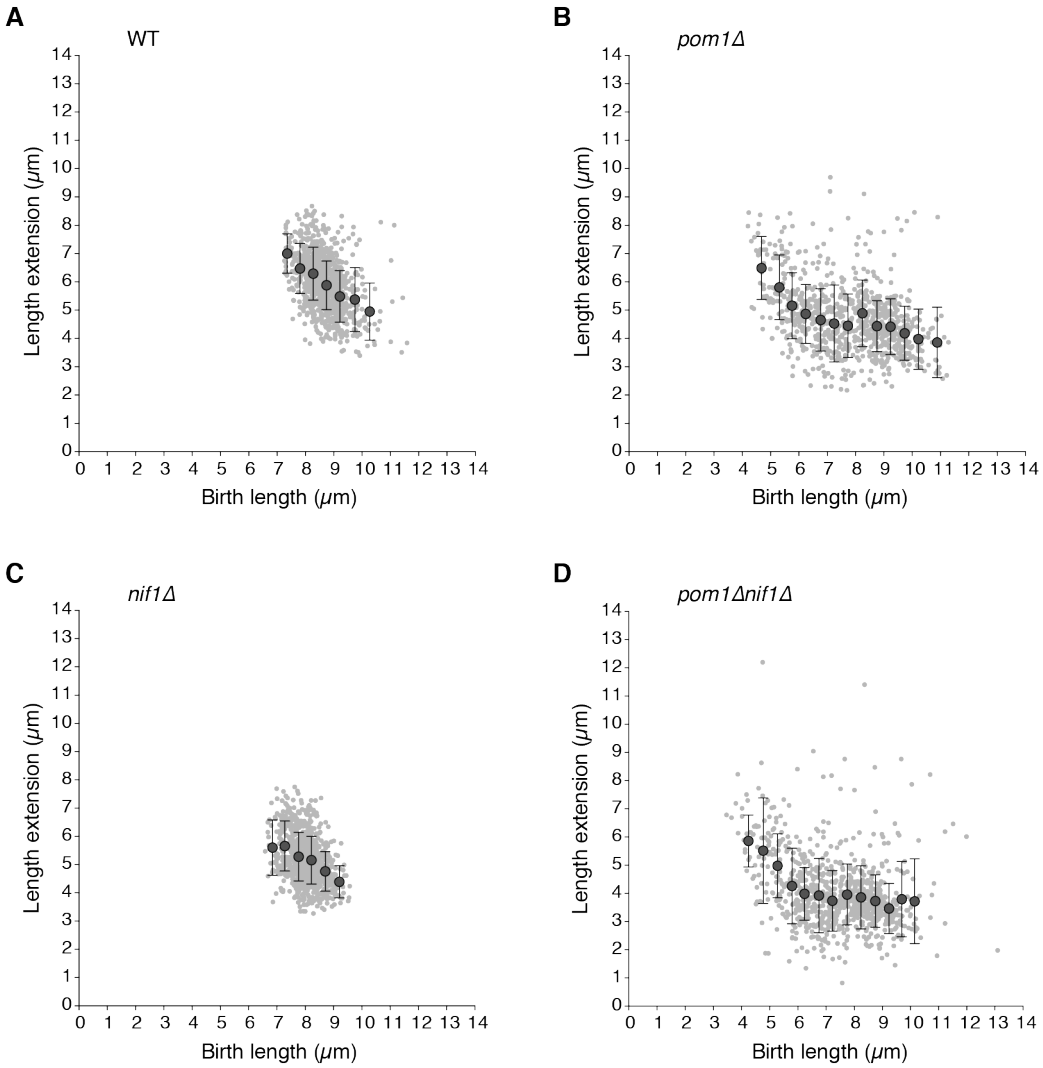

Figure 2.12|Size homeostasis analysis of *pom1*∆, *nif1*∆ and *pom1*∆*nif1*∆ cells

(A)-(D) Cell length at birth plotted against length extension for the strains indicated. Measurements taken from brightfield time-lapse images of around 800 cells for each strain. Length extension calculated from birth and division length measurements. Data shown excludes the outer 2% of birth length and length extension values. Small light grey dots show individual cells. Larger dark grey points show mean values of cohorted data. Bars represent standard deviation. All cells grown in YE4S at 32°C in a microfluidic chamber.

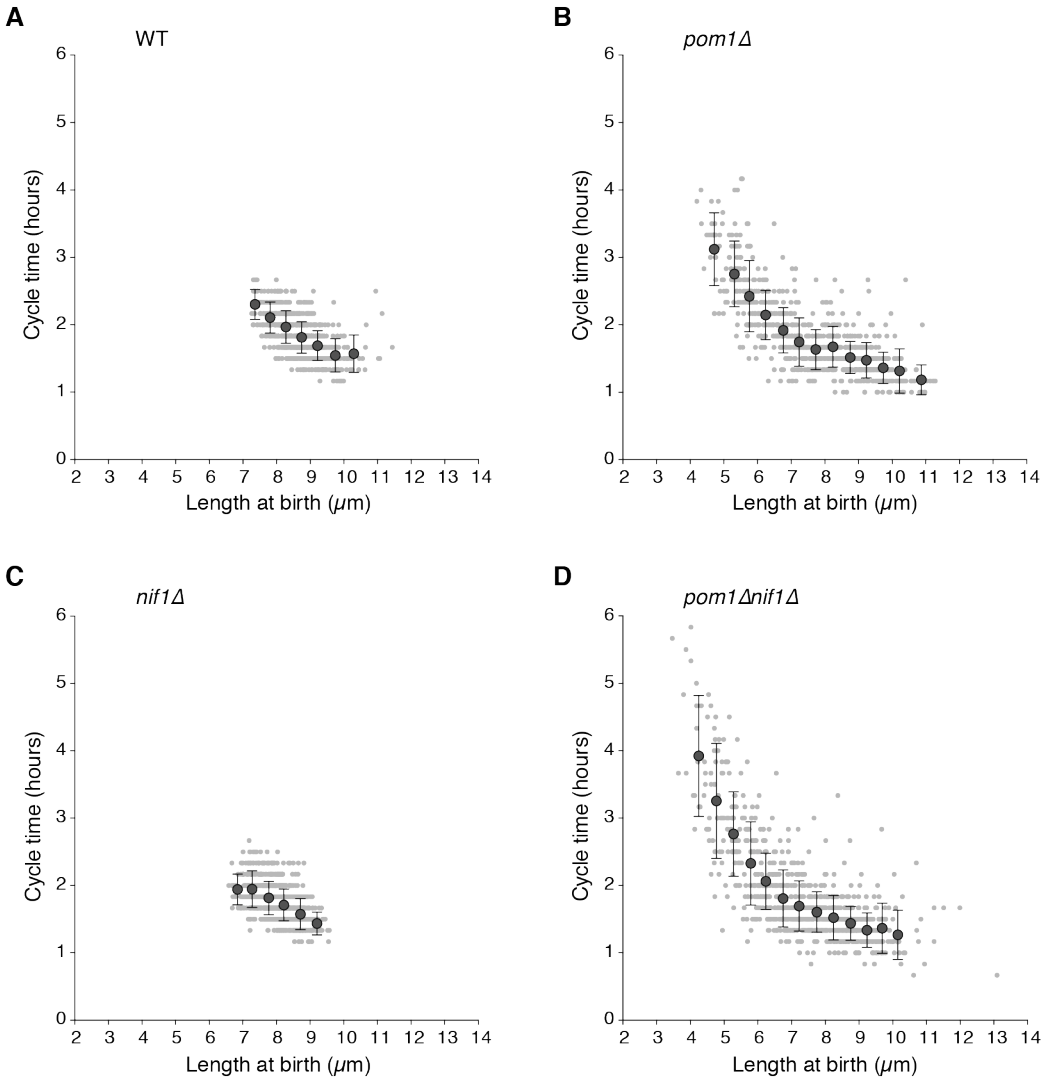

Figure 2.13|Relationship between BL and E is due to altered cycle times

(A)-(D) Cell length at birth plotted against cycle time for the strains indicated. Data is from the same cells shown in Figure 2.12. Cycle time is the time between birth and septation measurements. Data shown excludes the outer 2% of birth length and cycle time values. Small light grey dots show individual cells. Larger dark grey points show mean values of cohorted data. Bars represent standard deviation. All cells grown in YE4S at 32°C in a microfluidic chamber.

These data indicate that the strength of cell size homeostasis, that is the ability of naturally varying cell sizes in a population to return to the mean size, is not significantly changed in *pom1*Δ, *nif1*Δ and *pom1*Δ*nif1*Δ cells compared with wild type. Due to the asymmetry of division seen in both the *pom1*Δ and *pom1*Δ*nif1*Δ populations, a larger range of birth lengths is observed which uncovers the incompressible G2 period where for cells born longer than around 7 μm the

homeostatic mechanism is much less effective. For these long cells correction occurs over more than one cell cycle due to the minimum time that has to be spent growing in G2. This reduction in BL/E relationship can be visualised in WT cells recovering from hydroxyurea block and release, indicating that this effect is not only observed in the mutant populations. This suggests that neither Pom1 nor Nif1 are directly involved as essential players in the size sensing mechanism in fission yeast.

2.2.9 Cells deleted for *pom1* and *nif1* have a functioning G2 timer and sizer

The data presented above indicate that cells lacking Pom1 and/or Nif1 have good cell size homeostatic mechanisms. One possible explanation could be that these cells are controlling cell size at division through a G1/S size threshold followed by a G2 timer reflecting the minimum cell cycle time (also referred to as the incompressible G2 period).

The G2 timer was studied in these mutants using a cell cycle arrest. Addition of the DNA replication inhibitor hydroxyurea arrests cells in S phase without affecting cell growth (Mitchison and Creanor, 1971). Cells therefore undergo a cell cycle arrest but continue to grow and this results in cells elongating to lengths much longer than those seen in wild type cycling cells. After incubation with the drug for 4 hours, cells are extended to around 20-26 μm in length. For a wild type population, since the cells will have surpassed the G2/M size threshold, upon release from the arrest cells will undergo rapid cycles of synchronous divisions controlled only by the G2 timer (Mitchison and Creanor, 1971). The cell cycle time will therefore indicate the length of this G2 timer. The cells divide at progressively smaller sizes until they reach the G2/M size threshold, when this sizer will come back into play. A population of wild type cells returns to the average size within 2 cell cycles (Figure 2.14A). It would be expected that cells with a perturbed G2 timer would recover to their normal size at a faster or slower rate compared with wild type cells, or perhaps not return at all.

To investigate this in *pom1*Δ, *nif1*Δ and *pom1*Δ*nif1*Δ cells, cell size was measured at successive cell divisions after release from a 4-hour hydroxyurea arrest to observe how rapidly cells recover to a normal size at division. All three populations show the same response as wild type cells, returning to a normal size

at the same rate and within two cell cycles after washout of hydroxyurea (Figures 2.14B-D). This indicates that these genes do not have a significant role in determining the length of the G2 timer.

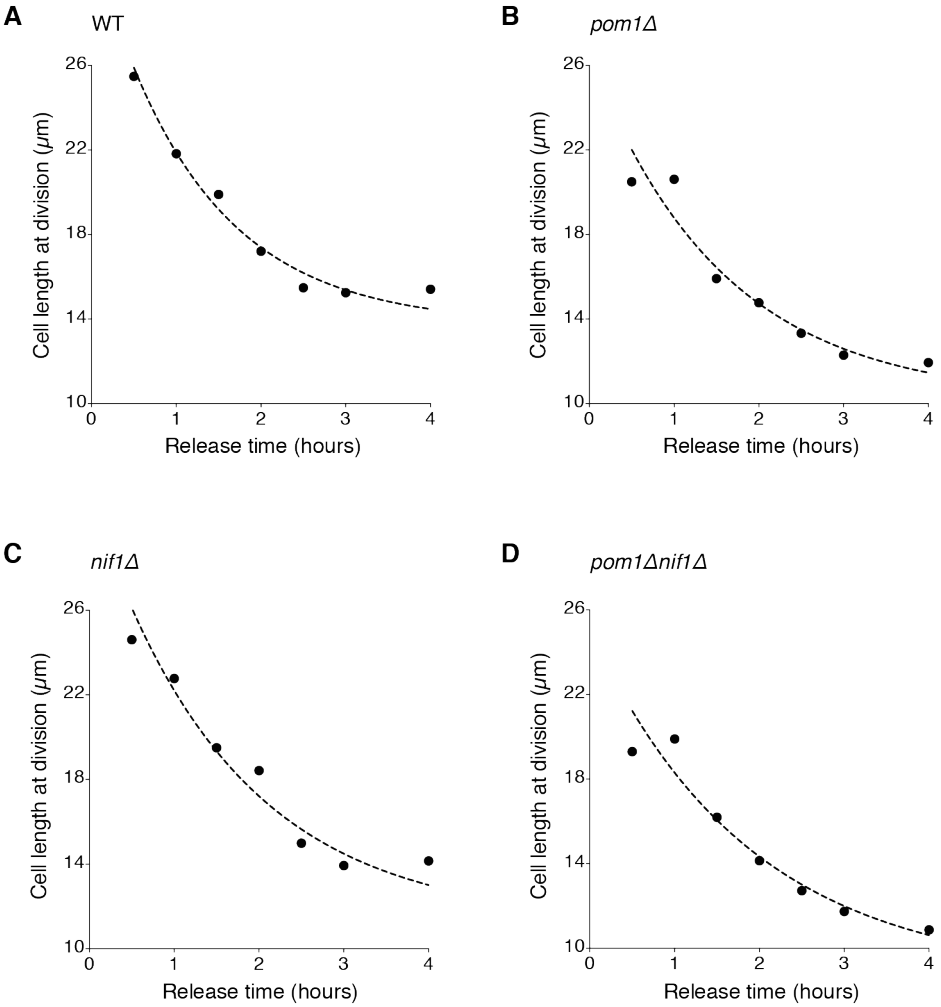

Figure 2.14|Hydroxyurea arrest and release

(A)-(D) Cell length recovery of the indicated strains after elongation with the S phase inhibitor hydroxyurea. Cells grown in EMM4S at 32°C. 11mM HU added for 4 hours then washed out at time zero. Average cell length at division measured for each time point and exponential curves fitted to the data (black dotted line).

The next aim was to check whether these mutant cells are maintaining cell size homeostasis through this timer alone plus the G1/S size threshold. If this were the case then the sizing mechanism at G2/M would be absent. This can be tested by exploiting the ability of the G2/M size threshold to be modulated by changes in the nutrient conditions that the cells are growing in. In wild type cells, shifting the

cells from nitrogen-rich to nitrogen-poor media lowers the G2/M size threshold and therefore accelerates cells through the cell cycle resulting in a peak in the septation index (Fantes and Nurse, 1977). This response has been previously demonstrated to be lacking in *wee1-50* cells (Fantes and Nurse, 1978). Wild type, *wee1-50*, *pom1*Δ, *nif1*Δ and *pom1*Δ*nif1*Δ cells were grown at 25°C in minimal media containing glutamate as a nitrogen source. Cells were then shifted to the restrictive temperature for two cell cycles to inactivate *wee1-50* and then transferred to minimal media containing proline. In the wild type population a peak in the number of septated cells is observed between 30 and 60 minutes of the nitrogen shift-down, confirming the presence of a nutrient-sensitive size threshold at mitosis (Figure 2.15A). In the *wee1-50* population no such peak is observed, since these cells have no G2/M size threshold, rather a G1/S threshold followed by a G2 timer (Figure 2.15A and B). The *pom1*Δ, *nif1*Δ and *pom1*Δ*nif1*Δ cells all show a peak in septation index similar to that seen in the wild type population (Figures 2.15A-C). This confirms the presence of a size threshold at the G2/M transition in these single and double mutant populations that is able to respond to changes in nutrient conditions. These data argue against *pom1*Δ, *nif1*Δ and *pom1*Δ*nif1*Δ cells lacking a G2/M size control.

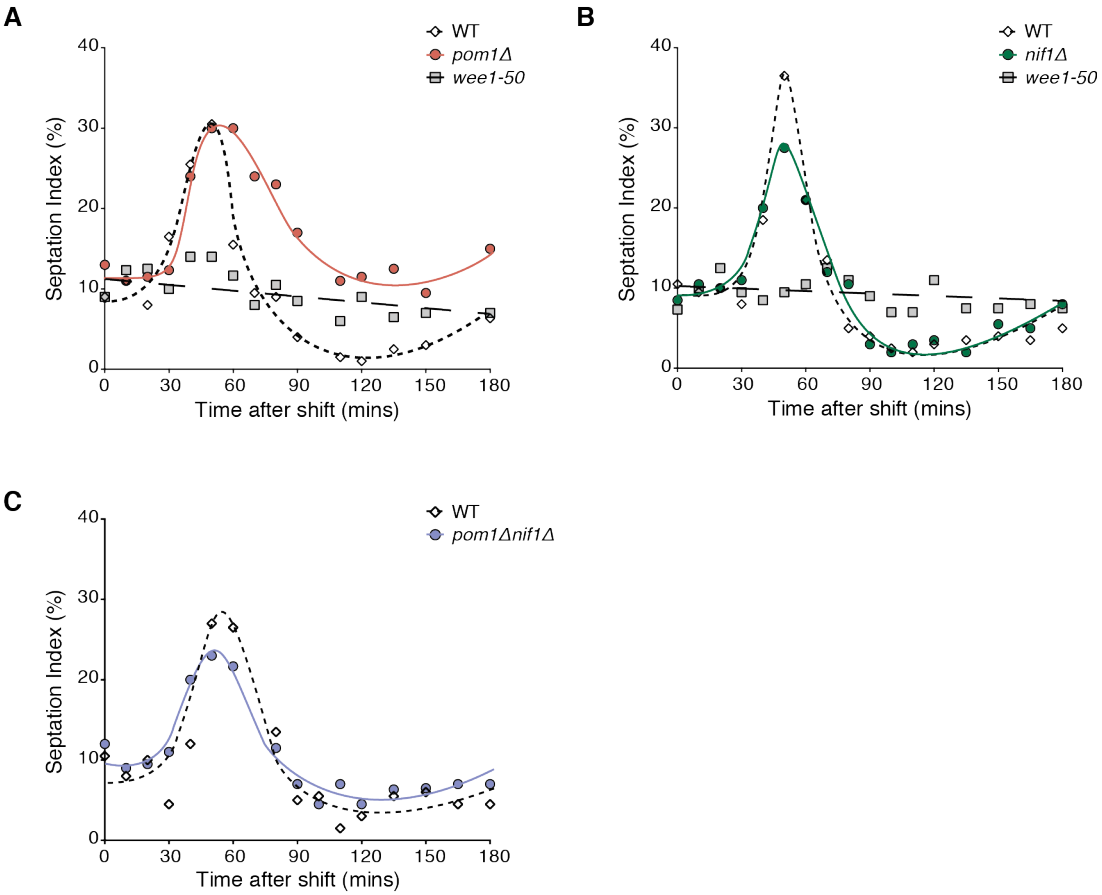

Figure 2.15|Nutrient shift-down reveals G2/M size threshold

(A) Septation index of a *pom1*Δ population compared with wild type and *wee1-50* cells after nutritional shift-down from glutamate to proline as a nitrogen source. **(B)** Experiment as in **A** with *nif1*Δ cells compared with wild type and *wee1-50* controls. For **A** and **B** cells grown at 25°C in EMM-N + 20 mM glutamic acid and shifted to 36°C for 2 cycles before being washed 3 times and resuspended at time zero in EMM-N + 10 mM proline. **(C)** Septation index of a *pom1*Δ*nif1*Δ population compared with wild type cells after nutritional shift-down from glutamate to proline as a nitrogen source. Cells grown at 32°C in EMM-N + 20 mM glutamic acid before being washed 3 times and resuspended at time zero in EMM-N + 10 mM proline. All graphs show number of septated cells represented as a percentage of the whole population. Lines are manual input showing general trend of the data.

2.3 Discussion

Pom1 and Nif1 have previously been reported to act as negative regulators of the G2/M transition and to have roles in setting a threshold size for entry into mitosis. The aim of this work was to test whether these proteins act as direct sensors of cell size.

2.3.1 Protein gradients of Pom1 and Nif1 act independently to set a threshold size for entry into mitosis in wild type cells

A possible model supported by the tip localisation of Pom1 and Nif1 is that in late G2 cells, when they are present at both ends of the cell, these proteins are acting together as gradient sensors of cell size and inputting information into the cell cycle controls through Cdr2, and therefore Wee1, present in a band of medial cortical nodes. A prediction of this model is that deletion of *pom1* or *nif1* will result in premature inactivation of Wee1 by Cdr1/Cdr2 and therefore entry into mitosis at a smaller cell size. The data here supports this, since *pom1*Δ and *nif1*Δ cells divide around 10% smaller than wild type cells. These genes have an additive effect on cell length at division, since the double *pom1*Δ*nif1*Δ mutant divides at a shorter length than either single mutant. This suggests that these genes are acting in independent pathways to feed size information into the cell cycle controls. Epistasis analysis using the known cell cycle regulators Cdr1 and Sty1, acting upstream of Wee1 and Cdc25 respectively, provides further data supporting the independent roles of Pom1 and Nif1. Cell length studies of *pom1* and *nif1* deletions together with *cdr1*Δ and *sty1*Δ indicate that Pom1 acts through Cdr1 whereas Nif1 is able to act through both Cdr1 and Sty1. This supports previously reported data (Navarro and Nurse, 2012).

Since Pom1 inhibits the localisation in addition to the activity of Cdr2, in *pom1*Δ cells the cortical nodes, which are organised by Cdr2, spread from a tight medial band overlaying the nucleus to the entire non-growing half of the cell (Martin and Berthelot-Grosjean, 2009, Moseley et al., 2009). It remains unknown what is preventing Cdr2 from spreading to the growing half of the cell; an obvious candidate is Nif1 yet Cdr2 localisation is unaffected in *nif1*Δ cells. Despite this, the double *pom1*Δ*nif1*Δ mutant has a more severe septation phenotype compared with the *pom1*Δ single mutant. The phenotype is more similar to that of *mid1*Δ cells,

which often place the septum at an angle to the cell periphery and occasionally form septa along the long axis of the cell (Chang et al., 1996, Sohrmann et al., 1996). This result cannot be explained with the data presented here.

Mid1 is a component of the medial cortical node domain organised by Cdr2 (Moseley et al., 2009). Due to the effect on Cdr2 localisation by Pom1 described above, cells deleted for *pom1* show an asymmetric septation phenotype caused by the mislocalisation of Mid1. This asymmetry results in an increase in the coefficient of variation in size at division. The displacement of the septum in both *pom1*Δ and *pom1*Δ*nif1*Δ is similar, around 2 μm from the centre of the cell, and in both mutants is independent of cell length. Mid1 is important for the medial positioning of contractile ring assembly (Sohrmann et al., 1996). When Mid1 is localised throughout the entire non-growing half of *pom1*Δ cells, one might expect a random positioning of the contractile ring anywhere in this region. The length-independent offset from the cell middle of the septum however suggests the possibility of sliding of the actomyosin ring from the cell middle. In these *pom1*Δ cells nuclear positioning is unaffected. Since Mid1 medial localisation is set up by nuclear shuffling (and then reinforced by medial Cdr2) (Moseley et al., 2009, Padte et al., 2006, Sohrmann et al., 1996), the central positioning of the nucleus in *pom1*Δ cells supports a model whereby the contractile ring is initially established in the middle of the cell and then slides towards the non-growing end due to mislocalised Mid1. Further testing of this model is required and could involve time-lapse studies of the components of the contractile ring and positioning factors.

It has also been shown here that the cortical node domain containing Cdr2 widens with increasing cell length. Since this work was carried out this finding has been published by other groups and modified models for Pom1 size sensing have since been proposed (Bhatia et al., 2014, Pan et al., 2014). This finding was therefore not pursued further with additional studies, and the alternative models proposed in the literature will be discussed more in the General Discussion.

2.3.2 Multinucleate cells reveal the presence of a global cytoplasmic signal coordinating mitotic entry

In wild type cycling cells there is sufficient evidence to suggest that both Pom1 and Nif1 could be acting through their gradient distribution to provide a read-out of cell length to the cortical nodes overlaying the nucleus in the middle of the cell. This model was further tested using multinucleate cells. The temperature-sensitive *cdc11-119* mutant when incubated at the restrictive temperature undergoes multiple rounds of nuclear division without intervening cytokinesis (Nurse et al., 1976). This results in single cells containing multiple nuclei.

In these multinucleate cells both Pom1 and Nif1 show wild type localisation at the cell tips. Cdr2 is seen in nodes overlaying all of the nuclei, which can be spread throughout the entire length of the cell. The gradient model would suggest that the outermost nodes are sensing a higher Pom1 and Nif1 concentration compared with the nodes overlaying the innermost nuclei. The inner nuclei should therefore enter mitosis earlier than the outer nuclei, if the Pom1 and Nif1 gradients are indeed dose-dependent inhibitors of mitotic entry and acting as the major read-out of cell length.

The data presented in this chapter, showing that nuclear divisions in a common cytoplasm are mostly synchronous, could be concluded to mean one of two things. One possibility is that nuclei receive individual signals to indicate the timing of the G2/M transition. This would lead to the suggestion that the Pom1 and Nif1 gradients are not the only major players in this decision making process, since nuclei behave in a synchronous fashion despite being in different positions within the protein gradient. An alternative possibility is that the Pom1 and Nif1 gradients are important to signal timing to the outer nuclei and a global signal then acts to coordinate the decision to divide among all nuclei within the common cytoplasm. Previous work suggests that this might be the case and that Wee1 is important for this synchrony (Kiang, 2010).

2.3.3 Size homeostasis analyses suggest that Pom1 and Nif1 do not have major roles in the sensing and correction of cell size at division

The early data discussed above indicate that both Pom1 and Nif1 act as negative regulators of the G2/M transition and have roles in setting a threshold size for entry into mitosis. However, by studying multinucleate cells it appears that these two proteins are not the only major players in coordinating cell length with mitotic entry. The aim was to further test whether Pom1 and Nif1 are acting as direct sensors of cell size. Two approaches were used. The first, population studies of size variability, suggests that cells deleted for either *pom1* or *nif1* are still able to restrict size at division to either fall within the wild type range (as is the case for *nif1*Δ) or to be reduced compared to the variation in size at birth (*pom1*Δ). The second approach, single cell size homeostasis studies, supports the finding that Pom1 and Nif1 are not essential in correcting for deviations in cell size.

In a population of exponentially growing cells, cell size deviations from the mean can arise at random, perhaps caused by an asymmetric division or an activated checkpoint in the previous cycle. The single cell measurements presented here demonstrate that deviations in birth length are corrected for through altered time spent, and thus length extended, in the subsequent cycle. Graphs of birth length plotted against length extension show a relationship close to -1 for both wild type and the mutant strains, implying that this correction occurs within almost one cell cycle (in other words for every 1 μm deviation in birth length the cell corrects by 1 μm in length extension). Where the asymmetric divisions of the *pom1*Δ populations lead to a wider range of birth lengths, the incompressible G2 period becomes clear. For cells greater than around 7-8 μm, corrections take longer than one cycle due to a minimum time requirement of this gap phase. This minimum time appears to be approximately 1 hour and the corresponding length extension is between 3-4 μm. This relationship is also seen in a wild type population recovering from a cell cycle arrest, demonstrating that this lack of homeostasis in longer cells is not unique to *pom1*Δ cells.

Implicit in these findings is that Pom1 and Nif1 are not essential for sensing deviations in cell size. Size corrections, and thus maintenance of size homeostasis, require cells to sense how much bigger or smaller they are from the desired size. Since both *pom1*Δ and *nif1*Δ populations are able to correct for deviations to the

same extent as wild type cells, this suggests that these cells are not defective in this sensing mechanism.

The work described in this chapter has revealed a new method for investigating the cell size sensing mechanism, which has revealed additional information regarding suggested size sensing genes. In the next chapter we use similar size homeostasis studies to probe other components thought to be important for the timing of the G2/M transition, with particular focus on *wee1*.

Chapter 3. An investigation of cell size homeostasis at the G1/S and G2/M transition

3.1 Introduction

The size homeostasis analyses in the previous chapter have suggested that the protein kinase Pom1, which has been shown to have a role in determining the size at which cells undergo the G2/M transition, is not required for a size sensing and correction mechanism. Cells deleted for *pom1* enter mitosis at a small cell size, however these cells are as effective as wild type cells in correcting natural size deviations that occur within the population.

The focus of this chapter is the use of similar size homeostasis studies to uncover additional information about the current size sensing model, both at G2/M and G1/S. Size thresholds have been instrumental in the discovery of key cell cycle regulators such as Wee1 and Cdc2 (Nurse, 1975, Nurse et al., 1976). The aim of this work is to see if more can be learnt about these mechanisms by looking at how size variability is corrected within a population.

The studies will focus on Wee1, since it has been previously shown that *wee1*Δ cells lack the G2/M size threshold and therefore the cell cycle is run on a G1/S size threshold followed by a timer in G2 (Fantes and Nurse, 1978, Nurse, 1975, Nurse and Thuriaux, 1977). Cells deleted for *wee1* are therefore a useful tool to study the G1/S size threshold, which in wild type cycling cells is usually cryptic since the G2/M size threshold means cells enter G1 at a size which surpasses the threshold for entry into S phase (Nurse and Thuriaux, 1977). Mik1 is a protein kinase which acts alongside Wee1 in phosphorylating Cdc2 (Lundgren et al., 1991).

The work described here shows that size homeostasis may be present at the G1/S transition, but that the timer period in G2 could complicate the analysis, since small cells have a slower growth rate compared to larger cells. The conclusions derived from this work are based on an assumption that the G2 timer period is a fixed timer that does not vary according to factors such as cell size or nutrients. It must be noted that this timer has not been extensively investigated however and therefore any further investigations would require additional study of this period of the cell cycle.

In addition, studies using the non-phosphorylatable Cdc13-L-Cdc2 fusion protein show that this strain may operate within a new system of maintaining size homeostasis independently of Wee1 and Cdc2-Tyr15 phosphorylation.

This work has shown that size variability is a useful tool for studying cell size control throughout the cell cycle and size homeostasis studies, alongside the study of cell size mutants, can provide additional information regarding a cell size sensing mechanism.

3.2 Results

3.2.1 Growth rate is not inherited

As part of an investigation into the growth conditions within the CellASIC microfluidic plates, a careful analysis of cell morphology and growth patterns was carried out for wild type cells growing in this microfluidic device. For 630 cells (42 lineages spanning 3 generations), a growth rate value, G, was calculated based on the assumption that growth rate per cell is proportional to cell size: $G = E/(BL \cdot CT)$, where E is length at septation minus birth length (BL) and CT is cycle time. For the population of cells analysed, G varies around a mean of 0.4 t^{-1}, with a coefficient of variation of 12% (cells growing in complex media at 32°C). Figure 3.1A shows images of wild type cells from a typical time-lapse film used for this analysis.

An analysis of the growth rate of single cells within lineages enabled a study into whether there is any heritability in growth rate. Across the whole population the difference in the growth rate value between two sister cells (0.04 t^{-1}) is equal to the difference in growth rate between a single sister cell and the average of the population (0.04 t^{-1}). Figure 3.1B shows the growth rate of individual mother cells plotted against the growth rate of the corresponding daughter cell. This shows no relationship: the slope of the regression line in red is -0.01 and r^2=0.0001. Plotting the growth rate of single mother cells against the average growth rate of the 14 progeny over 3 generations also shows no relationship: slope 0.04, r^2=0.01 (Figure 3.1C). These data indicate that there is no significant heritability in growth rate within wild type cell lineages.

In addition to heritability in growth rate, a limited analysis was carried out to investigate whether the growth conditions in the microfluidic chambers may

adversely affect the cells. First an analysis was carried out into the effect of the position of a cell within a colony that forms within the chamber. Cells completely surrounded on all sides by other cells have a G value only 2.5% higher than those cells on the edge of the colony (Figure 3.1D). Second, an analysis over 6-8 hours over the three generations shows that the growth rate value increases on average 3.7% with each successive generation (Figure 3.1E). We conclude that cells are not significantly affected by growth in the microfluidic chambers within the first three generations.

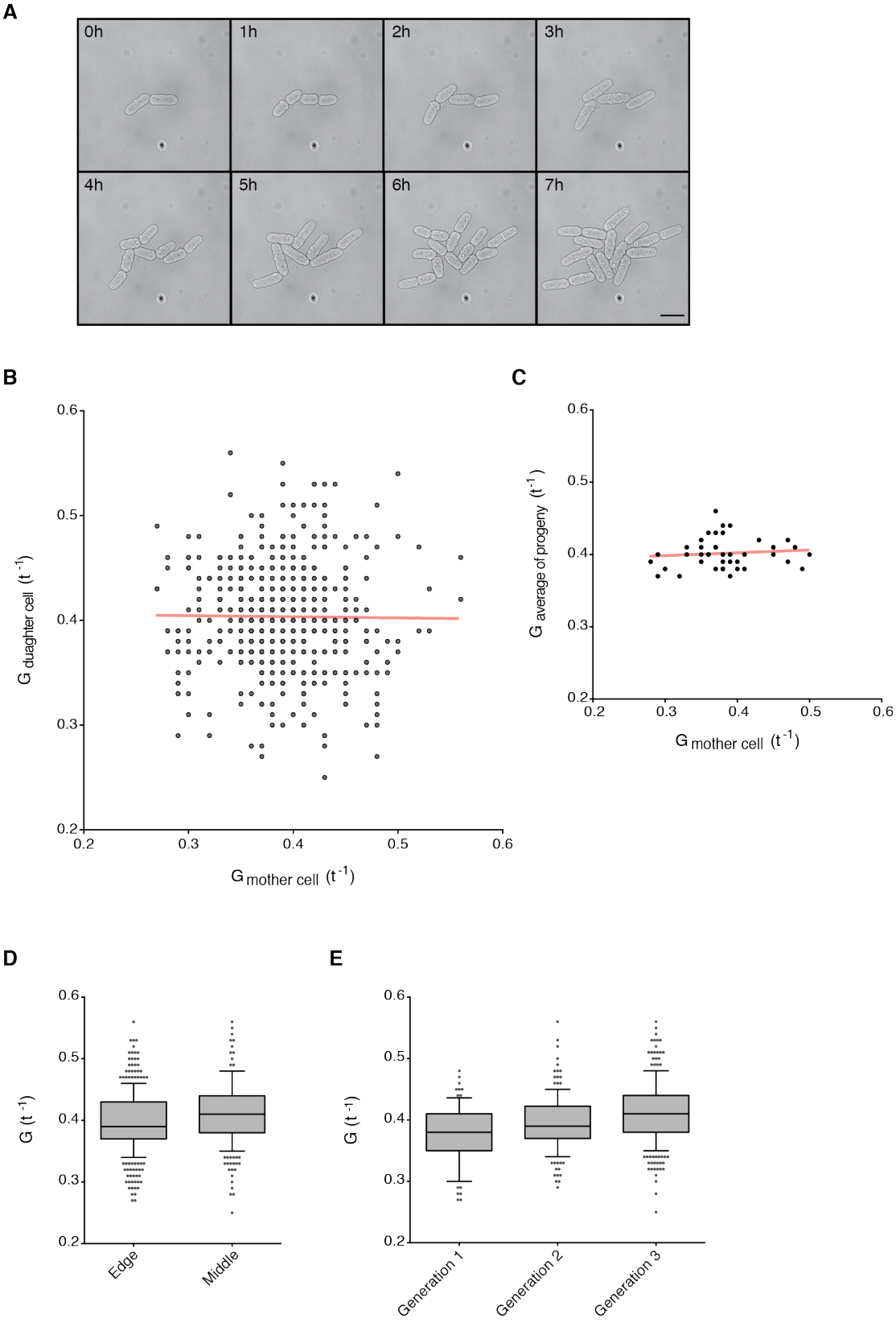

Figure 3.1 |Growth rate analysis of cells in the microfluidic chamber

Figure 3.1|Growth rate analysis of cells in the microfluidic chamber

All cells for **A-E** growing in a microfluidic chamber in YE4S at 32°C, brightfield images taken every 10 minutes. G=E/(BL·CT), where E is length at division minus length at birth. **(A)** Representative brightfield images of wild type cells taken from a time-lapse film at the times indicated. Scale bar represents 10 μm. **(B)** Growth rate values of mother cells plotted against respective daughter cells. Mother cells, n=290. Daughter cells, n=580. Regression slope -0.01, r^2=0.0001. **(C)** Growth rate values of mother cells plotted against the average values calculated for the 14 progeny (same cells as in **B**). Regression slope 0.04, r^2=0.01. **(D)** Growth rates of all cells from **B** annotated as either at the edge of a colony or in the middle (surrounded on all sides by other cells). Boxes delimited by first quartile, median and third quartile and whiskers mark maximum and minimum values within a 10-90% range. Values outside this range displayed as single points. **(E)** Same as **D** with cells annotated according to generation. Boxes delimited by first quartile, median and third quartile and whiskers mark maximum and minimum values within a 10-90% range. Values outside this range displayed as single points.

3.2.2 Wee1 is required for a wild type birth length/length extension relationship

As described in Chapter 2, size homeostasis can be investigated at a single cell level by measuring the birth length, length extension, and cycle time using time-lapse microscopy of single cells growing in a microfluidic chamber. In section 2.2.8, such analysis on *pom1*Δ cells reveals that although Pom1 has a role in setting the threshold size at the G2/M transition, this kinase is not required for a population of cells to maintain size homeostasis. In 1996 a similar study was carried out on a *wee1*Δ population, which found that these cells do have size homeostasis (Sveiczer et al., 1996). This study of *wee1* was repeated in order to further investigate the role of the G1/S transition on cell size homeostasis.

Wee1 is a major component of the G2/M transition and without this protein kinase cells are born sufficiently small to activate a second size checkpoint at the G1/S transition. These cells have an elongated G1 phase in order to attain the required size for S phase, and G2 is shortened due to the absence of the G2/M checkpoint. When the 1996 study (Sveiczer et al., 1996) was repeated, the results of this work could not be replicated. A graph of birth length against extension (BL/E) of 827 *wee-50* cells at 36.5°C shows only a limited relationship, with a regression slope of -0.3 (95% confidence interval (CI) -0.41 to -0.13) (Figure 3.2A and C, Table 3.1). This slope significantly deviates from zero but is significantly different to a wild type population growing at the same temperature, which has a slope of -0.7 (95% CI -0.80 to -0.60) (Figure 3.2A and B, Table 3.1).

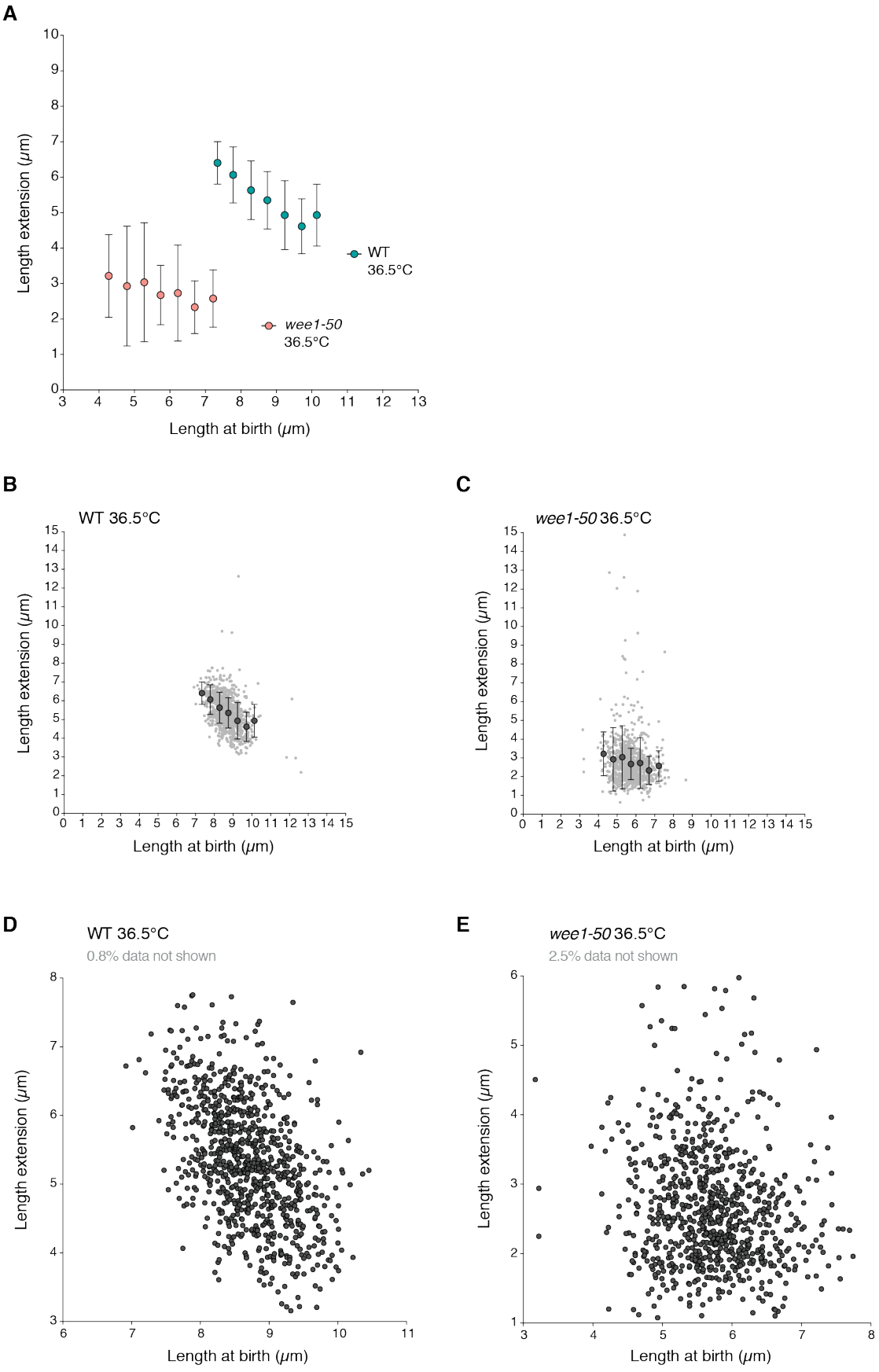

Figure 3.2|Cells deleted for *wee1* show a weak BL/E relationship

Figure 3.2|Cells deleted for *wee1* show a weak BL/E relationship

(A) Cell length at birth plotted against length extension of wild type and *wee1-50* cells from brightfield time-lapse images. Length extension calculated from birth and division length measurements. Points show mean values of cohorted data, bars represent standard deviation. **(B)** and **(C)** Individual graphs of WT and *wee1-50* cells, respectively. Small light grey dots show individual cells. Larger dark grey points show mean values of cohorted data as shown in **A**. **(D)** and **(E)** Raw data from plots **B** and **C**, respectively, with reduced axis scales for clarity. Percentage of data excluded shown. All cells grown in YE4S at 36.5°C in a microfluidic chamber.

Genotype	Temperature (°C)	Number of cells	Cell length at division		BL/E Slope	BL/CT Slope
			Mean (µm)	CV (%)		
Wild type	**32.0**	895	14.7	8	-0.7	-0.3
Wild type	**36.5**	857	14.1	6	-0.7	-0.2
wee1-50	**36.5**	827	8.5	17	-0.3	-0.3
***wee1*Δ**	**32.0**	623	8.5	15	-0.3	-0.5
***mik1*Δ**	**36.5**	726	14.4	8	-0.7	-0.2
Cdc13-L-Cdc2	**32.0**	769	16.1	7	-0.5	-0.2
Cdc13-L-Cdc2AF	**32.0**	829	13.1	15	-0.9	-0.4
***wee1*Δ Cdc13-L-Cdc2**	**32.0**	804	11.5	16	-0.4	-0.3
***wee1*Δ Cdc13-L-Cdc2AF**	**32.0**	779	12.9	18	-0.5	-0.3

Table 3.1|BL/E and BL/CT relationships for all strains measured

Relationship between birth length and length extension and cycle time for all strains investigated in this chapter. BL = birth length (µm), E = length extension in the subsequent cycle (µm), CT = cycle time of the subsequent cycle (hours). Mean cell length at division (1d.p.) and coefficient of variation (to the nearest percent) also included.

To ensure that temperature is not playing a role in this observation, the same experiment was repeated at 32°C with *wee1*Δ. Figure 3.3A and B and Table 3.1 show that there is very little difference between a population of *wee1-50* cells at 36.5°C and *wee1*Δ cells at 32°C when birth length is plotted against length extension. As well as suggesting that temperature is having no significant effect on the behaviour of the cells, this also indicates that there is no effect from the temperature sensitive allele and that the *wee1-50* strain is likely to have no or only limited Wee1 kinase activity at the restrictive temperature.

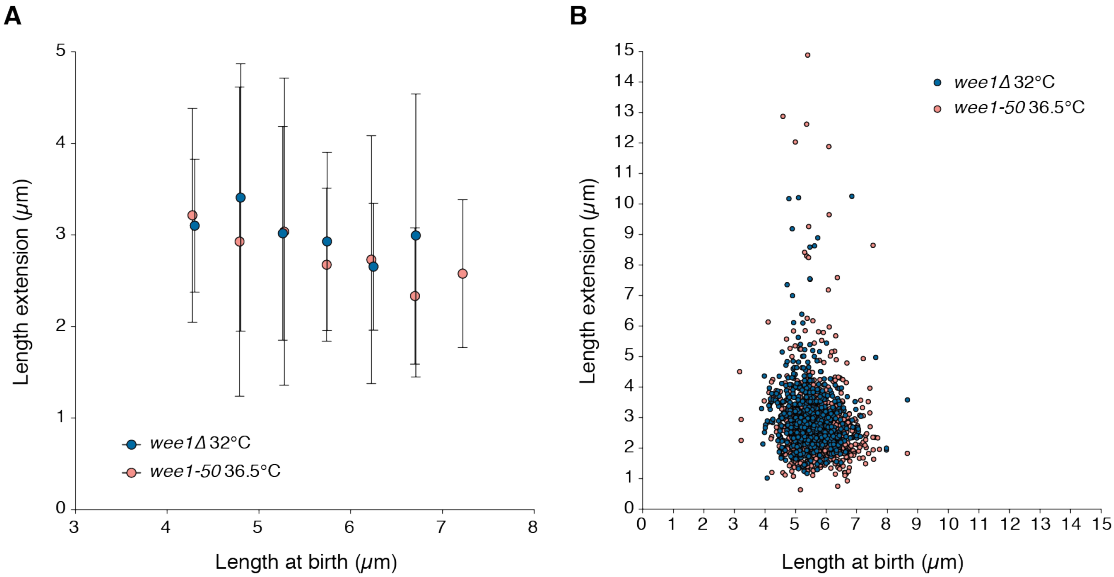

Figure 3.3|*wee1-50* and *wee1*Δ cells show the same BL/E relationship

(A) Cell length at birth plotted against length extension of *wee1-50* and *wee1*Δ cells from brightfield time-lapse images. Length extension calculated from birth and division length measurements. Points show mean values of cohorted data, bars represent standard deviation. **(B)** Raw data of measurements in **A**. Each dot corresponds to a single cell. Cells grown in YE4S at 32°C or 36.5°C, as indicated, in a microfluidic chamber.

These data suggest that in cells lacking Wee1 activity, the G1/S size threshold followed by a G2 timer has only limited size homeostasis. The large distribution of the data on the BL/E plot and the reduced correlation indicate that the majority of cells will extend by approximately 3 μm, irrespective of their birth length. This suggests that a G2/M size checkpoint, and thus Wee1, is required for cells to correct efficiently for deviations in cell size that arise within the population.

3.2.3 The birth length/length extension relationship of *wee1-50* cells is not reflected in cycle time

In order to investigate this further, a graph of birth length against cycle time was plotted for *wee1-50* cells. It has been previously reported that changes in length extension to correct for birth length deviations are through altered cycle times rather than altered growth rates (Fantes, 1977), and this can be seen in the wild type population; a graph of birth length against cycle time (BL/CT) shows a negative relationship, slope -0.2, r^2=0.4 (Figure 3.4A and C, Table 3.1). If the G1/S

size threshold cannot maintain size homeostasis, a prediction from the *wee1-50* BL/E data is therefore that cycle time is no longer inversely related to birth length. In other words, small cells cannot extend the time spent in the following cycle in order to extend more in length.

However this is not the case, and a graph of birth length against cycle time for *wee1-50* cells at 36.5°C shows a relationship with a similar slope to wild type cells (Figure 3.4A and D). The cycle time data in the *wee1-50* population is slightly more variable compared with wild type, indicated by the larger standard deviation bars of the cohorted data (Figure 3.4A) and a slightly lower r^2 value of 0.2 compared to 0.4 for wild type (Figure 3.4D and Table 3.1).

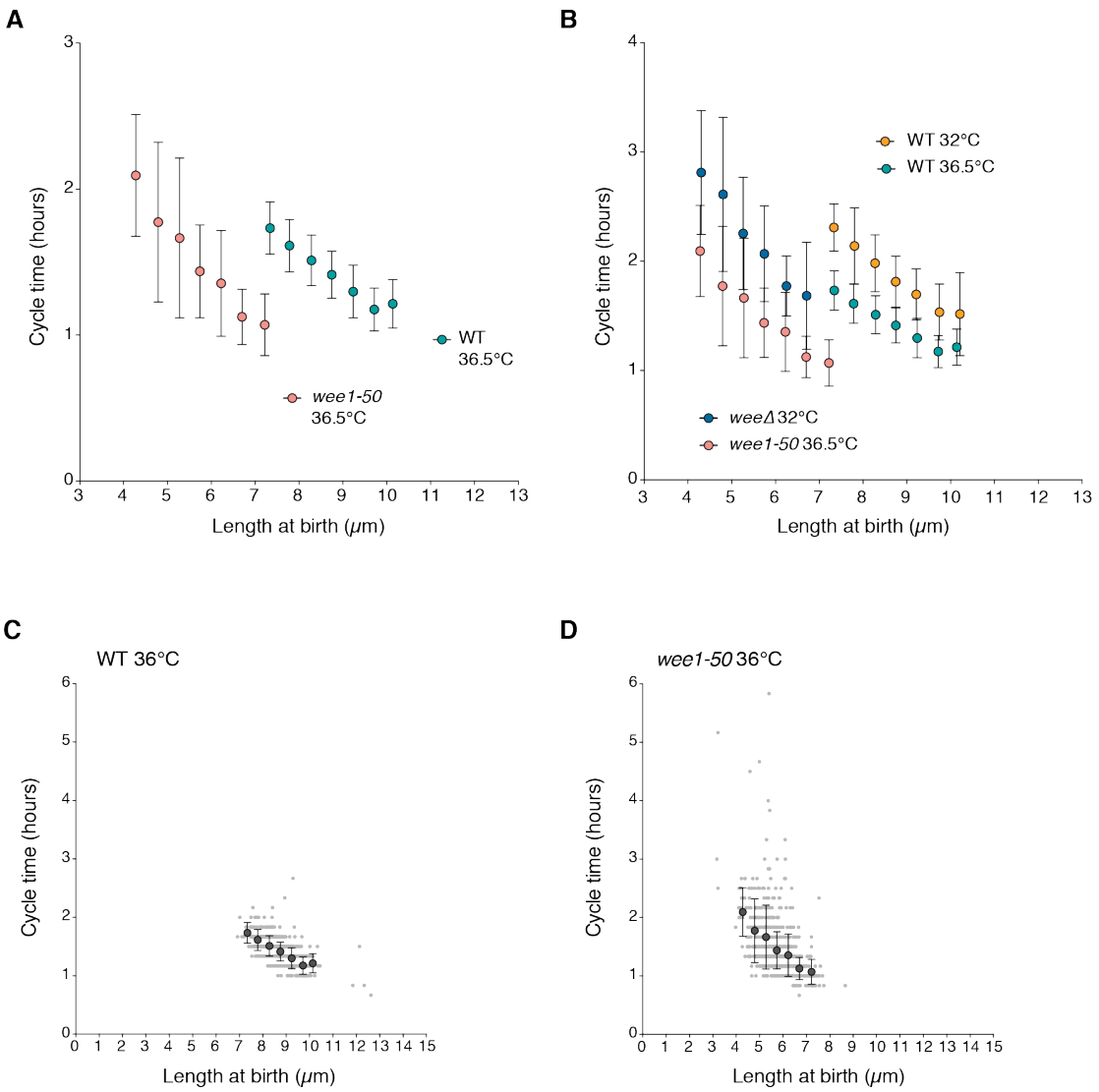

Figure 3.4|Cells deleted for *wee1* show a wild type BL/CT relationship

Figure 3.4|Cells deleted for *wee1* show a wild type BL/CT relationship

(A) and **(B)** Cell length at birth plotted against cycle time of the strains indicated. Cycle time calculated as the time between birth and division length measurements. Points show mean values of cohorted data, bars represent standard deviation. **(C)** and **(D)** Individual graphs of WT and *wee1-50* cells, respectively. Small light grey dots show individual cells. Larger dark grey points show mean values of cohorted data as shown in **A**. All cells grown in YE4S at 32°C or 36.5°C, as indicated, in a microfluidic chamber.

A slight difference between *wee1-50* and *wee1*Δ is seen on the BL/CT plot (Figure 3.4B). In addition to an overall increase in cycle time for the population of *wee1*Δ cells, which is expected due to the lower temperature, the *wee1*Δ population also has a slightly steeper slope compared with *wee1-50* cells (Figure 3.4B, Table 3.1). This increase in the slope value is suggested to be due to the temperature difference as a similar trend is seen when comparing wild type populations growing at 32°C and 36.5°C (Figure 3.4B).

These data suggest that small cells are spending longer in the subsequent cycle compared with longer cells. The indication is that a size threshold must be surpassed before cells can enter S phase, causing smaller cells to delay in the cell cycle. Importantly, the experimental measurements are taken at septation and therefore include not only the G1/S sizer but also the G2 timer. Small cells have a slower growth rate compared with longer cells, therefore during a fixed G2 timer period small cells grow less than larger cells and may mask any corrections made earlier in the cycle at the G1/S transition. Therefore it is possible that a BL/E relationship at G1/S could be weakened during the G2 timer period and therefore not be seen in the measurements taken at septation.

3.2.4 There is no width increase in small *wee1-50* cells experiencing a cell cycle delay

A second possibility which could explain the *wee1-50* and *wee1*Δ data is that length is not a good surrogate for cell size for these cells, perhaps because very short cells increase in width as they grow. If the G1/S threshold is measuring cell volume and not cell length, it is possible that a homeostatic mechanism leading to a birth length/cycle time relationship would not translate to a relationship in cell length extension. Figure 3.5 suggests that this is not the case. A graph of cell length against cell width (using all measurements, taken at birth and division)

shows no relationship for either WT cells (Figure 3.5A, regression slope -0.02, r^2=0.06) or *wee1-50* cells (Figure 3.5B, regression slope -0.02, r^2=0.007) and thus smaller cells do not appear to be increasing in volume by increasing their width. In addition to this, there is no increase from the average width at birth to that at division for either strain (Figure 3.5C), suggesting there is no increase in width during the cell cycle of WT or *wee1-50* cells at 36.5°C.

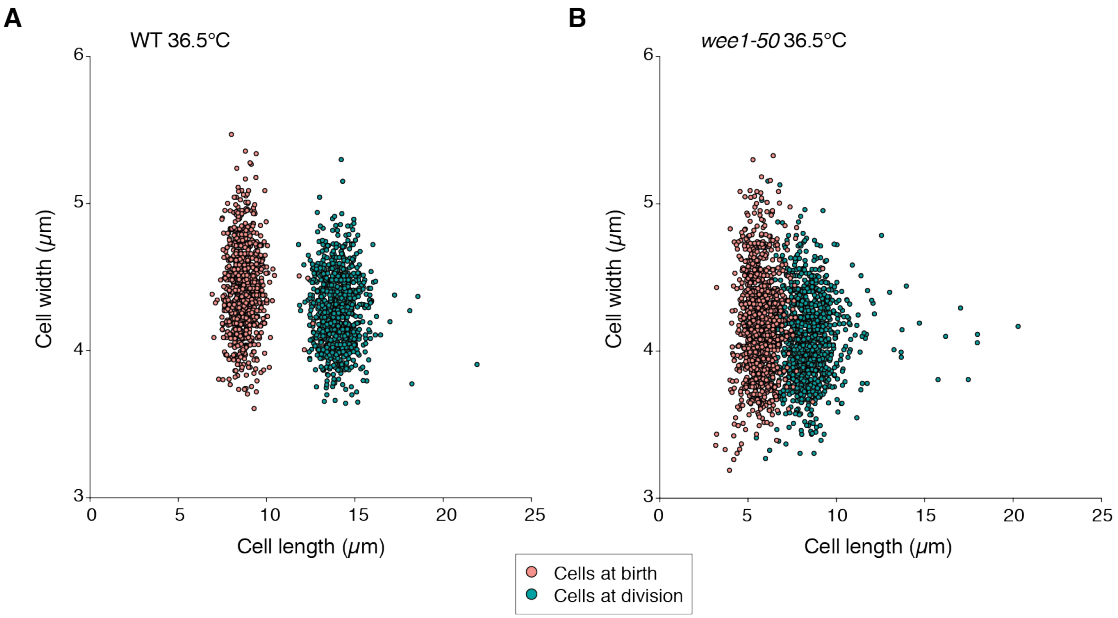

C

	Average width at birth (μm)	Average width at division (μm)
WT	4.4	4.3
wee1-50	4.2	4.1

Figure 3.5|Cell width does not change with increasing cell length

(A) Cell length plotted against cell width for WT cells growing in a microfluidic chamber in YE4S at 36.5°C. n=1,714, regression slope -0.02, r^2=0.06. **(B)** Cell length plotted against cell width for *wee1-50* cells growing in a microfluidic chamber in YE4S at 36.5°C. n=2,198, regression slope -0.02, r^2=0.007. Cell measurements plotted are those taken from time-lapse movies for Figure 3.2 and 3.4. Measurements are therefore a mixture of cells at birth and at division. **(C)** Table showing average cell width values at birth and division for WT and *wee1-50* cells at 36.5°C.

3.2.5 Mik1 is not required for cell size homeostasis

Mik1, like Wee1, is a tyrosine kinase that phosphorylates and inhibits Cdc2. Although deleting *mik1* does not cause a size phenotype, it was investigated whether Mik1 has a role in size homeostasis. BL/E and BL/CT plots reveal that *mik1*Δ cells respond in a very similar manner to wild type cells, with a BL/E slope of -0.7 (95% CI -0.81 to -0.56), and a BL/CT r^2 value of 0.3 (Figure 3.6A-D, Table 3.1). Mik1 therefore does not have a role in size sensing and correction.

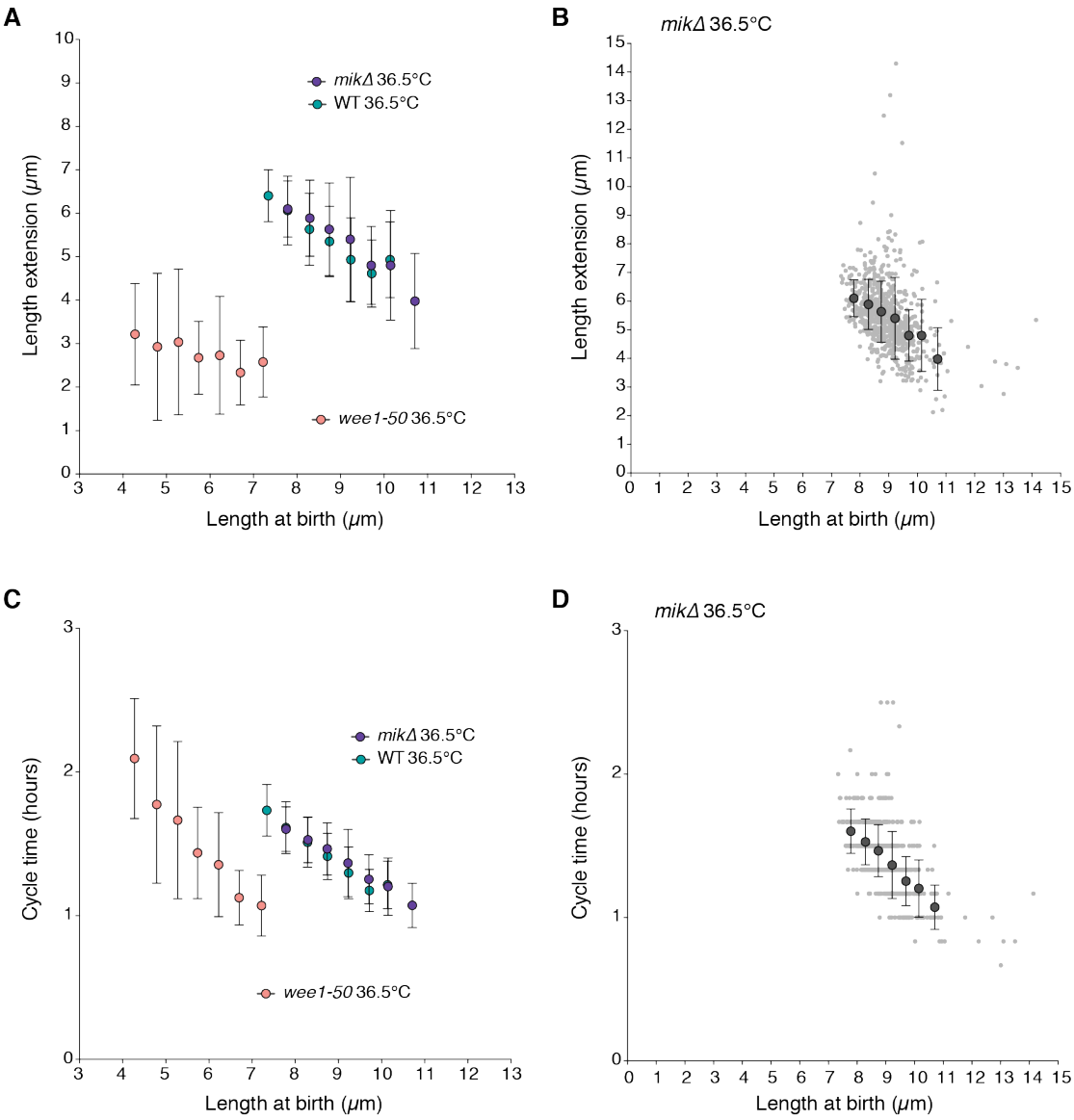

Figure 3.6|Mik1 does not have a role in cell size homeostasis

Figure 3.6|Mik1 does not have a role in cell size homeostasis

(A) Cell length at birth plotted against length extension of wild type, *wee1-50*, and *mik1*Δ cells from brightfield time-lapse images. Length extension calculated from birth and division length measurements. Points show mean values of cohorted data, bars represent standard deviation. **(B)** Raw data of *mik1*Δ cells. Small light grey dots show individual cells. Larger dark grey points show mean values of cohorted data as shown in **A**. **(C)** and **(D)** Same as **A** and **B**, respectively, with birth length plotted against cycle time. All cells grown in YE4S at 36.5°C in a microfluidic chamber.

3.2.6 Cdc2-Y15 phosphorylation is required for the G2/M size threshold

The data presented above suggests that cell size sensing and correction is achieved through control at the G2/M transition and therefore requires Wee1. In the absence of this G2/M size threshold, the G1/S sizer is revealed. The data from *wee1-50* and *wee1*Δ populations suggest that although cells do not have strong size homeostasis in the absence of the G2/M size threshold, the G1/S size threshold does require the achievement of a particular cell size and so contributes to cell size homeostasis by delaying small cells in G1. Smaller cells therefore have a longer cycle time compared to longer cells. Given this result the G1/S size threshold was investigated further using cells defective in Cdc2-Y15 phosphorylation.

Wee1 phosphorylates and inhibits the cyclin-dependent kinase Cdc2 – it is therefore predicted that size homeostasis at the G2/M transition requires Cdc2-Tyr15 phosphorylation. This can be tested by making use of a strain containing a minimal CDK control network. The orderly progression through the major cell cycle events can be driven by the oscillation of a monomolecular CDK module, a single Cdc13-L-Cdc2 fusion protein, in a cell with much of the core cell cycle machinery removed (Coudreuse and Nurse, 2010). This minimal control network allows an investigation of the role of Cdc2-Tyr15 phosphorylation, since this fusion protein strain is able to tolerate a mutant Thr14Ala Tyr15Phe (AF) Cdc2 kinase, rendering the kinase non-phosphorylatable on these residues. This mutation is lethal in a wild type stain expressing Cdc13 and Cdc2. As a control, a wild type fusion protein strain is used and both fusion strains are deleted for the wild type copies of *cdc2* and *cdc13* in addition to the other three mitotic cyclins, *cig1*, *cig2* and *puc1*.

A nutrient-shift experiment similar to that described in section 2.2.9 was carried out for wild type, Cdc13-L-Cdc2 and Cdc13-L-Cdc2AF cells. The wild type

fusion protein strain behaves in a similar manner to cells in a fully wild type population, with a characteristic peak in septation at around 30-60 minutes after the shift from glutamate to proline (Figure 3.7). This indicates that these cells have a functioning G2/M size threshold that is responsive to changes in the surrounding nutrient conditions. The AF fusion protein strain on the other hand does not show this characteristic peak in septation index (Figure 3.7) and behaves instead more similarly to a *wee1-50* population (Figure 2.15). This suggests that cells of the AF fusion protein strain do not have a size threshold at G2/M that can input information regarding the nutritional state of the cell and therefore may be operating using the G1/S size control.

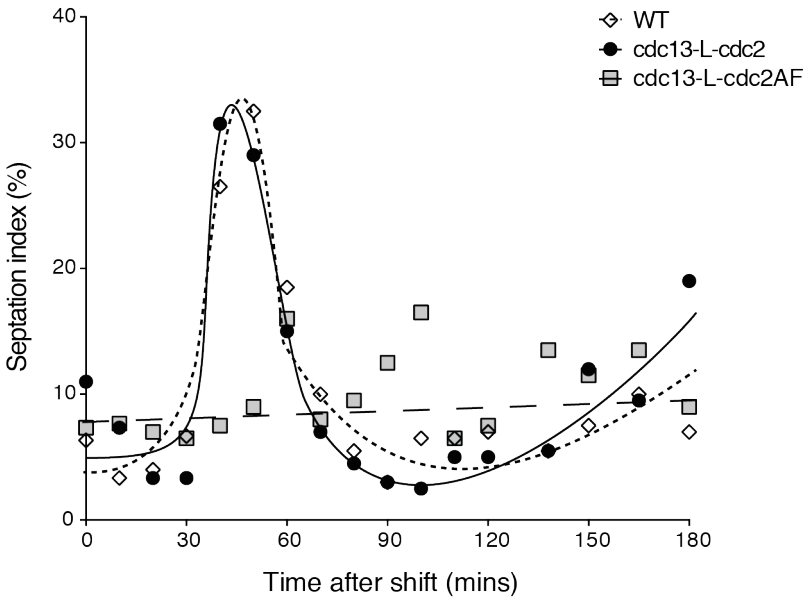

Figure 3.7|Cdc2-Tyr15 phosphorylation is required for a nutrient-sensitive G2/M size threshold

Septation index of WT, Cdc13-L-Cdc2 and Cdc13-L-Cdc2AF populations after nutritional shift-down from glutamate to proline as a nitrogen source. Cells grown at 32°C in EMM-N + 20 mM glutamic acid before being washed 3 times and resuspended at time zero in EMM-N + 10 mM proline. Graph shows number of septated cells represented as a percentage of the whole population. Lines are manual input showing general trend of the data.

3.2.7 An effective size homeostatic mechanism is present in cells lacking Cdc2-Y15 phosphorylation

Wild type, Cdc13-L-Cdc2, and Cdc13-L-Cdc2AF cells were grown in microfluidic chambers at 32°C. Figure 3.8A shows the cell length at division of cells from all three strains. As previously reported, the AF mutant divides at a slightly smaller size compared with the wild type fusion strain and its variability in cell size at division is greater (Coudreuse and Nurse, 2010). This can be seen more clearly in the histogram distributions of cell size at division (Figure 3.8B). Both wild type and the fusion strain divide with a coefficient of variation of 7-8%, whereas the AF mutant has a coefficient of variation in size at division of 15%.

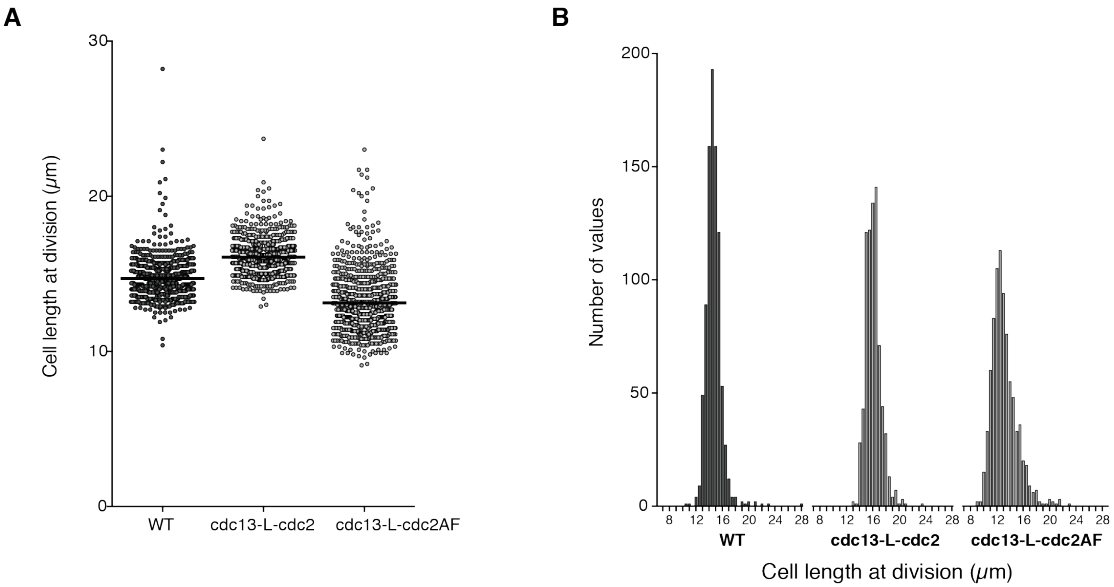

Figure 3.8|Cells with the AF fusion protein construct have increased size variability at division

(A) Scatter dot plots showing cell length at division of WT, Cdc13-L-Cdc2 and Cdc13-L-Cdc2AF cells. Line drawn at mean, dots represent individual cells. **(B)** Data from **A** represented as a frequency distribution. Bin size 0.5 μm. n=700-900 cells for each strain.

The BL/E plots for the wild type fusion protein and AF fusion protein strains show a relationship similar to WT cells, whereby small cells extend more than longer cells in order to maintain a constant size at division (Figure 3.9A, C and E, 3.10A and B). The slightly different positions of the slopes compared with WT (Figure 3.9A) reflect the different mean sizes of the fusion and AF fusion protein

populations. The regression slopes for these strains are -0.5 (95% CI -0.62 to -0.35) for cells with the fusion construct and -0.9 (95% CI -1.0 to -0.77) for cells with the AF fusion protein (both slopes are not significantly different to the wild type slope of -0.7, 95% CI -0.84 to -0.60, at 32°C). As with wild type cells, the BL/E relationship is due to altered cycle times rather than altered growth rates (Figure 3.9B, D and F).

For the wild type fusion protein strain this is the expected result, since these cells have been shown to have a G2/M size threshold (Figure 3.7) and are therefore predicted to behave in a similar manner to wild type cells. The data from the AF fusion protein cells suggests that without a G2/M size threshold, size control at the G1/S transition followed by the G2 timer is able to maintain size homeostasis in cells within a wild type size range. This is in contradiction with the data from the *wee1-50* and *wee1*Δ populations.

One possibility is that cells containing the non-phosphorylatable fusion protein have established another mechanism by which to effectively sense and correct for size deviations independently of *wee1* and Cdc2-Tyr15 phosphorylation, such that a strong relationship is maintained between cell length at birth and length extension during the subsequent cycle. A second possibility is that the phenotype seen in the *wee1-50* and *wee1*Δ populations is due to the small size of these cells. Perhaps cells below 7 μm cannot effectively establish a growth zone and therefore are accumulating mass but are not able to elongate. If the G1/S size threshold is measuring protein amount for example, a size homeostasis mechanism may not always be evident from cell size measurements alone. Thirdly, *wee1* may have a role in cell size homeostasis that is independent of Cdc2-Tyr15 phosphorylation.

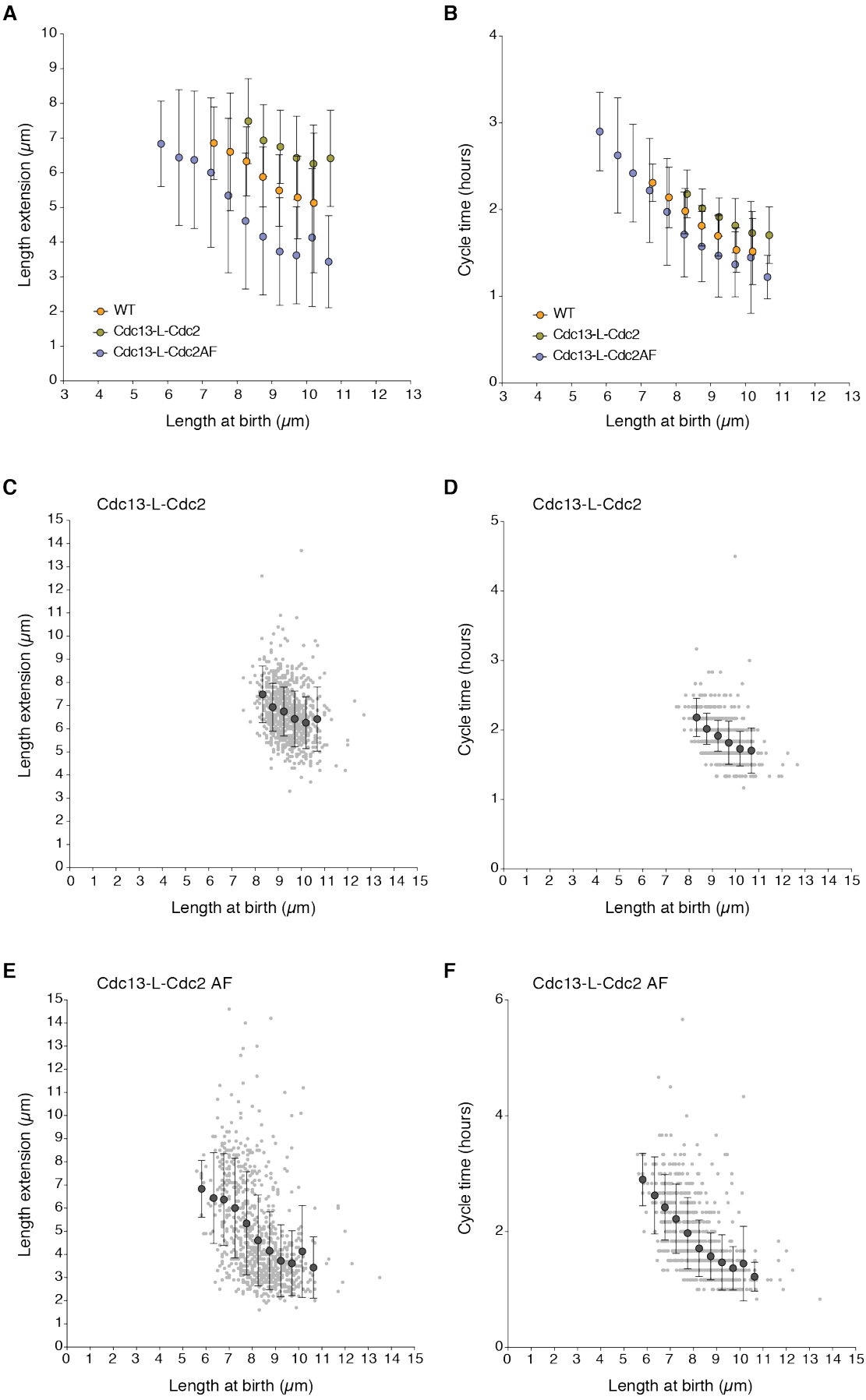
A
Length extension (μm)
Length at birth (μm)
WT
Cdc13-L-Cdc2
Cdc13-L-Cdc2AF
B
Cycle time (hours)
Length at birth (μm)
WT
Cdc13-L-Cdc2
Cdc13-L-Cdc2AF
C
Cdc13-L-Cdc2
Length extension (μm)
Length at birth (μm)
D
Cdc13-L-Cdc2
Cycle time (hours)
Length at birth (μm)
E
Cdc13-L-Cdc2 AF
Length extension (μm)
Length at birth (μm)
F
Cdc13-L-Cdc2 AF
Cycle time (hours)
Length at birth (μm)

Figure 3.9|Cells with the fusion protein and AF fusion protein show size homeostasis

(A) Cell length at birth plotted against length extension of wild type, Cdc13-L-Cdc2 and Cdc13-L-Cdc2AF cells from brightfield time-lapse images. Length extension calculated from birth and division length measurements. Points show mean values of cohorted data, bars represent standard deviation. **(B)** Same as **A** with length at birth plotted against cycle time. **(C)** and **(D)** Raw data of Cdc13-L-Cdc2 cells, with birth length plotted against length extension and cycle time, respectively. Small light grey dots show individual cells. Larger dark grey points show mean values of cohorted data as shown in **A** and **B**. **(E)** and **(F)** Same as **C** and **D**, respectively, for Cdc13-L-Cdc2AF cells. All cells grown in YE4S at 32°C in a microfluidic chamber.

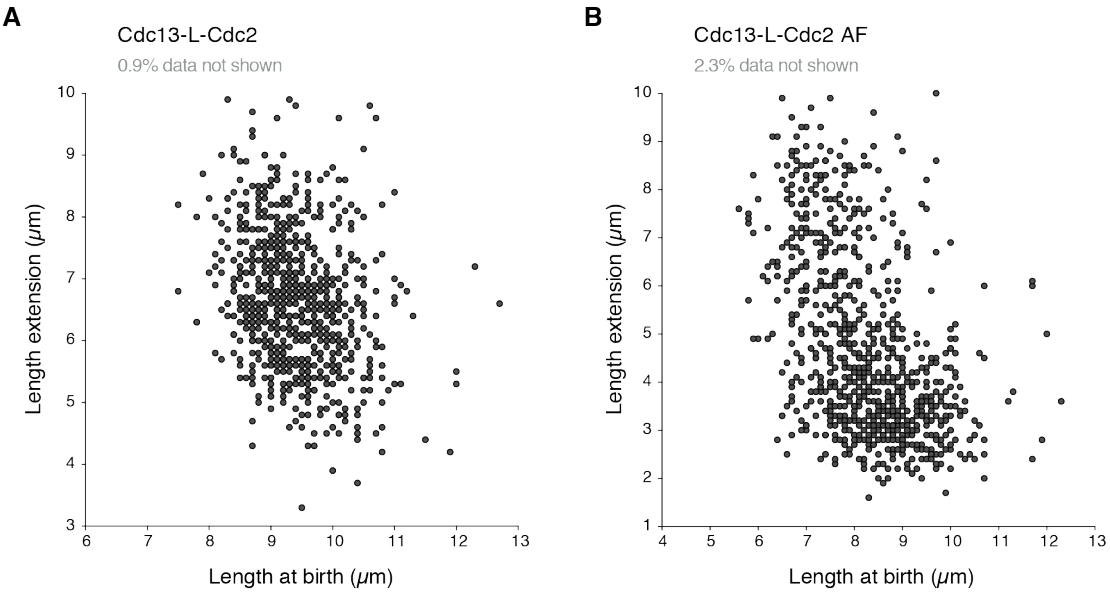

Figure 3.10|BL/E data of the fusion and AF fusion protein strains

(A) and **(B)** Raw data from plots in Figure 3.9C and E, respectively, with reduced axis scales for clarity. Percentage of data not shown here for clarity is indicated.

3.2.8 Cells containing the Cdc13-L-Cdc2AF construct behave differently to *wee1*∆Cdc13-L-Cdc2 cells

In order to further investigate these possibilities, both fusion constructs (wild type and AF) were combined with *wee1*∆. The BL/E and BL/CT plots are shown in Figure 3.11 and 3.12.

Since Wee1 is thought to act on the G2/M transition through Cdc2-Tyr15 phosphorylation only, deleting *wee1* in a strain containing a non-phosphorylatable Cdc2 protein should not have any additional effect on cell size. This is indeed the

case and the *wee1*∆Cdc13-L-Cdc2AF cells behave similarly to the AF fusion protein cells in terms of both the length extension and cycle time relationships with length at birth (although the 95% CI for the BL/E slope of *wee1*∆Cdc13-L-Cdc2AF cells falls just outside the 95% confidence interval of the AF fusion protein strain, the slope does not significantly differ from the wild type slope and therefore we conclude these cells have size homeostasis) (Figure 3.11, Table 3.1). This indicates that Wee1 does not have a role in cell size homeostasis independent of Cdc2-Tyr15 phosphorylation.

Deleting *wee1* in the wild type fusion protein strain on the other hand does have an effect and it has previously been shown that *wee1*∆Cdc13-L-Cdc2 cells divide at a smaller size compared to the fusion construct in a *wee1+* background (Coudreuse and Nurse, 2010). These cells are not reduced to the size of *wee1*∆ cells however and this is thought to be due to the absence of *cig1*, *cig2* and *puc1* in these cells (Martin-Castellanos et al., 2000). This enables an investigation of *wee1*∆ cells which are shifted towards the wild type cell size range and therefore may identify effects which are only due to the very small size of *wee1*∆ cells. Figure 3.12 shows that *wee1*∆Cdc13-L-Cdc2 cells behave in manner similar to *wee1*∆ cells, showing a weak relationship between birth length and length extension (significantly different to wild type however significantly non-zero, as with the *wee1*∆ population) with a wild type relationship between birth length and cycle time (Figure 3.12 and Table 3.1).

The data presented here suggest that in a wild type background deleting *wee1* removes the G2/M size threshold and that the G1/S size threshold followed by a G2 timer is not sufficient for cells to make effective cell length corrections in response to natural variations in birth length. The cycle time data does suggest however that cells do make corrections in response to birth length variations, by delaying small cells in the cell cycle. Since the G2 timer is, by its nature, predicted to be a fixed duration of time, this response in the cycle time must be occurring in G1. A prediction therefore is that the correction occurring at the G1/S is counteracted in the G2 timer phase. The data has also demonstrated that cells carrying a non-phosphorylatable Cdc2-Tyr15 residue may have come up with an alternative method of maintaining size homeostasis in the absence of *wee1* and tyrosine phosphorylation. The analysis of *wee1*∆Cdc13-L-Cdc2 cells, which are

longer than *wee1*Δ cells, has shown that the weak BL/E relationship seen in *wee1*Δ is likely not to be caused by the small size of these cells.

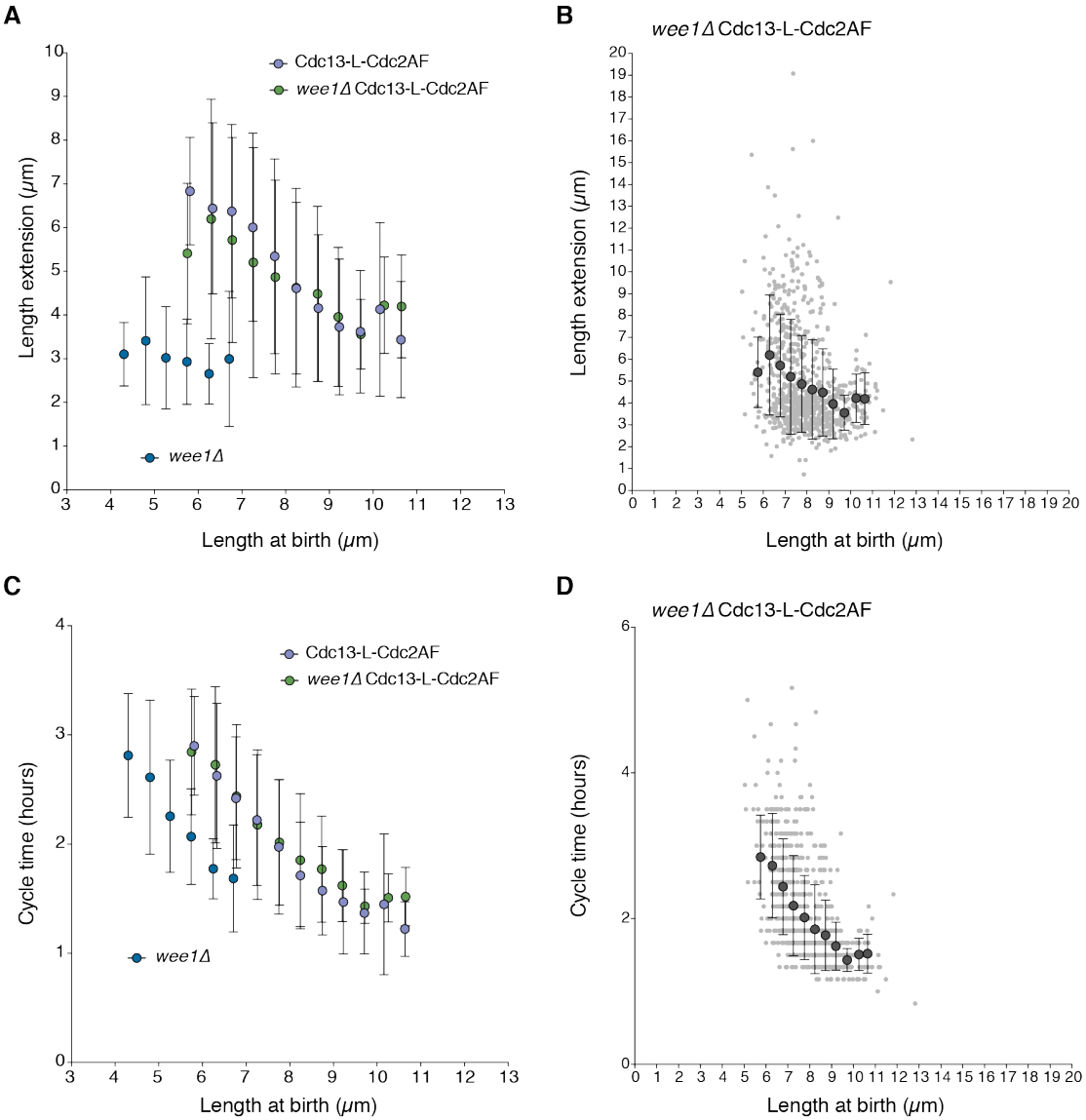

Figure 3.11|Deleting *wee1* in the AF fusion protein background has no additional effect on size homeostasis

(A) Cell length at birth plotted against length extension of *wee1*Δ, Cdc13-L-Cdc2AF and *wee1*ΔCdc13-L-Cdc2AF cells from brightfield time-lapse images. Length extension calculated from birth and division length measurements. Points show mean values of cohorted data, bars represent standard deviation. **(B)** Raw data of *wee1*ΔCdc13-L-Cdc2AF cells. Small light grey dots show individual cells. Larger dark grey points show mean values of cohorted data as shown in **A**. **(C)** and **(D)** Same as **A** and **B**, respectively, with birth length plotted against cycle time. All cells grown in YE4S at 32°C in a microfluidic chamber.

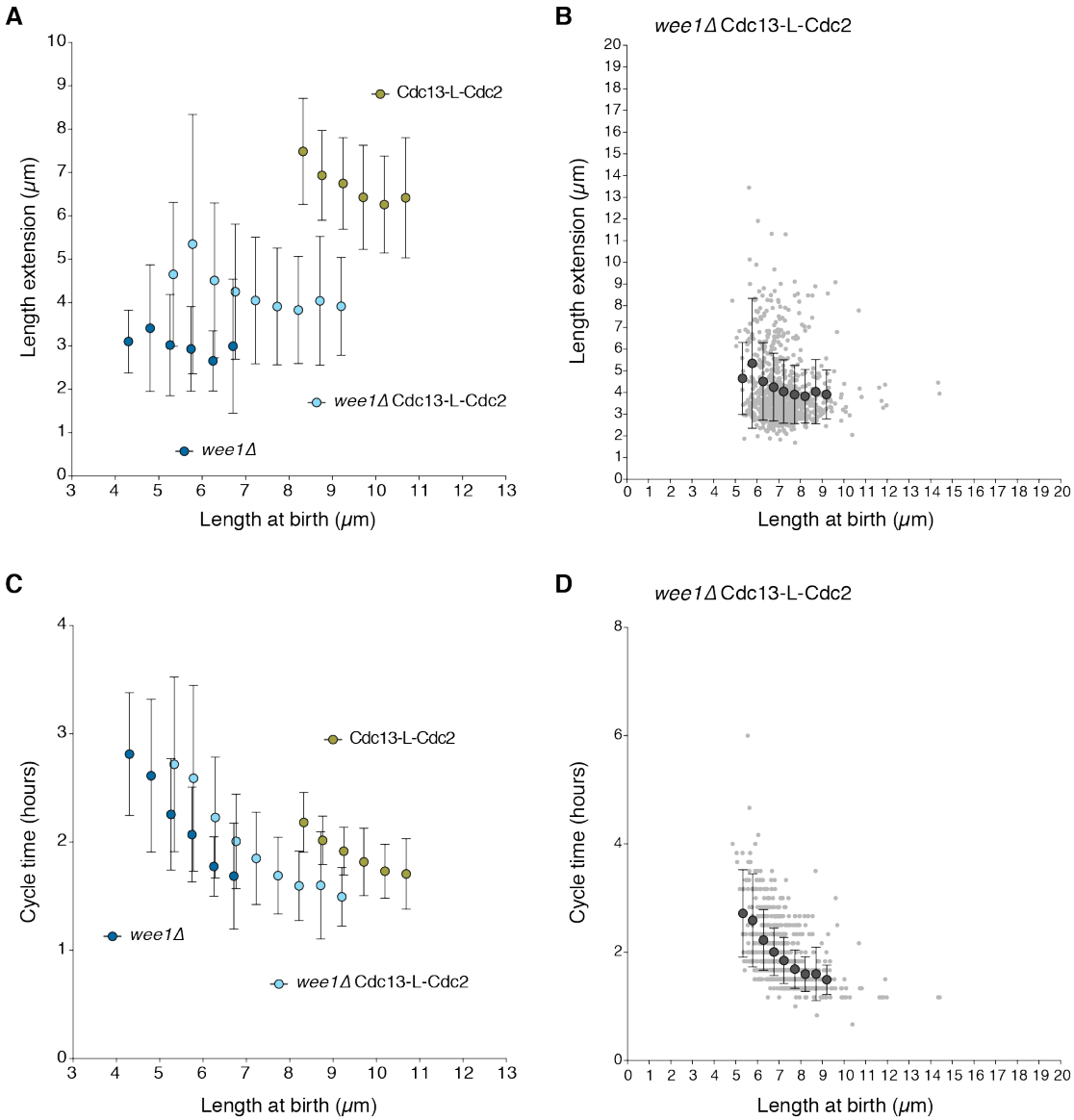

Figure 3.12|Wee1 is required in the fusion protein background to maintain size homeostasis

(A) Cell length at birth plotted against length extension of *wee1*Δ, Cdc13-L-Cdc2 and *wee1*ΔCdc13-L-Cdc2 cells from brightfield time-lapse images. Length extension calculated from birth and division length measurements. Points show mean values of cohorted data, bars represent standard deviation. **(B)** Raw data of *wee1*ΔCdc13-L-Cdc2 cells. Small light grey dots show individual cells. Larger dark grey points show mean values of cohorted data as shown in **A**. **(C)** and **(D)** Same as **A** and **B**, respectively, with birth length plotted against cycle time. All cells grown in YE4S at 32°C in a microfluidic chamber.

3.3 Discussion

3.3.1 Growth rate is not inherited

An analysis of the growth of wild type cells within the microfluidic chambers (in which all the subsequent homeostasis experiments were carried out) was done in order to investigate whether this growth environment has any adverse effects on cell growth or cell morphology. From the time-lapse images it is clear that cell morphology is not affected, and cell length and width measurements reflect those taken in liquid culture. Cycle time values also match those of cells growing in liquid culture. There also does not appear to be an effect of position or generation number of individual cells on their growth rate that would suggest any unfavourable effects which might affect the results from data collected from these time-lapse videos. Therefore it is concluded that the microfluidic chambers are adequate to carry out the subsequent cell size homeostasis analyses discussed in this chapter. All data in these investigations was collected within the first three generations after cell loading, as covered by the growth analysis.

The data collected from the growth analysis enabled an investigation into the growth rate patterns within cell lineages. By calculating a pseudo-exponential growth rate for every cell within 42 lineages spanning 3 generations ($G = E/(BL \cdot CT)$) a comparison could be carried out between mother and daughter cells. This analysis shows that growth rate is not inherited by individual daughters, and that there does not appear to be a larger structure of growth rate patterns within whole lineages within the time frame of 3 generations. This suggests that growth rate potential does not have a genetic element, for which inheritance from mother to daughter cell might be expected.

3.3.2 Wee1 is required for cells to maintain size homeostasis

The main aim of this chapter was to investigate known cell cycle regulators for their role in cell size homeostasis. A similar investigation was carried out in 1996 (Sveiczer et al., 1996) and the work here sought to expand on this with measurements from a greater numbers of cells. The first finding was that whereas in the earlier study *wee1*Δ cells were found to show size homeostasis, with a BL/E

relationship similar to wild type cells (Sveiczer et al., 1996), both *wee1-50* and *wee1*Δ cells in the investigation here show a weaker BL/E response. It is possible that this is due to the much larger numbers of cells measured here, or perhaps the growth conditions during filming. It should be noted that the previous investigation used minimal medium EMM3 whereas all cells measured in this work were grown in complex YE4S media.

Both *wee1-50* and *wee1*Δ cells show a very similar response to variations in birth length, both with BL/E regression slopes of -0.3. On its own this data would suggest that without Wee1, cells can no longer sense cell size effectively and so cannot rapidly make the appropriate corrections in the subsequent cell cycle. The prediction therefore would be that the cycle time relationship with birth length seen in wild type cells would be lost. However this is not the case and in fact the BL/CT slope of both *wee1-50* and *wee1*Δ cells is similar to that of a wild type population. From this observation there are a number of possibilities.

Firstly, size correction may be occurring in cells deleted for *wee1*Δ but due to the small size of these cells it is possible that they are not able to immediately establish growth at the cell poles following cell division. It is conceivable that cells born below a length of 6 μm, for example, may have difficulty establishing polarity due to a more spherical cell shape. In this case it is possible that these small cells will alter the time spent in the subsequent cycle to correct for size deviations, but the corresponding size increase is not seen in cell length but rather in cell volume. In this case, cell width would be expected to increase. This was tested directly by analysing the cell length and cell width values of individual cells. For both wild type and *wee1-50* cells at the restrictive temperature, no relationship is seen between cell length and cell width. Both WT and *wee1-50* populations have a mean cell width at division of 4.3 μm and 4.1 μm, respectively, values which are not increased compared to the values at birth, thus suggesting that *wee1-50* cells are not increasing in width.

The second possibility is similar to the first and postulates that small *wee1-50* cells, although elongating their cell cycle to try and correct for their small size, cannot begin elongation immediately following cell division. Rather than measuring cell size however, it may be possible that the G1/S transition is measuring another factor of cell growth, such as the accumulation of a transcript or protein, or total protein amount. If this factor/these factors were to accumulate in the absence of an

absolute increase in cell size, it is possible for a cell to correct its cycle time according to its birth length but for this correction not to translate into a length extension relationship. However, in its simplest form this does not seem to be the case. In this situation it would be expected that *wee1-50* cells within the wild type birth length range would show a more wild type response, since this model relies on the idea that length extension is only disrupted in very small cells (below 6 μm) and hence the effect is only seen in a *wee1-50* population. However, data from the *wee1*∆Cdc13-L-Cdc2 strain, cells of which lack *wee1* but are not as reduced in cell size, show a very similar response to *wee1*∆ and *wee1-50* cells, despite many cells being in the wild type size range. This suggests that cells born longer than 6 μm are not showing any additional elongation despite the increased cycle time. This model could be further tested by measuring cell density, since accumulation of mass without an increase in cell length or volume would lead to an increase in cell density.

The third possibility is based on the differing growth rates of small and large cells. For fission yeast it has been established that cells do not accumulate mass in a linear fashion for extended periods of time (Baumgartner and Tolic-Norrelykke, 2009, Creanor and Mitchison, 1982, Mitchison, 2003, Mitchison and Nurse, 1985). Data supporting this comes from the growth of *wee1-50* and *cdc25-22* cells at the semi-restrictive temperature. Despite a greater than three-fold size difference between these two cell types, cells of both strains double their mass in the same time. *Cdc25-22* cells must therefore be accumulating mass at a higher rate compared with *wee1-50* cells (Nurse and Fantes, 1981). From this we can therefore speculate that within a population of *wee1-50* cells at 36.5 °C, the smaller cells may be growing slower than the larger cells. The cell cycles of these *wee1-50* cells consist of a G1, followed by a G1/S size threshold (the nature of which is unknown), followed by a G2 timer (the incompressible G2 period), followed immediately by entry into mitosis. During G1, some size correction may be taking place, such that the cycle times of cells born small are extended compared to those born longer (hence the BL/CT relationship, the slope of which may seem increased compared to wild type due to a slight delay in the establishment of growth zones in the smallest cells). A possible reason for the lack of a BL/E relationship could be the following G2 timer period. Following correction in G1, cells then enter G2 for a fixed period of time (which will therefore leave the CT correction unaffected and

increase the CT of all cells by the same amount). If small cells are growing slower than larger cells, cells entering G2 at a smaller size will extend less during this fixed G2 period. Therefore it can be envisaged that any BL/E relationship resulting from a G1/S size threshold might be weakened during the following incompressible G2 period.

This last prediction implies that the G1/S size threshold is able to sense and correct for deviations in cell size but that due to the pseudo-exponential growth pattern of these cells, this size homeostasis is not efficiently maintained due to the subsequent G2 timer period.

3.3.3 Introducing a Cdc2AF mutation restores size homeostasis to *wee1*Δ cells

The data from the *wee1-50* and *wee1*Δ cells indicates that without a G2/M size threshold, size homeostasis is weakened. Another system in which to investigate this is with cells carrying the Cdc13-L-Cdc2 fusion protein. These cells have been shown to tolerate a Cdc2AF mutation (T14A, Y15F) which renders the Cdc2-Thr14 and Cdc2-Tyr15 residues non-phosphorylatable and is lethal in wild type cells (Coudreuse and Nurse, 2010). In these AF fusion protein cells therefore, Wee1 is unable to phosphorylate and inhibit Cdc2, and it is expected that these cells should behave similarly to *wee1*Δ cells without a G2/M size threshold. However this is not what is seen and the cells of the AF fusion protein show both a wild type BL/E and BL/CT response.

Two possibilities which could explain this data are as follows. Firstly it is possible that cells with this AF fusion protein have established a completely different mechanism for controlling cell size at division that is independent of Wee1 and Cdc2-Tyr15 phosphorylation. This could also explain why these cells are not reduced to the size of *wee1*Δ cells. A second possible interpretation of this data is that Wee1 has another role in cell size control that is independent of Cdc2-Tyr15 phosphorylation. In this case, deleting *wee1* in the AF fusion protein background should reduce size homeostasis to the level seen in *wee1*Δ cells.

However the data presented does not support this. Deleting *wee1* in a cell expressing the Cdc13-L-Cdc2AF fusion protein does not reduce size homeostasis

to the level seen in *wee1*Δ cells, and the BL/E and BL/CT graphs of the AF fusion protein strain with and without *wee1* are not significantly different to wild type. This suggests that carrying a Cdc2-AF mutation may have resulted in cells establishing a size control mechanism that is independent of *wee1*. This hypothesis can explain why these cells are a wild type size and yet have a long G1 similar to *wee1-50* cells.

3.3.4 The G1/S versus G2/M size threshold

The data presented in this chapter does not give direct and absolute answers to the question of the mechanism of cell size control at G1/S and G2/M. The most fitting interpretation of the data as it stands however is as follows. Cells with a G2/M size threshold can maintain effective size homeostasis such that small cells extend more in the subsequent cycle in order to correct for size deviations that arise. This is seen in plots of birth length against length extension. It must be noted here that the experimental measurements are being taken at entry into mitosis (measurements taken at septation correspond to those at mitosis due to the constant length period) and it is predicted that the cell is also 'measuring' length at or close to this control point in the cell cycle.

Cells without the G2/M size threshold are running on a G1/S size threshold followed by a G2 timer period. These cells appear to show weak size homeostasis as measured by cell length at division (and plotted as BL/E), however in this case the experimental measurements are being taken some time after the G1/S control point. Due to the fixed G2 timer period and the growth rate differences of small and large cells, it is possible that a size control mechanism acting to maintain size homeostasis at G1/S could be masked such that these are not picked up in measurements taken later in the cycle at G2/M.

The work presented here has shown how size homeostasis studies have been used to probe known cell cycle regulators and provide additional information regarding the cell size control at both the G1/S and G2/M transitions. The next chapter aims to use similar studies to screen for novel components of the size sensing mechanism at G2/M.

Chapter 4. Finding candidate genes that affect cell size variability at division

4.1 Introduction

Studying size homeostasis through population variability and single cell analysis has proved to be a valuable tool in understanding what is important for the sensing and regulation of cell size during the cell cycle. In the previous chapter, this type of analysis was used to probe and further understand the current components of the size checkpoint. This investigation has shown that Wee1, acting through Cdc2-Tyr15 phosphorylation, is essential for a population to maintain size homeostasis through a size checkpoint at the G2/M transition. Without this G2/M control, the G1/S size threshold may be able to make corrections for size deviations, but these corrections in cell length are weakened by the time the cells enter mitosis, possibly due to the growth rate differences between small and large cells.

The final aim of this work was to see if size homeostasis analysis could be used in this way to find new components which may be involved in size sensing and correction at the G2/M transition. This type of analysis is possible in fission yeast since these cells divide at a constant cell length with very little variation about the mean (Mitchison, 1957, Nurse, 1975). Wild type cells must therefore have a mechanism to actively sense their size and rapidly correct for any deviations that arise. A mutant that disrupts this tight regulation can be predicted to have a role in either the sensing or the correction of these size deviations.

To this end, a previous cell size screen carried out in the lab (Navarro and Nurse, 2012) was utilised and the data was mined for gene deletions that lead to increased variability in cell size at division. Similar approaches to those discussed in the previous chapters were then used to further investigate the gene deletion strains, including single cell size homeostasis studies and observing nuclear divisions within a common cytoplasm.

The screen reveals Mga2 as a potential component involved in regulating size homeostasis. In addition to having much greater variation in cell size at division, cells deleted for *mga2* do not show any relationship between birth length

and length extension. Thus a cell that is born too short or too long does not rapidly correct for this size defect. This predicted regulator of fatty acid biosynthesis could form a link between cellular membranes and cell size sensing through a pathway independent of Cdc2 tyrosine phosphorylation, although more evidence is required to support this hypothesis.

This is the first time that size variation has been used in this way to investigate the problem of cell size sensing. It has proved to be a useful tool in identifying possible candidates involved in size control in this single-celled organism. The investigation has uncovered Mga2 as a potential new component of the G2/M size regulation, a gene with no previously annotated cell cycle role (PomBase). Further mechanistic evidence is required to validate this result and find a mechanism for its role in the decision to enter mitosis.

4.2 Results

4.2.1 A near genome-wide screen reveals 15 genes which when deleted lead to increased cell size variability at division

The hypothesis is that any population of cells showing increased size dispersion at mitosis may be defective in size sensing or correction. An increase in size variability will not necessarily change the average size of the population and therefore on a population level these cells will not appear as size mutants.

The *S.pombe* haploid gene deletion strain collection (Kim et al., 2010) was previously screened in the lab to search systematically for gene deletion mutants that divide prematurely at a smaller cell size (Navarro and Nurse, 2012). The aim of this screen was to further characterise the components and mechanisms acting to negatively control the onset of mitosis. 82% of all the non-essential genes in fission yeast were screened and any size and growth phenotypes were recorded (Figure 4.1A). This screen aimed at identifying only small size mutants using the population mean and therefore strains with potentially increased cell size variability at division were noted but not chosen for further characterisation. The comprehensive nature of the screen enabled the dataset to be reanalysed for this investigation, looking specifically for gene deletions which were recorded as causing increased variability in the size of cells at division.

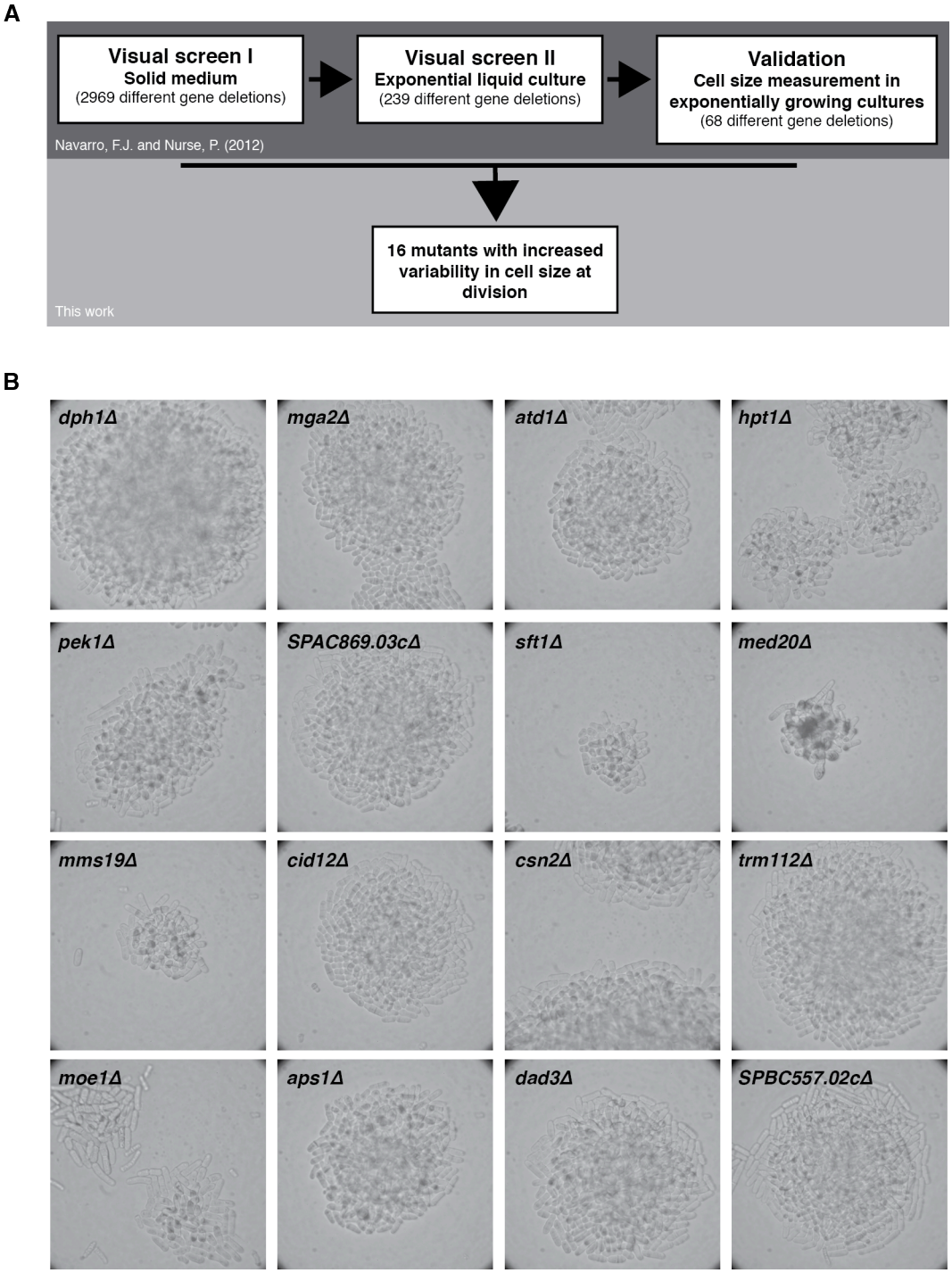

Figure 4.1|A screen for gene deletions that cause increased size variability

(A) Strategy for the identification of variable mutants in the fission yeast gene deletion collection. Results from all three phases of a previous screen (Navarro and Nurse, 2012) were taken and searched for any gene deletion annotated as giving an increase in variability in cell size at division. Original screen was of microcolonies of 2,969 strains carrying individual deletions of different non-essential genes. 16 of these strains were described as having increased size variation. **(B)** Images of microcolonies of the 16 candidates.

From the original screen results, 16 genes were found which were annotated as variable in size growing on solid YE4S medium, some having been further confirmed as variable in exponential liquid culture (Figure 4.1A). No further investigation of these genes was carried out as part of the original investigation.

In order to validate these results, all 16 possible variable candidates were re-isolated from the haploid gene deletion collection. First, the phenotype on solid medium was checked by examining cells growing in microcolonies, formed by approximately 50-100 cells (Figure 4.1B). Of these candidates, 15 were validated as being variable in size at division. One of the gene deletions, *med20*Δ, forms very small microcolonies and the cells appear sick and multiseptated (Figure 4.1B). For this reason *med20* was not taken any further in this investigation.

This left 15 candidate genes, which were grown in exponential liquid culture. Length measurements were taken from brightfield images of between 50 and 150 cells for each strain. For eight of the candidates, the mean size at division is not significantly different compared to wild type, while seven candidates have a mean cell length at division which is significantly greater or smaller than wild type ($p \leq 0.0005$) (Figure 4.2A). All 15 candidates have a coefficient of variation in size at division greater than the wild type value of 5%, ranging from 6% to 21% (Figure 4.2B).

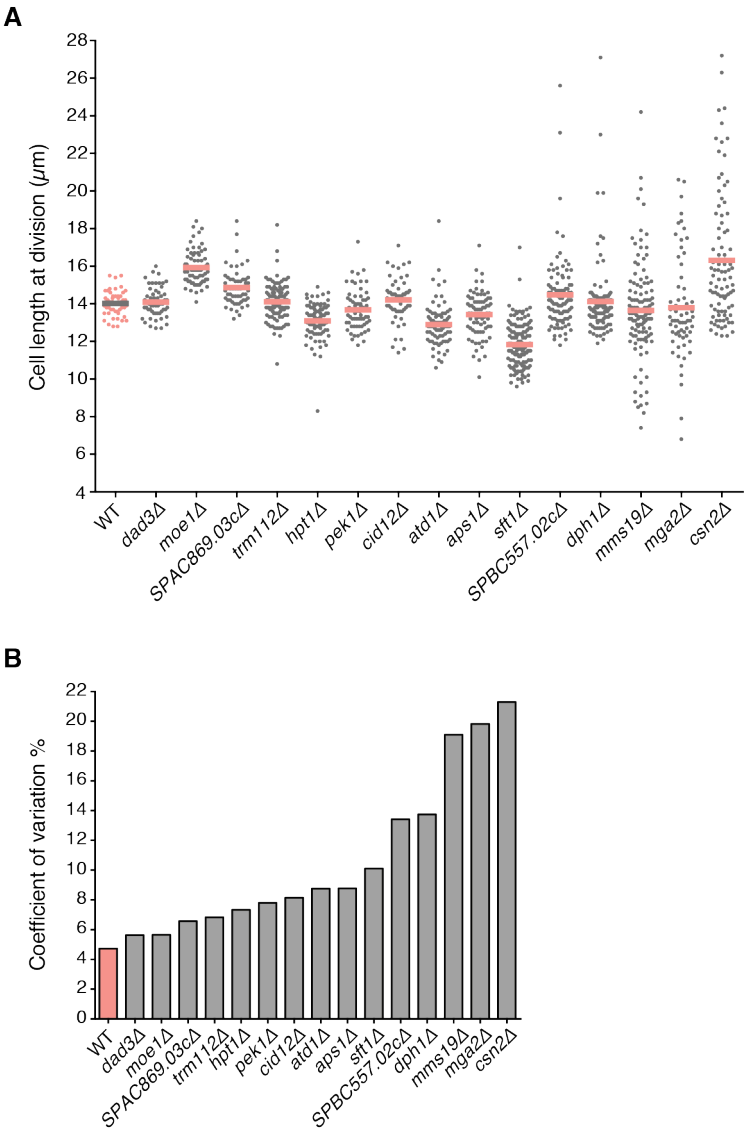

Figure 4.2|Variable cell size candidates

(A) Scatter dot plots showing 15 variable gene deletion strains from the screen and a wild type strain (far left). 50-150 cells measured for each strain. Line drawn at mean, each dot corresponds to a single cell. Cells measured in exponential growth at 32°C in YE4S. **(B)** Coefficient of variation of cell length at division measured for the cells shown in **A**.

4.2.2 Single cell analyses reveal two genes which when deleted lead to reduced size homeostasis

The next step was to analyse these candidate genes for a role in size homeostasis, aimed at identifying a possible mechanism for cell size sensing. From the above screen validation, eight genes were chosen for further analysis based on

their increased size variability at division and even distribution about the mean. These eight genes are *aps1*, *atd1*, *cid12*, *mga2*, *mms19*, *pek1*, *sft1* and a sequence orphan (systematic ID, SPBC557.02c). Two genes not chosen were *dph1* and *csn2*, since despite having a high coefficient of variation in cell size at division, both mutants show a skewed distribution towards longer cells which could be a result of checkpoint activation.

In order to investigate size homeostasis in the eight chosen strains, single cell studies were carried out using time-lapse microscopy. As described in the previous chapters, cells were grown in microfluidic chambers within a temperature-controlled microscope chamber and brightfield images were taken every 10 minutes over 12 hours.

For one of these gene deletion strains, *mms19*Δ, it became clear from the time-lapse microscopy that much of the size variation previously measured from still images of the cells may have been a result of septating cells continuing to extend in length before cell separation (Figure 4.3). In wild type cells the septum is usually visible for around 30 minutes and cells do not elongate during this time. Therefore in still images the length of any septated cell will be a close approximation of the cell length at mitosis (this constant length period usually starts at mitotic entry and persists until cell separation). If cells continue to elongate once a visible septum has formed, as appears to be the case for *mms19*Δ, this could distort the data and may cause an apparent increase in variability in size at division. The cell indicated in Figure 4.3 septates 3 hours 30 minutes into the film and this septum is not resolved for the duration of the movie, yet cell length continues to increase and more septa form within this cell. Due to the potential for misinterpretation, this strain was therefore not taken any further in the investigation.

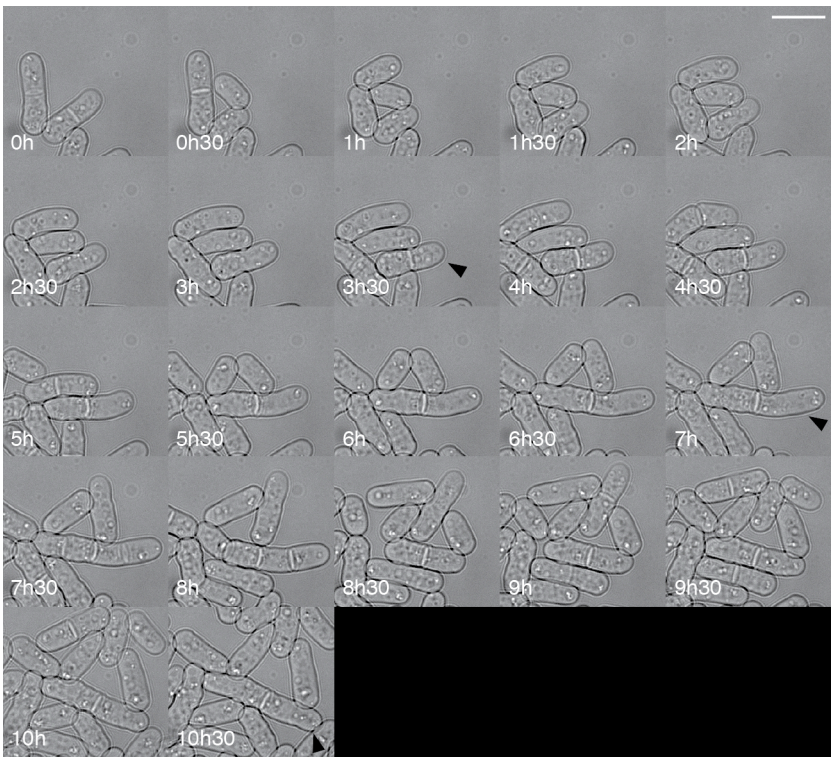

Figure 4.3|*mms19*Δ causes cells to delay during septum formation

Stills taken from a brightfield time-lapse movie of *mms19*Δ cells growing in a microfluidic plate. Times indicate the time lapsed from the start of imaging, which was 1 hour after loading the cells into the plate. Arrows indicate cell described in the text. Cells grown at 32°C in YE4S. Scale bar represents 10 μm.

The length at birth and division of between 200-900 cells was measured for the remaining seven strains, and graphs of birth length against length extension (BL/E) were plotted. The results can be seen in Figure 4.4 and the values of the BL/E slopes, in addition to length and cycle time data, is presented in Table 4.1. Of the seven strains investigated in this manner, five show a wild type relationship between birth length and length extension, that is, small cells extend more than long cells in order to maintain a constant size at division (Figure 4.4B, C, F, G and H and Table 4.1). In fact for four of these strains, *aps1*Δ, *atd1*Δ, *pek1*Δ and *sft1*Δ, the coefficient of variation for size at division is no longer increased compared to the wild type strain, since under these time-lapse conditions the wild type population has a coefficient of variation of 8% (Table 4.1). This could be due to the microfluidic plate not being an optimal growth environment for the cells, or it could be due to the transillumination adversely affecting the cells (the cells are imaged by brightfield every 10 minutes), or perhaps a combination of both. For

*SPBC557.02c*Δ although the coefficient of variation in size at division is greater than wild type, with a value of 15% (Table 4.1), the BL/E relationship is -0.6 and therefore we conclude that these cells are showing some size homeostasis (Figure 4.4H).

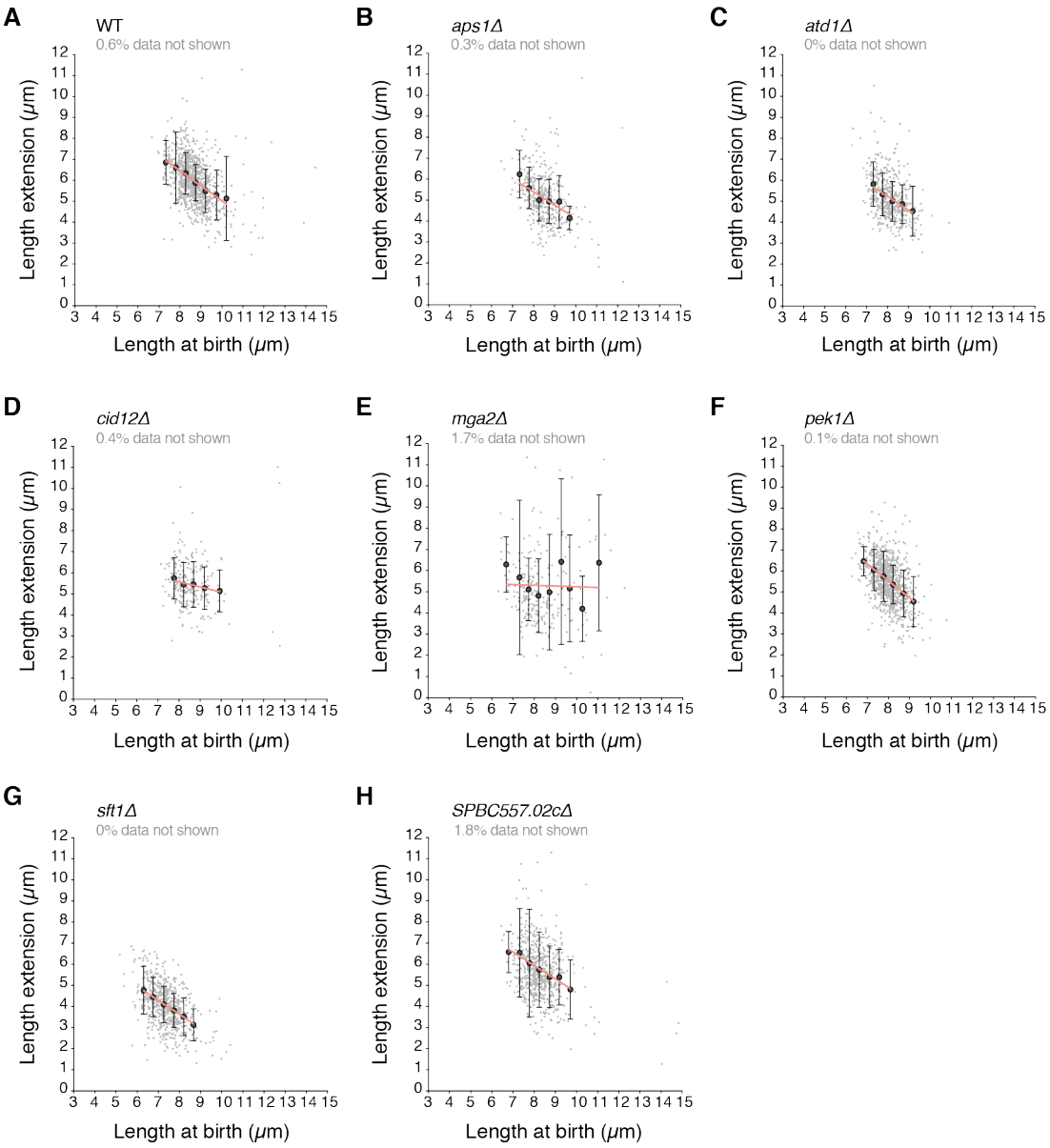

Figure 4.4|Single cell size homeostasis analysis of variable candidates

(A)-(H) Cell length at birth plotted against length extension for the strains indicated. Measurements taken from brightfield time-lapse images of 200-900 cells for each strain. Length extension calculated from birth and division length measurements. Small light grey dots show individual cells. Larger dark grey points show mean values of cohorted data. Bars represent standard deviation. Percentage of data not shown here for clarity is indicated. All cells grown in YE4S at 32°C in a microfluidic chamber.

Gene	Cell length at birth		Cell length at division		Cycle Time		BL v E slope value (1 s.f.)	Molecular function	Biological process
	Mean (µm)	CV (%)	Mean (µm)	CV (%)	Mean (hours)	CV (%)			
aps1	8.5	9	13.6	9	1.9	21	-0.6	Phosphatase	Nucleobase-containing small molecule metabolic process
atd1	8.1	7	13.3	8	2.3	19	-0.7	Aldehyde dehydrogenase (predicted)	Nucleobase-containing small molecule metabolic process
cid12	8.5	10	14.0	10	2.0	18	-0.2	Poly(A) polymerase	Chromosome segregation; Cytoskeleton organisation; Transcription
mga2	8.3	13	13.6	20	2.5	41	-0.03	Transcription regulator (predicted)	Lipid metabolism; Transcription
pek1	8.0	8	13.5	8	2.1	18	-0.8	Kinase	Cell wall organisation; Mitotic cytokinesis; Signaling
sft1	7.4	10	11.4	8	2.3	37	-0.7	SNARE	Vesicle-mediated transport
SPBC557.02c	8.3	12	14.1	15	2.1	28	-0.6	NA	NA
WT	8.7	10	14.7	8	1.9	18	-0.7		

Table 4.1|Candidate genes from the screen

Cell length at birth, cell length at division and cycle times for the seven candidate genes. Cells grown in YE4S at 32°C in a microfluidic chamber. Mean values to 1 decimal place (d.p.) and coefficient of variation (CV) values to the nearest percent. Values of the regression slope of birth length against length extension calculated from Figure 4.4, quoted to 1 significant figure (s.f.). Molecular function and biological process from PomBase (PomBase).

Two of the seven strains, *mga2*Δ and *cid12*Δ, show a different homeostatic response compared to the wild type cells. For both of these strains the relationship between birth length and length extension is reduced, the value of the BL/E slopes being -0.003 for *mga2*Δ and -0.2 for *cid12*Δ (Figure 4.4D and E and Table 4.1). Mga2 is a predicted transcription regulator of fatty acid biosynthesis based on its two orthologs in budding yeast, which are involved in the regulation of OLE1 transcription (OLE1 in budding yeast is a fatty acid desaturase). Cid12 is a poly(A) polymerase.

In order to validate this result, *mga2* and *cid12* were individually deleted in a wild type background generating new isolates of these gene deletion strains (to rule out the effect of auxotrophies on the phenotype). These strains were measured in time-lapse movies (as described above), this time with increased numbers of cells: 777 cells for *mga2*Δ and 1138 cells for *cid12*Δ. The graphs of birth length against length extension for these cells can be seen in Figure 4.5, and frequency distribution plots of cell length at division in Figure 4.6. Cells deleted for *cid12* show a BL/E slope of -0.5, which is slightly higher than measured using the deletion collection strain but still less than wild type. The coefficient of variation in cell length at division is 11% around a mean of 14.8 μm. Cells deleted for *mga2* show a BL/E slope of -0.07 and a CV in length at division of 16% around a mean of 14 μm, strongly suggesting that these cells are not able to adequately sense and/or correct for size deviations that arise in the population. Both strains show a slightly reduced growth rate at the population level compared with wild type cells (slightly more pronounced in the *mga2*Δ population), as assessed by a serial dilution assay (Figure 4.6D).

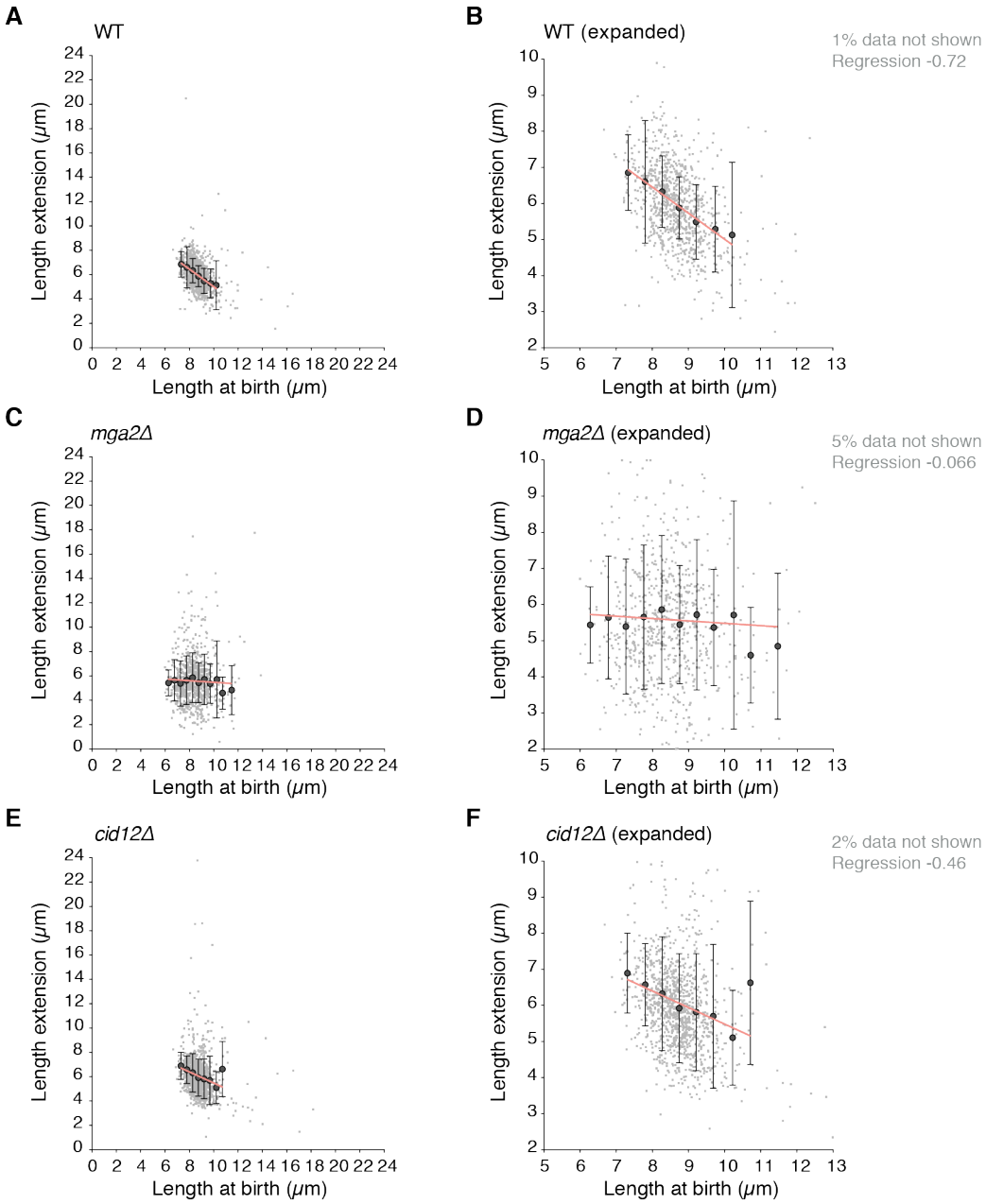

Figure 4.5|Cells deleted for *mga2* and *cid12* show reduced size homeostasis

(A),(C),(E) Cell length at birth plotted against length extension for the strains indicated. Measurements taken from brightfield time-lapse images of 750-1150 cells for each strain. Length extension calculated from birth and division length measurements. Small light grey dots show individual cells. Larger dark grey points show mean values of cohorted data. Bars represent standard deviation. All cells grown in YE4S at 32°C in a microfluidic chamber. **(B),(D),(F)** Plots as in **A**, **C** and **E**, respectively, with reduced axis scales for clarity. Percentage of data excluded shown on the right along with regression slope.

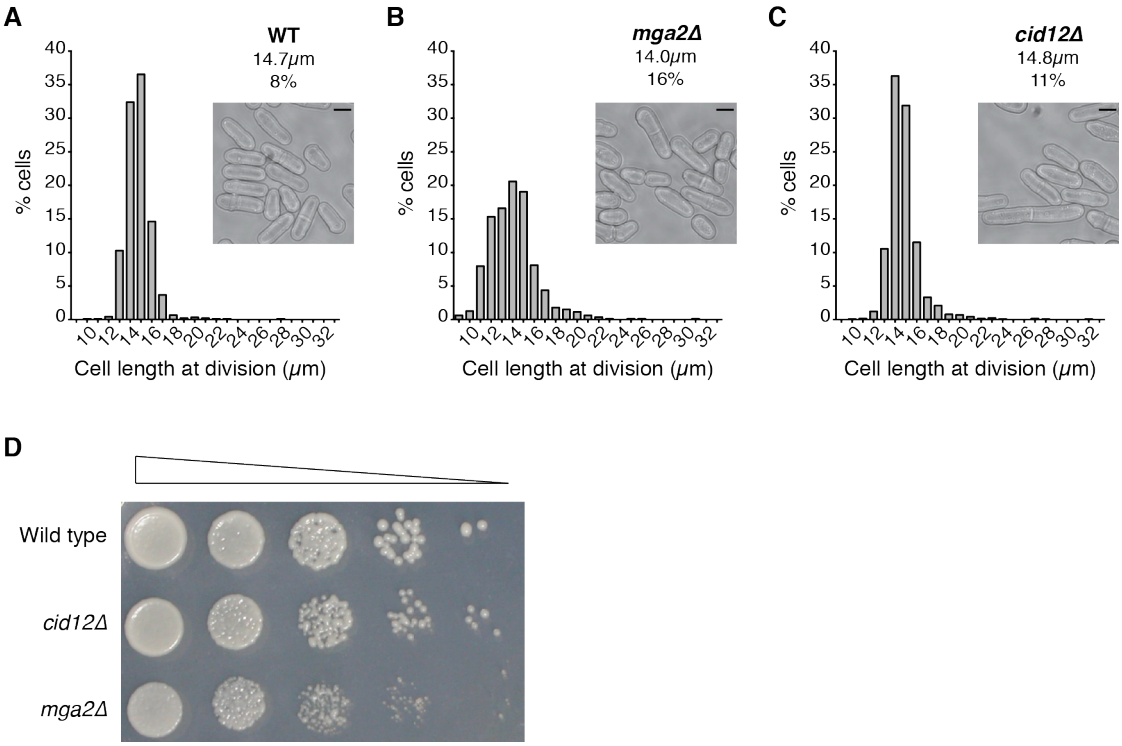

Figure 4.6|Frequency distribution of cell length at division

(A)-(C) Frequency distribution of cell length at division for WT, *mga2*Δ and *cid12*Δ, respectively. Same cells as plotted in Figure 4.5. Cells grown in YE4S at 32°C in a microfluidic plate. Bin size 1 μm. Mean cell length at division value shown, with coefficient of variation. Images show representative cells of each strain. Scale bar represents 5 μm. **(D)** Serial dilution assay showing relative growth of wild type, *cid12*Δ and *mga2*Δ on YE4S at 32°C. 10 fold dilution from $2x10^6$ cells/ml to $2x10^2$ cells/ml.

4.2.3 Cells deleted for *mga2* and *cid12* have a functional G2 size threshold

The results presented above could suggest that *mga2* and *cid12* have a role in either size sensing or correction, since deletion of either of these genes results in cells being unable to make the appropriate corrections for any size deviations that arise in the population. Another possibility is that these cells have lost the G2/M size threshold altogether and are behaving like a *wee1*Δ population, the cell cycle of which runs on a G1/S size threshold followed by a G2 timer. As discussed in the previous chapter, this G1/S sizer plus timer is not sufficient to maintain size homeostasis in *wee1*Δ cells, however a plot of birth length against cycle time for these cells shows a wild type relationship. The cycle time relationship was therefore investigated for *cid12*Δ and *mga2*Δ cells.

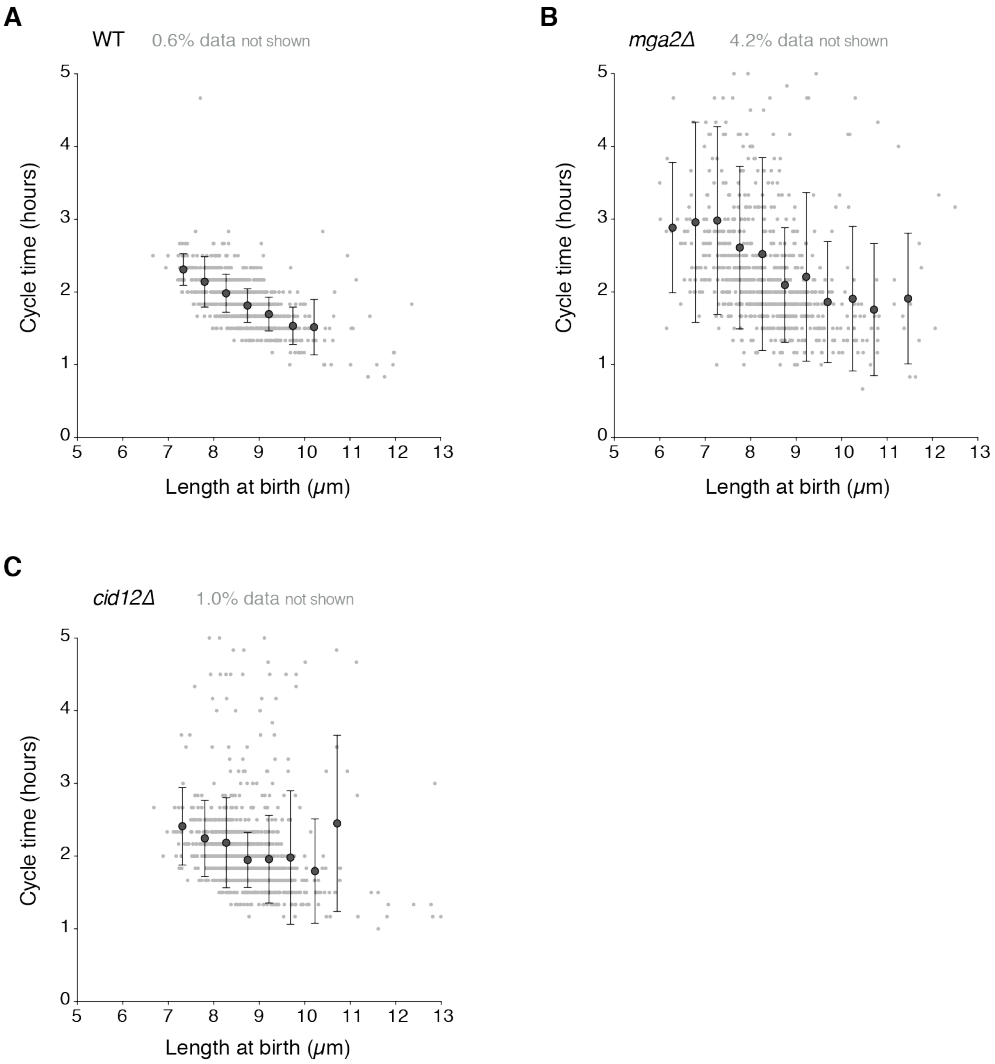

Figure 4.7|Cells deleted for *mga2* and *cid12* show reduced BL/CT relationship

(A), (B) and **(C)** Cell length at birth plotted against cycle time of the strains indicated. Cycle time calculated as the time between birth and division length measurements. Small light grey dots show individual cells. Larger dark grey points show mean values of cohorted data, bars represent standard deviation. Percentage of data not shown here for clarity is indicated. All cells grown in YE4S at 32°C or 36.5°C, as indicated, in a microfluidic chamber.

Both *mga2*Δ and *cid12*Δ cells show a weaker relationship between birth length and cycle time compared to a wild type population, with r^2 values of 0.08 and 0.03, respectively (compared to an r^2 value of 0.3 for wild type and *wee1-50* cells). This suggests that these cells are not behaving like a *wee1-50* population with a G1/S size threshold followed by a G2 timer.

In order to investigate this further, nutrient shift experiments were carried out as described in Chapter 2.2.9 with the candidates *mga2*Δ and *cid12*Δ. Shifting the cells from media containing glutamate (nitrogen-rich) to media containing proline (nitrogen-poor) shows a wild type response for both *mga2*Δ and *cid12*Δ populations. Both strains show the characteristic peak in septation index at around 1 hour suggesting that both populations have a G2/M size threshold that is responsive to changes in the surrounding nutrient conditions (Figure 4.8A and B).

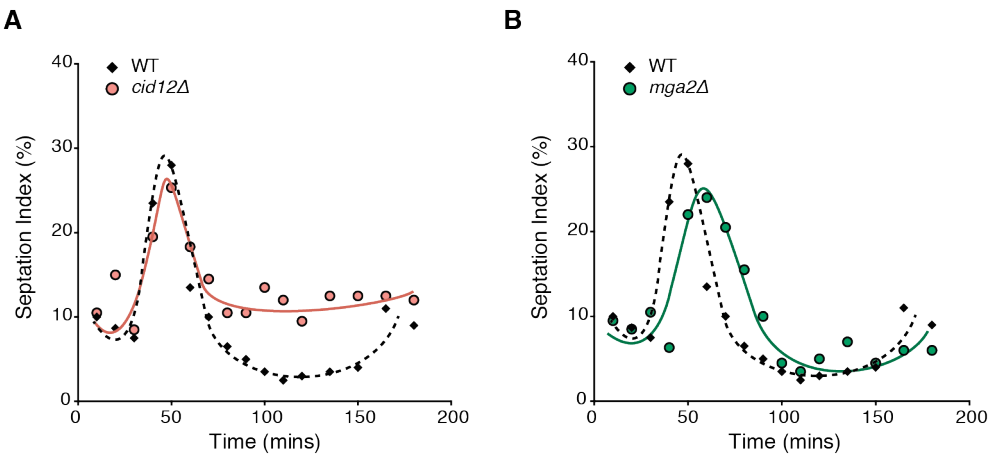

Figure 4.8|*cid12*Δ and *mga2*Δ cells have a size threshold that is responsive to changes in nutrient conditions

(A)-(B) Septation index of a *cid12*Δ and *mga2*Δ population, respectively, compared to wild type cells after nutritional shift-down from glutamate to proline as a nitrogen source. Cells grown at 32°C in EMM-N + 20 mM glutamic acid washed with EMM-N + 10 mM proline at time zero then resuspended in EMM-N + proline. Number of septated cells counted and represented as a percentage of the population.

4.2.4 Multinucleate cells deleted for *mga2* show asynchronous nuclear divisions

In order to further investigate the variability in the timing of mitotic entry in these two candidates, multinucleate cells were used. This system allows the variability to be studied in a single cell system and therefore in a common cytoplasmic environment. The nuclei in multinucleate cells have been shown in Chapter 2 to divide synchronously (Section 2.2.6). Any variability in the timing of division between different nuclei in a single cell can be identified by simply counting the numbers of nuclei within the cell. Synchronous divisions will result in cells with

one, two, four or eight nuclei. Any deviations from this indicates that some asynchrony has occurred. Since the nuclei are sharing a common environment any timing effects due to cell to cell variability can be eliminated.

The temperature-sensitive mutation *cdc11-119* was crossed into the *mga2*Δ and *cid12*Δ strains. The cells were grown at the restrictive temperature for 8 hours and images were taken after 3, 4, 7 and 8 hours. Nuclei were visualised using the ER marker SPAC1B2.03c-mCherry and the numbers of nuclei in each cell were counted and then combined across all time points for each strain. Figure 4.9A shows this quantification. Cells deleted for *cid12* show a similar response to *cid12+* cells in the cdc11-119 background, the most common numbers of nuclei per cell being two, four and eight. Very few cells have three, five, six or seven nuclei. In cells deleted for *mga2*, the most common numbers of nuclei are two and four, however there is a much higher percentage of cells with three, five and six nuclei compared to *cdc11-119* and *cid12*Δ *cdc11-119* cells.

These quantities of nuclei per cell can be annotated as either being the result of synchronous or asynchronous divisions. Cells with one, two, four or eight nuclei could either arise from successive rounds of synchronous divisions or a mixture of synchronous and/or asynchronous divisions. Cells containing three, five, six or seven nuclei on the other hand can only arise if at least one asynchronous division has occurred. A minimum estimation of asynchrony can therefore be calculated using this latter category of cells, and the percentage of these in the population is displayed in Figure 4.9B. This graph shows that *mga2*Δ *cdc11-119* cells have a higher proportion of asynchronous nuclear divisions compared to wild type and *cid12*Δ multinucleate cells.

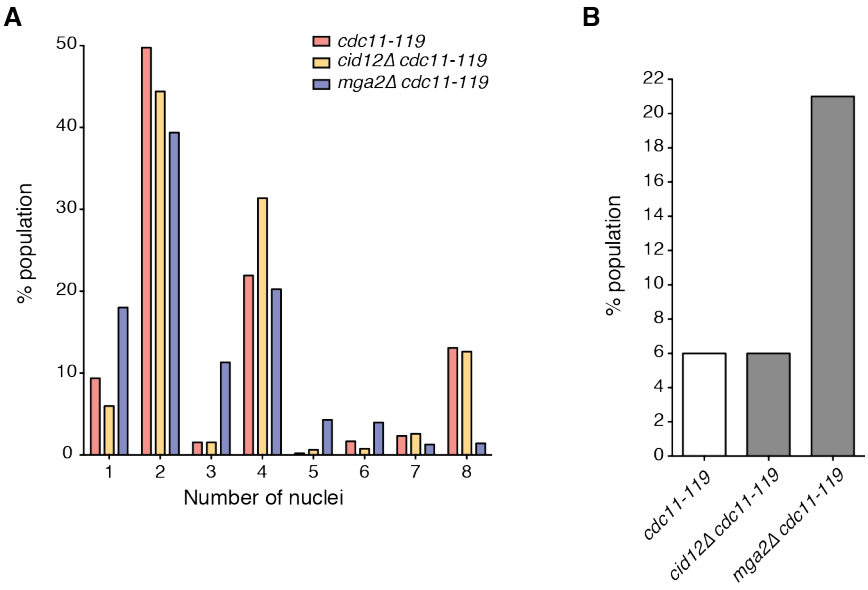

Figure 4.9|Deleting *mga2* leads to asynchronous nuclear divisions in *cdc11-119*

(A) Quantification of numbers of nuclei per cell, represented as a percentage of the population. Cells incubated at 36.5°C for a total of 8 hours, with nuclei quantified at 3, 4, 7 and 8 hour time points. Total n=600-900 cells for each strain across all time points. **(B)** Percentage of cells showing asynchronous nuclear divisions (data from **A**). A cell with 3, 5, 6 or 7 nuclei was recorded as asynchronous.

4.2.5 Mga2 is a predicted regulator of fatty acid biosynthesis

Mga2 has a predicted role in fatty acid biosynthesis through possible regulation of Ole1, as predicted by the orthologs MGA2 and SPT23 in budding yeast. To this end, Ole1-GFP was tagged in both wild type and *mga2*Δ cells (Figure 4.10A). In wild type cells, Ole1 localises to the endoplasmic reticulum and is evenly distributed between cells. In cells deleted for *mga2*, Ole1 remains localised to the ER however there is variation in the intensity of signal between cells.

This varying intensity of Ole1-GFP signal could be merely due to sick or dying cells fluorescing more intensely, however to further explore a possible link between Mga2, the ER and cell size at division, cell length studies were carried out at varying temperatures. Since the temperature can affect the fluidity of membranes within the cell (Gennis, 1989), it is possible that *mga2*Δ cells grown at different temperatures may have different degrees of variability in cell length at division. Wild type and *mga2*Δ cells were grown in complex media at 25°C, 32°C and 36°C for 36 hours in exponential phase (diluting when appropriate). The coefficient of variation in size at division for the wild type cells varies between 5.3%

and 6.9% and is not correlated with temperature (Figure 4.10B). The *mga2*Δ cells on the other hand show an increase in coefficient of variation from 13.7% at 25°C to 20.4% at 36°C (Figure 4.10B). Together with its predicted role in fatty acid biosynthesis, this suggests a possible link between the internal cellular membranes and cell length at division.

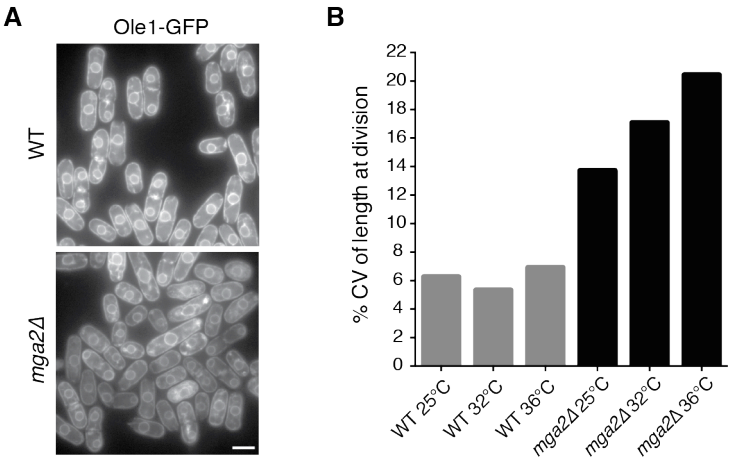

Figure 4.10|The variation in cell length at division of *mga2*Δ cells is temperature-dependent

(A) Cells tagged with Ole1-GFP. Top image wild type cells, lower image *mga2*Δ cells. Maximum intensity projections of deconvolved images. Scale bar represents 6 μm. **(B)** Coefficient of variation in cell length at division of wild type and *mga2*Δ cells incubated at various temperatures. n=80-320 cells. Cells grown in YE4S.

4.2.6 Mga2 may be acting independently of Cdc2-Tyr15 phosphorylation

In order to investigate where Mga2 may be acting at the G2/M transition, the Cdc2-Tyr15 phosphorylation and cyclin Cdc13 levels were investigated in this strain. Cells lacking *wee1* were used as a control since these cells also have increased variability in size at division and Wee1 is known to act through Tyr15 phosphorylation.

The phosphorylation levels of Cdc2 at Tyr15 are similar in *mga2*Δ cells compared to those in the wild type strain, whereas *wee1*Δ shows significantly reduced levels (Figure 4.11A and B). This suggests a role for Mga2 in the G2/M transition independent of Tyr15 phosphorylation regulation, although we cannot rule out increased variability of Tyr15 phosphorylation which would appear to be

the same mean level as wild type on a population level. Cdc13 levels remain similar across all three strains (Figure 4.11A).

To add further support to this observation with regards to the Cdc2 phosphorylation levels, variability analyses were carried out to evaluate whether the increased coefficient of variation in size at division in the *mga2*Δ strain is observed in a background containing a non-phosphorylatable Cdc2 mutant fusion protein. The strain described in Chapter 3, expressing a mutant Thr14Ala Tyr15Phe Cdc2 kinase fused to Cdc13 (Cdc13-L-Cdc2AF), was crossed into an *mga2*Δ and a *wee1*Δ background and cell length at division was measured. A control fusion strain with a wild type Cdc2 (Cdc13-L-Cdc2) was also used. Both *wee1*Δ and *mga2*Δ cells show a similar increase in variation in cell size at division, which is maintained in a wild type *cdc13-L-cdc2* background (Figure 4.11C). The non-phosphorylatable *cdc13-L-cdc2AF* strain has a coefficient of variation in cell size division of 16.2%, more than double that of the wild type fusion protein strain. Epistasis analyses using cell size variation is therefore more difficult with this strain, especially since size variation has not been studied in this way before and so it is unknown how much variation is tolerated before this becomes a lethal phenotype. Deleting *wee1* in this background increases the coefficient of variation by only 0.3% (Figure 4.11C), supporting the idea that the increased size variation in the *wee1*Δ strain is not additive and is therefore dependent on phosphorylation of Cdc2. Deleting *mga2* in the AF fusion background increases the coefficient of variation by 2.2% (Figure 4.11C). This suggests that some of the size variation seen in *mga2*Δ could be independent of tyrosine phosphorylation.

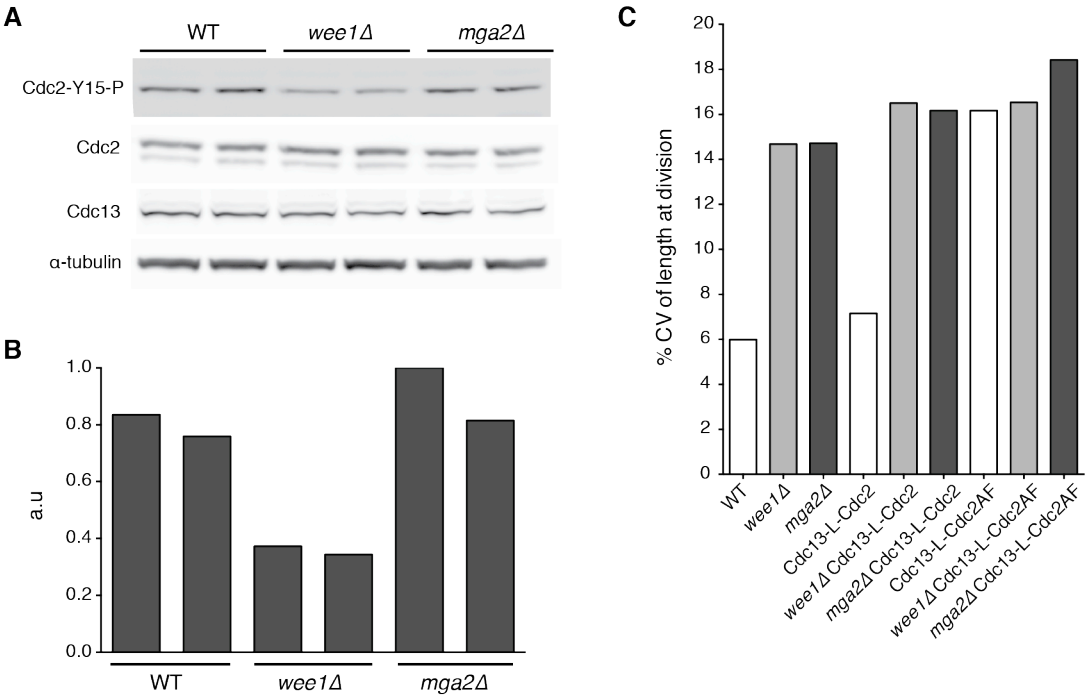

Figure 4.11|Mga2 does not appear to be acting through Tyr15 phosphorylation

(A) Western blot of total cell lysates for phosphorylated-Tyr15 Cdc2, Cdc2, Cdc13 and α-tubulin protein levels in WT, *wee1*Δ and *mga2*Δ cells. **(B)** Quantification of phosphorylated-Tyr15 Cdc2 from Western blot in **A**, normalised against Cdc2 levels. **(C)** Coefficient of variation in cell length at division for the strains indicated. Cells grown in YE4S at 32°C (*wee1+*) or 36.5°C (*wee1Δ).* n=160-600.

4.3 Discussion

4.3.1 Size variability at division can be used as a tool to identify genes involved in size control

Wild type fission yeast cells divide at a length of 14 μm with very little variation around this threshold. It is therefore hypothesised that these cells actively sense and regulate size at division to maintain a very tight distribution of sizes within a population. Work carried out as part of the investigations described in the previous chapters reveals that in addition to the threshold size at which cells enter mitosis, the variation around this threshold is an important aspect of size control in fission yeast. To this end, it was hypothesised that additional genes acting at the G2/M transition might be identified by investigating cell size variability rather than cell size thresholds alone.

A near genome-wide screen of the fission yeast haploid gene deletion collection had been previously carried out in the lab to identify new elements acting at the G2/M transition (Navarro and Nurse, 2012). The aim of this screen was to systematically search the fission yeast genome for gene deletions that advance cells into mitosis at a small cell size. Approximately 3,000 gene deletion mutants were screened and 18 genes were identified that act negatively at mitotic entry resulting in cells which divide at a smaller size compared with wild type cells. Seven of these genes had not been previously reported as cell cycle regulators and three genes were shown to act independently of Cdc2-Tyr15 phosphorylation and therefore potentially define additional uncharacterised molecular control mechanisms (Navarro and Nurse, 2012). This study demonstrated that small size mutants can be used to successfully identify genes acting at the G2/M transition.

The aim was to investigate whether size variability could be used in a similar way to reveal additional components of this key cell cycle transition, specifically probing for genes involved in size sensing. The initial screen had annotated any size phenotype associated with a gene deletion and this included increased cell size variability. The results from the study were therefore re-addressed and the 3,000 gene deletion annotations were searched for mutants with increased variability in size at division. This second screen identified 16 genes which when deleted lead to greater size variability compared with wild type and these results were validated in exponential culture. Wild type fission yeast cells maintain a coefficient of variation in cell size at division of approximately 5% and these mutants have values ranging from 6-21%. The mean cell size of the population was not important for this investigation, although using the cut-off of 1 μm from the initial screen, *sft1* and *atd1* would be classed as small size mutants. Both of these were annotated as small in the initial screen but were not carried forward for reasons not discussed here.

Of the 16 variable mutants identified, eight were chosen for further analysis. These mutants have a coefficient of variation in cell size at division of 8% or above and an even distribution of sizes around the mean. Both *dph1*Δ and *csn2*Δ were excluded due to not falling into this latter category despite having a CV of 14% and 21%, respectively. Both of these mutants show a skewed distribution towards longer cell lengths and were concluded to possibly be involved in DNA damage repair causing activation of the checkpoint and cell elongation.

4.3.2 Mga2 and Cid12 are involved in size sensing and/or correction

Single cell studies were carried out on the eight gene deletion strains chosen from the screen. An advantage of single cell studies compared to snapshots of cells growing in exponential liquid culture is the ability to observe how the variation in cell size at division arises. This investigation has until now assumed that variation observed in the length of septated cells is indicative of variation in the size at which cells enter mitosis. In turn, this is presumed to be due to cells spending a variable length of time in G2, since it has been shown previously that the adjustment of cell elongation is due to altered cell cycle times rather than altered growth rates. For one of the candidates, *mms19*, time-lapse data reveals that a possible cause of the perceived increase in size variability is cells becoming delayed in septation and continuing to elongate before cell separation. Since these cells are showing an additional length extension phenotype which could mislead the interpretation of any length data, this strain was not investigated further for this study.

The remaining seven deletion strains show wild type growth patterns and length data was used to assess size homeostasis. It has been discussed in previous chapters that a graph of birth length against length extension for wild type cells has a regression of -0.8, indicating that small cells extend more than long cells to compensate for any deviation from the average size. The small error bars suggest that within any particular cohort of birth lengths the variation in length extension is minimal, indicating that wild type cells are able to carry out the correction with relative accuracy.

Four of the variable candidates show a very similar relationship between birth length and length extension compared with the wild type cells both in terms of the regression analysis and the error bars in the cohorted data. This suggests that these strains are relatively homeostatic and are able to make the appropriate adjustments to correct for size deviations. These candidate genes are *aps1*, *atd1*, *pek1* and *sft1*. The question remains, therefore, what the cause of the variability is in these populations, if deviations from the mean are sensed and corrected for. One possibility is asymmetric divisions which, as in the *pom1*Δ population, result in variation which cannot be corrected for in one cell cycle. However a strong asymmetric division phenotype was not observed for any of these candidates. An

alternative reason could be increased variability in growth rate independent of cell size which would lead to increased size dispersion despite the appropriate corrections being made during each previous cycle.

For one of the candidates, the sequence orphan, although the relationship between birth length and length extension is close to wild type, the cohorted data shows slightly more variability in length extension within each group of birth lengths. For this strain it could be suggested that cells are able to sense for size deviations but that the correction mechanism is not as accurate as that in wild type cells.

Two candidates did not show a strong relationship between birth length and length extension. Cells deleted for *cid12*Δ and *mga2*Δ had a BL/E relationship of -0.2 and -0.03, respectively. This suggests that these genes may have a role in the control of cell size homeostasis since deviations in cell size are not rapidly corrected for in the subsequent cycle. One possibility is that these cells are extending by a given amount regardless of their initial size. This response would lead to a BL/E slope of zero corresponding to the number of micrometres by which each cell extends. This “constant adder” principle has been recently suggested for bacterial cell size homeostasis (Campos et al., 2014, Taheri-Araghi et al., 2015). This could be the case for the *cid12*Δ cells, where there is only a small amount of variation in length extension across the range of birth lengths measured. With regards to the *mga2*Δ population however, this does not seem to be the case since there is large variation in length extension, evident from the large error bars in the cohorted data compared with the other strains. This suggests that regardless of initial size, cells elongate by a seemingly random amount before dividing.

To further investigate these two genes they were deleted in a wild type background to eliminate any effect of auxotrophies (which are present in the strains of the deletion collection) and to confirm the phenotype observed. Cells deleted for *mga2* behave in a similar way to those in the collection, showing a weak relationship between birth length and length extension, with large deviations in the extent of elongation observed for any given birth length cohort. The *cid12*Δ cells show a slightly more wild type BL/E relationship compared with the data from the deletion collection strain, possibly due to the reduction of growth defects caused by auxotrophies. The prototrophic strains carrying these deletions do still show a slight growth defect, which is more pronounced in the *mga2*Δ population. This could be due to the fact that without a size correction mechanism extreme cell sizes become

lethal and therefore there could be a higher proportion of cell death in these deletion strains.

It can be concluded from this investigation that Mga2, and to a lesser extent Cid12, have a role in either the sensing or correction of cell size.

4.3.3 Mga2 and Cid12 could be involved in size control at the G2/M transition

This is not the first time a loss of size homeostasis has been observed. In the previous chapter *wee1*Δ cells are also shown to have a weak relationship between birth length and length extension. One possible reason for this is because these cells lack any G2/M size threshold and therefore the cell cycle is running on a G1/S size threshold followed by a G2 timer to mitosis. It is quite possible that the G1/S size threshold, which is not necessary in rapidly growing wild type cells, cannot achieve such accurate size measurements compared to the G2/M size checkpoint. However, since a BL/CT relationship similar to that in wild type cells is seen for a *wee1*Δ population, an alternative possibility was suggested, which is not in regards to a less accurate sizer at G1/S but due to the subsequent G2 timer which may not be sufficient to maintain such tight size control through to the onset of mitosis.

In order to investigate whether this could be the cause of the loss of size homeostasis seen in *mga2*Δ and *cid12*Δ populations, firstly BL/CT plots were analysed for these two strains. Both show a weaker relationship compared with wild type and *wee1*Δ cells. Secondly, nutrient shift experiments were carried out to test for the presence of a G2/M size threshold. As described in Chapter 2, the G2/M size threshold is sensitive to changes in local nutrient availability and can therefore be detected by shifting cells from nutrient-rich to nutrient-poor media and observing a peak in the number of septated cells, characteristic of a sub-population of cells advancing into mitosis due to the newly-reduced size threshold. In both gene deletion strains this characteristic peak in septation is observed suggesting that these cells do possess a G2/M size threshold that is sensitive to changes in nutrient conditions. This argues against a hypothesis that these cells have a *wee1*-like cell cycle and instead suggests that the size variability is due to a loss of size

control at the G2/M transition. Mga2 and Cid12 could therefore have a role in either the sensing or correction of cell size as part of a size control mechanism at the onset of mitosis.

4.3.4 Mga2 may form part of the G2/M regulation independent of Cdc2-Tyr15 phosphorylation

The screen has revealed Mga2 as the strongest candidate for being involved in size sensing at the G2/M transition. To further investigate the role of this gene in the decision to enter mitosis, multinucleate cells of the temperature-sensitive *cdc11-119* mutant were used. This enabled an investigation into whether this gene is part of a nuclear-autonomous or cytoplasmic signal to enter mitosis at a given size. Multinucleate cells deleted for *mga2* show asynchronous nuclear divisions, with an elevated frequency of trinucleate cells compared with wild type and *cid12*Δ *cdc11-119* cells. It has previously been suggested that a global signal acts in multinucleate cells to coordinate nuclear division and that Wee1 activity may be important for this (Kiang, 2010). The work here suggests that Mga2 may also be part of this global cytoplasmic signal for mitotic entry.

A clue to a possible mechanistic role for Mga2 in the control of the timing of mitotic entry comes from the role of the two orthologs in budding yeast, MGA2 and SPT23. These are ER membrane proteins involved in the regulation of the transcription of OLE1, which is required for monounsaturated fatty acid synthesis. This provides a possible link between membrane synthesis and cell cycle control. The fission yeast Ole1 tagged with GFP localises to the ER and in *mga2*Δ cells appears to have cell-to-cell variability in the intensity of the signal. It could be that this reflects a difference in the amount of membrane or perhaps a difference in the recruitment of Ole1 to the ER. This differing intensity of Ole1 signal does not seem to be dependent on cell length, however time-lapse data would be required to test whether it is related to the size of the cell at division (since cell length is no longer indicative of cell cycle stage in these cells). It could be hypothesised that the amount of membrane synthesis is linked to the cell cycle controls, so that membrane availability can influence the timing of mitosis and therefore nuclear and cell division. Cells deleted for *mga2* have increased variability in cell size at division

at higher temperatures, when membranes are predicted to be more fluid, thus suggesting a possible link between the regulation of membrane proteins and the G2/M transition.

Cdc2 tyrosine phosphorylation and cyclin levels were investigated in the *mga2*Δ strain to examine whether this gene is acting through known cell cycle regulators or through an as-yet unidentified pathway. There are no differences in the levels of the mitotic cyclin Cdc13 or the levels of Cdc2-Tyr15 phosphorylation between wild type and *mga2*Δ cells. However this is an average level of phosphorylation for the population and does not eliminate the possibility of variable Tyr15 phosphorylation within a population of *mga2*Δ cells. In order to investigate this, single cell immunofluorescence analysis would be required. However the population level data, together with genetic interaction studies using the non-phosphorylatable Cdc2 fusion protein that suggests *mga2*Δ can further increase size variability in this AF mutant background, suggests that Mga2 may be functioning independently of tyrosine phosphorylation. However, in light of the investigations carried out in Chapter 3, which suggest that the Cdc2AF mutation may lead to a different size control system altogether, this analysis with *mga2*Δ requires further investigation.

Chapter 5. General Discussion

Wild type fission yeast cells growing in nutrient rich conditions have a cell cycle of approximately 2 hours. After nuclear division cells enter G1 whilst they are binucleate (Nurse, 1975). Since the size threshold to enter S phase is already surpassed, G1 is short and cells enter S phase and undergo cytokinesis (Nurse and Thuriaux, 1977). Between nuclear division and cytokinesis cells are in the constant length phase and therefore no elongation occurs (Mitchison, 1957). Daughter cells are born in G2 at around 8 μm and spend time in G2 elongating in order to reach the required size to enter mitosis (Fantes and Nurse, 1977). Cells enter mitosis at 14μm with very little variation around this (Sveiczer et al., 1996). The major question surrounding the work in this thesis is how do cells measure their size in order to accurately divide at 14μm?

5.1 Using cell size homeostasis as a tool to study size control

The work presented here has focused on the use of cell size variability and size homeostasis analysis to investigate the cell size control mechanism in fission yeast. This has been a novel approach for identifying new cell size regulators and has revealed additional information regarding the components currently thought to be involved in cell size control at the G2/M transition. The idea behind this approach has been to move away from the classic cell size mutant analyses, which have been very successful in the past in the identification of genes involved in the coordination of cell growth and division (Nurse, 1975, Nurse et al., 1976). The hypothesis behind the work here was that despite the success of using size mutants to study this problem, a different technique may reveal additional information regarding the roles of genes thought to act at the G2/M transition and perhaps identify new components altogether, which may not be possible using size mutant analysis alone.

Rather than using the mean cell size of a population to look for mutant backgrounds which lead to increased or decreased cell sizes, the approach used here has therefore focused on the variability of cell sizes around the mean. The idea is that a population of cells which lacks size regulation may rely on a more

stochastic regulation of cell growth and division which could lead to a greater variation in cell size at division. Measurements of cell size at birth and at division can be used to investigate this at a single cell level and this has been the basis for the size homeostasis studies.

Within any population of cells, size deviations can arise naturally due to processes such as asymmetric divisions, the activation of a cell cycle checkpoint, or perhaps differences in cell growth rates (which, as we have shown here, are not inherited and could therefore be envisaged to arise stochastically within the population). In order to assess how rapidly these size deviations are corrected, an analysis of birth length and length extension can be carried out (Fantes, 1977). If a population of cells has rapid size homeostasis, meaning that cell size deviations are sensed and corrected for within one cell cycle, a graph of birth length against length extension (BL/E) will have a slope of -1. This means that for every 1μm either side of the mean that a cell is born, the subsequent length extension will be 1μm in the counteracting direction. This correction has been shown here and by others to be due to altered cycle times rather than altered growth rates (Fantes, 1977). Cells therefore sense that a size correction is required and alter the time spent in the subsequent cell cycle accordingly.

With the experimental conditions used in the studies described here, wild type cells have a BL/E slope of around -0.8. Therefore in wild type cells, size deviations are rapidly corrected within almost one cell cycle. Importantly, the addition of a cell cycle block to increase the birth length of wild type cells shows that cells born above a certain size, around 11μm, are no longer able to make cycle time or length extension corrections. This is thought to be due to an incompressible portion of the cell cycle during which the cell must make the appropriate preparations for mitosis (this part of the cycle is later referred to as the G2 timer). For these cells, size deviations will therefore take longer than one cell cycle to be corrected.

This type of size homeostasis analysis was used to screen the non-essential gene deletion collection for genes that might be involved in size sensing or correction. An initial visual screen was carried out on a group of deletions that had been previously annotated as having a variable size phenotype (Navarro and Nurse, 2012). This phenotype was then further investigated using single cell studies of size homeostasis.

This screen identified three potential candidates. The strongest candidate is Mga2, a predicted transcription regulator of fatty acid biosynthesis based on its orthologs in budding yeast. The other two candidates are a sequence orphan and a polyA polymerase, Cid12. The sequence orphan (SPBC557.02c), although showing an almost wild type slope on the BL/E graph, shows much greater variation in the length extension values for any given birth length. A possibility is that these cells are able to sense size deviations, however the correction mechanism is less accurate compared to wild type cells. Perhaps this gene could have a role upstream of Wee1 and feed information from a size sensing pathway into the cell cycle controls. Cells deleted for *cid12* show less size homeostasis compared to the wild type population and it is possible that its role in gene expression means that it could regulate another protein or group of proteins that is/are involved in cell size control. Mga2 however was the strongest candidate from this screen and this gene will be discussed in more detail in section 5.4.

Before considering this potential novel regulator of cell size, this discussion will first explore previously identified cell cycle regulators and their role in cell size homeostasis.

5.2 The control of cell size homeostasis

5.2.1 Pom1 and Nif1 are not essential for size sensing and correction

When work for this thesis began, the current model of size control involved the protein kinase Pom1, a gradient of which was hypothesised to act as a measure of cell size and relieve inhibition of mitotic entry only when cells reach a certain length (Martin and Berthelot-Grosjean, 2009, Moseley et al., 2009). The size sensing pathway was described as follows. Pom1, possibly together with another protein, Nif1, forms polar gradients along the length of the cell, enriched at the cell tips. In short G2 cells, Pom1 concentration in the cell middle is high enough to inhibit the mitotic activators Cdr1 and Cdr2, present in cortical nodes at the cell midline. Progression of cells through G2, coupled to cell elongation, results in late G2 cells having a lower concentration of Pom1 in the cell middle. Below a certain threshold Cdr1 and Cdr2 are activated and they therefore inhibit Wee1, which

relieves the inhibition of Cdc2 and allows active CDK to drive the cell into mitosis (Martin and Berthelot-Grosjean, 2009, Moseley et al., 2009).

Supporting this model is the size phenotype of *pom1*Δ and *nif1*Δ mutants. Single mutants divide at a smaller cell size compared with wild type cells and the additive phenotype of the double *pom1*Δ*nif1*Δ mutant suggests that these genes are working independently to regulate cell size at division. The aim of the work presented here was to further study the roles of these genes in cell size sensing by investigating whether or not Pom1 and Nif1 are required for size homeostasis.

The data discussed in Chapter 2 shows that neither Pom1 nor Nif1 is essential for a population of cells to maintain size homeostasis. Birth length plotted against length extension and cycle time for *pom1*Δ, *nif1*Δ, and *pom1*Δ*nif1*Δ cells shows that small cells spend longer in the subsequent cell cycle and therefore extend more than longer cells in order to attain the correct size at division. The populations therefore rapidly correct for any size deviations that arise. A loss of this relationship is seen for cells born longer than around 8μm for *pom1*Δ cells and 7μm for *pom1*Δ*nif1*Δ cells. It is hypothesised that this is due to the incompressible G2, a portion of the cell cycle that runs on a timer and is the minimum time that a cell can spend in G2 in order to make the necessary preparations to enter mitosis. From the graphs of birth length against cycle time this seems to correspond to a cycle time of roughly 1 hour. For cells above a certain size this G2 timer means that the cycle cannot be compressed any further and therefore size correction will take longer than one cell cycle to bring the cell back to its average size. The nature and implication of this G2 timer will be discussed in more detail in a later section of this discussion.

5.2.2 A G1/S size threshold plus G2 timer cannot maintain wild type cell size homeostasis

Since Pom1 and Nif1 are acting upstream of Wee1, the next stage of the investigation was to study size homeostasis in cells lacking Wee1 activity. A similar study was carried out in 1996, which showed that *wee1*Δ cells have a birth length/length extension relationship of -1, suggesting that size deviations are corrected within one cell cycle (*wee1-50* cells were shown to have a BL/E slope of

-0.55 however no explanation for this difference was provided) (Sveiczer et al., 1996). However when this experiment was repeated here, the BL/E relationship was found to be -0.3 for both *wee1*Δ and *wee1-50* cells. A possible reason for this difference is the much larger number of cells analysed in this study, which is around 7 times the number of cells analysed in the 1996 paper (Sveiczer et al., 1996). This enabled data to be collected over almost twice the birth length range compared to the previous analysis. During the process of analysing the data for this thesis it became clear that in order to obtain meaningful and interpretable data from single cell studies such as these, a large data set was required. With 100-200 cells the BL/E relationships were sometimes not as apparent as when 700-800 were measured. The difference in the data could therefore be due to the fewer number of cells and therefore the smaller range of birth lengths analysed in the 2006 study. An alternative possibility is that size homeostasis in these cells is affected by the media conditions that the cells are growing in. The experiments outlined here were all carried out in yeast extract complex media, whereas the 1996 study used minimal media (Sveiczer et al., 1996). Although there has been no indication that nutrients should alter cell size control at this level, it would be important to repeat these experiments in EMM before ruling out a possible nutrient effect.

The results from the investigation presented here suggest that cells lacking *wee1* are not able to rapidly correct for size deviations. However, the graph of birth length against cycle time for *wee1-50* and *wee1*Δ strains shows a wild type relationship whereby small cells spend longer in the subsequent cell cycle. Wee1 is a major component of the G2/M transition and cells lacking this gene divide prematurely at a small cell size (Nurse, 1975). It was *wee1-50* cells growing at the restrictive temperature which first led to the identification of an additional size control point at the G1/S transition (Fantes and Nurse, 1978, Nurse and Thuriaux, 1977). Since these cells are born at almost half the size of wild type cells, *wee1-50* cells must extend the time spent in G1 in order to grow to surpass the size threshold to enter S phase. This normally cryptic size threshold is therefore observed in *wee1-50* and *wee1*Δ cells and is characterised by an extended G1 phase. These cells lack a G2/M size control and therefore the G2 phase is short and is thought to be limited to the incompressible G2 timer (Fantes and Nurse, 1978).

The weak size homeostasis seen in cells lacking *wee1* activity suggests that the G1/S size threshold followed by a G2 timer is not sufficient to maintain size homeostasis within a population. From the BL/CT data, which shows a wild type relationship, it is possible that size corrections are being carried out in G1 so that very short cells extend their G1 more than longer cells in order to make the appropriate correction. However these corrections may not be seen in the measurements taken at septation due to the subsequent G2 timer period, during which, if it indeed does act as a fixed timer, smaller cells will extend less than longer cells due to the pseudo-exponential growth of fission yeast cells (Baumgartner and Tolic-Norrelykke, 2009, Creanor and Mitchison, 1982, Mitchison, 2003).

The G2 timer has not been extensively studied and was initially proposed based on nutritional shifts and S phase delay experiments (Fantes and Nurse, 1978). The data from these studies were consistent with a constant timer period connecting S phase and nuclear division in *wee1-50 cells*. It was therefore suggested that part of the G2 period is dispensable in wild type cells but that this part of the cycle cannot be indefinitely shortened, and in *wee1-50* cells it is at its minimum. Further studies would be important to investigate in more detail whether this is a truly fixed period of the cell cycle or whether its timing could depend on cell size or nutrient conditions for example. This would have important consequences for the interpretation of the results presented here.

An alternative possibility for the weak size homeostasis seen in *wee1-50* and *wee1*Δ cells is that due to the small size of these cells, cells that are born at the lower end of the range of birth sizes (perhaps below 6μm) are not able to immediately establish polarised growth. Since these cells will be almost spherical in shape, it is possible that there is a delay in the establishment of polarity and therefore the delivery of actin to the cell ends. If cell growth were to continue during this delay, cells may increase in volume but this will not translate into an elongation of cell length and will therefore not be seen in the experimental measurements. If this were the case however cell width might be expected to increase and a limited analysis of cell width in *wee1-50* cells suggests that this is not the case.

Another possibility is that during this delay in establishing polarised growth, the cell does not increase in volume at all. In this case small cells would be expected to show an increase in density which correlates with the G1 delay. Rather

than measuring cell size directly, this would require the G1/S transition to measure another factor of cell growth such as the accumulation of a specific transcript or protein, or perhaps total protein content. Therefore in order to attain the requirement for G1/S, smaller cells would delay in G1 in order to accumulate this factor/factors while not increasing in cell length or cell volume due to a delay in establishing polarised growth. In order to test this further, cells that are within the wild type size range but lacking Wee1 activity were investigated using the Cdc13-L-Cdc2 fusion protein strain. When Wee1 activity is removed from these cells they are not reduced to the size of *wee1-50* or *wee1*Δ cells, possibly due to the *cig1*Δ*cig2*Δ*puc1*Δ deletions (Martin-Castellanos et al., 2000). The idea was that if the weakened BL/E relationship is merely due to the small size of these cells, larger cells lacking Wee1 activity might show a more wild type response. This was not the case however and despite having a wild type range of birth lengths, these Cdc13-L-Cdc2 *wee1*Δ cells show a very similar BL/E response to *wee1*Δ cells with wild type copies of Cdc13 and Cdc2.

The model that most closely fits the data is therefore that in cells lacking Wee1 activity, and hence the G2/M size threshold, size correction occurs at the G1/S transition. A checkpoint upon entry into S phase acts to measure cell size (possibly cell length, cell volume or another indicator of cell size) and delay cells in G1 until they have surpassed the size threshold. On entry into S phase and subsequently G2, there will remain a variation of cell sizes due to the stochasticity of these processes and the range of larger cells already large enough to surpass the G1/S threshold. Since there is no G2/M size threshold in these cells, the idea is that G2 consists of a fixed timer period, after which cells enter mitosis regardless of their size. Due to the pseudo-exponential nature of fission yeast cell growth, the shorter cells will acquire less mass during this fixed timer compared with the longer cells. This could act to mask the earlier length corrections at the G1/S transition, since the experimental measurements are taken at septation, after this G2 timer period.

This suggests that a G1/S size control plus a G2 timer is not sufficient to maintain an efficient size homeostasis in fission yeast cells, although weak size homeostasis still takes place.

5.2.3 The Cdc2AF mutation seems to bypass the need for Wee1 in size homeostasis

The next stage of the investigation involved studying a simplified cell cycle in a system in which much of the core cell cycle machinery has been removed (Coudreuse and Nurse, 2010). Here, a fusion protein Cdc13-L-Cdc2 is able to drive the cell cycle in the absence of wild type copies of *cdc13* and *cdc2* in addition to the other mitotic cyclins, *cig1*, *cig2* and *puc1*. This strain is also able to tolerate a mutant Thr14Ala Tyr15Phe (AF) Cdc2 kinase, a mutation which is lethal in a wild type cell. This Cdc13-L-Cdc2AF protein therefore lacks any regulation through the phosphorylation of the Thr14 and Tyr15 residues and as a consequence lacks any input from the Wee1 and Mik1 kinases. The prediction is therefore that this strain should respond in a manner similar to *wee1*Δ cells, whereby there is only a weak relationship between length at birth and length extension and therefore that the cells are unable to maintain wild type size homeostasis.

However, size homeostasis analysis carried out on the AF fusion protein strain shows a wild type relationship between length at birth and length extension. From this result it is possible that Wee1 could have an as yet unidentified role in the cell cycle, which is independent of Cdc2-Tyr15 phosphorylation. However the observed BL/E relationship in these AF cells is not significantly different to wild type cells with or without Wee1, which implies that this is not the case. This suggests that these AF fusion protein cells may be relying on a different mechanism to maintain size homeostasis that does not require Cdc2-Tyr15 phosphorylation or Wee1 activity.

This finding could have implications for the investigations carried out both here and in other recent work. If the Cdc2AF mutation allows these cells to bypass the requirement of Cdc2-Tyr15 phosphorylation in size control, this could complicate the results of epistasis analyses carried out in this Cdc2AF background. For example both here and in a recent study (Navarro and Nurse, 2012), the AF fusion background has been used to investigate whether a gene might act through Cdc2-Tyr15 phosphorylation, which is currently the major input for information into CDK control at the G2/M transition. This has been favourable over genetic interaction studies using *wee1-50* since it can also bypass the requirement for Mik1 kinase. However, if this AF fusion protein strain can maintain size control through

an alternative mechanism, if a gene is found to have an effect in this AF background it cannot be concluded that this gene is acting independently of Wee1 and Cdc2-Tyr15 phosphorylation in wild type cells. Therefore a closer analysis of the controls operating within the AF fusion protein strain is required in order to understand how size information is being processed in these cells.

5.2.4 Further work

Further investigations could be carried out in order to assess whether the weakened size homeostasis seen in cells lacking Wee1 activity is due to the fixed G2 timer period and the nature of the pseudo-exponential growth of fission yeast cells. If a marker of the G1/S transition could be used to visualise the timing of the onset of S phase, experimental measurements could be carried out to investigate size homeostasis at this point in the cell cycle, before cells enter the G2 period. If a relationship between length at birth and length extension during G1 was seen, it could be concluded with greater certainty that a G1/S size control is able to sense and correct for size deviations. This would support the earlier idea that the weakened size homeostasis seen in these *wee1-50* and *wee1*Δ cells is due to the fixed G2 timer during which small cells elongate less than longer cells, which acts to reduce any homeostatic response at the onset of S phase. An alternative investigation could involve measuring the length of G1 in short *wee1*Δ cells compared to long *wee1*Δ cells, since if the above hypothesis is true, shorter cells should spend longer in G1 in order to correct for size deviations. This could be investigated using an Imaging Flow Cytometer, which can measure DNA content and also measure cell length from the images acquired (Patterson et al., 2015). The advantage of this analysis is that using a Flow Cytometer would greatly increase the numbers of cells that can be analysed.

If it were found that cells do not have size homeostasis at the G1/S transition according to cell size measurements, it would be interesting to explore the idea of cells growing in G1 without growing in volume. In this case, cells would be expected to increase in density and protein content. Cell density has been previously measured using interference microscopy (Mitchison et al., 1956, Mitchison, 1957) and a suspended microchannel resonator (SMR) (Bryan et al.,

2010, Godin et al., 2010), although the latter has not yet been done in fission yeast. Digital holographic microscopy however has been demonstrated to be a useful tool for deriving dry mass production in *S. pombe* cells (Rappaz et al., 2009). Alternatively individual protein levels could be analysed by immunofluorescence (targeting specific proteins) or total protein amounts could be observed using a fluorescein dye. Alternatively perhaps mass spectrometry could measure the global or specific protein content of small versus long G1 cells.

5.3 The role of Pom1 and Nif1 in the cell cycle

The conclusion from the data presented in Chapter 2 and discussed above is that Pom1 and Nif1 are not the major sensors of cell size, since in the absence of these genes, cells are able to sense and correct for size deviations that naturally arise in the population.

Whilst work for this thesis was being carried out, work was published hypothesising a number of alternative size sensing models (Bhatia et al., 2014, Deng et al., 2014, Pan et al., 2014). Both in the work here and in the recent studies it has been found that the band of cortical nodes increases in width with increasing cell length (Bhatia et al., 2014, Pan et al., 2014). One model postulates that the increasing length of the Cdr2 cortical node domain, together with the Pom1 gradient, could act to measure the length of the cell (Bhatia et al., 2014). Another model postulates that cell size could be measured through the ratio of Pom1-bound cortex to total cortex, which diminishes as cells elongate (Bhatia et al., 2014). Both of these models however are not supported by the data presented here since they describe Pom1 as the major player in the size sensing mechanism. An alternative model has been described which places more focus on the cortical nodes containing Cdr2 (Pan et al., 2014). This alternative model states that Cdr2 probes the surface area of the cell and feeds this information into the medial cortex and cell cycle controls. Since I have suggested here that Pom1 is not a major component of the size sensing mechanism, this model, placing Cdr2 as the major size sensor, is not incompatible with my data.

An alternative hypothesis is that Pom1 and Nif1 are acting together with the cortical nodes to ensure that there is a minimum size below which nuclear division

cannot occur (Wood and Nurse, 2013). In this instance, Pom1 is not acting directly to *sense* cell size, but is acting to *set* a threshold size for entry into mitosis. Since these cells are rod-shaped and restricted to a cell width of 4μm, the polarity of spindle formation must be aligned along the length of the cell. It could be suggested, therefore, that a minimum cell length must be set in order to ensure that there is enough cytoplasmic space to fully separate the two nuclei and leave enough space for septum formation. The high levels of Pom1 and Nif1 at the cell tips would also act to prevent nuclear division occurring too near the cell tips in the case of a mis-positioned off-centre nucleus. In order to test this, an analysis could be carried out whereby the nucleus is displaced from the centre of the cell towards the cell tip by MBC treatment and centrifugation. Tracing the subsequent nuclear division by time-lapse microscopy in WT versus *pom1*Δ cells may reveal whether Pom1 is acting to inhibit nuclear division close to the cell ends.

Lastly, Pom1 and Nif1 may not be involved in size control at all and may simply affect the levels of active CDK (perhaps acting as a buffer for additional signals such as stress or nutrient conditions), which indirectly affects the size at which cells enter mitosis (Bhatia et al., 2014, Wood and Nurse, 2013).

5.4 The role of Mga2 in cell size homeostasis

As discussed at the beginning of this chapter, a screen was carried out to look for non-essential genes which when deleted result in greater variability in cell size at division and cause cells to show a weaker size homeostatic response. Mga2 and Cid12 were candidates from this screen and both genes could act as regulators of other transcripts involved in cell size sensing.

5.4.1 Mga2 is essential for size homeostasis

The strongest candidate from the screen was Mga2. Mga2 is a predicted transcription regulator of fatty acid biosynthesis due to the role of its orthologs, MGA2 and SPT23, in budding yeast which regulate the transcription of OLE1 (Chellappa et al., 2001, Kandasamy et al., 2004). The birth length and length extension data of *mga2*Δ cells suggest that regardless of the size that a cell is born

it will extend by a seemingly random, stochastic amount in the subsequent cell cycle. The spread of the data is similar to that seen in the *wee1*Δ population, albeit over a larger range of birth lengths, and the regression slope is less than that of the *wee1*Δ population. Unlike the *wee1*Δ cells however, the relationship between birth length and cycle time is not as strong as wild type cells and the standard error bars of the cohorted data show a large variation of cycle times for any given birth length. Together with the nutrient shift experiment suggesting that *mga2*Δ cells possess a G2/M size threshold that is responsive to changes in nutrient conditions, these data suggest that deleting *mga2* results in loss of size homeostasis at a G2/M size threshold rather than during a G2 timer. In order to further investigate this, an S phase marker could be used to visualise the G1/S transition and confirm that the variability is occurring in G2 rather than G1.

The growth rate of a population of *mga2*Δ cells is slower than a wild type population and is more variable between different colonies. This may be influenced by the lack of size homeostasis in these cells. Cells that are born small are not able to sense and correct for this, therefore in the subsequent cell cycle if they do not extend by enough to allow full separation of the daughter nuclei the likelihood of cell death, by mitotic catastrophe for example, is increased. This is supported by the single cell cycle time data from the time-lapse films which show a shorter generation time for some cells than that measured by optical density of liquid cultures. This therefore suggests increased cell death in *mga2*Δ populations compared to wild type and it would be interesting to look at this directly.

An analysis of multinucleate cells enabled a study of the variability in the timing of mitosis in the absence of any cell-to-cell growth rate differences. By studying multiple nuclei in the same cytoplasmic environment, any timing effects caused by differing growth rates could be minimised. This analysis shows that in an *mga2*Δ *cdc11-119* multinucleate cell, nuclear divisions are not synchronous, which they are in a WT *cdc11-119* cell. One possibility is that the synchrony in wild type cells is due to a global cytoplasmic signal which acts to coordinate mitotic entry. This would suggest that Mga2 has a role in this global signal, possibly upstream of Wee1, the deletion of which has also been shown to disrupt the synchrony of nuclear divisions (Kiang, 2010). In this case, it would be interesting to use time-lapse microscopy to observe the divisions and the relationship between nuclear

position and the timing of mitosis. In the absence of a global cytoplasmic signal the roles of the polar Pom1 and Nif1 proteins could also be investigated more directly.

Another possibility is that the synchrony seen in wild type cells is nuclear autonomous and due to the very little variation in the timing of mitotic entry. In this case Mga2 would have a more local role within or directly surrounding each nucleus to control the timing of mitotic entry. In the first instance an investigation of the localisation of Mga2 in multinucleate cells may shed light on these two possibilities.

Further investigation is required to analyse how Mga2 might be feeding size information into the cell cycle controls. The usual method for finding which pathway a gene is acting in is to use genetic interaction studies and this has been instrumental in the annotation of the current size sensing and nutrient sensing pathways feeding into Cdc2 and mitotic entry. Epistasis analyses in this case have been more complicated due to the subtle phenotype: cell size differences are more easily analysed than size variability differences. Preliminary analysis presented in Chapter 4 suggests that Mga2 may be acting independently of Cdc2-Tyr15 phosphorylation, however further research is required to support this hypothesis.

5.4.2 The role of fatty acid biosynthesis in cell size control

One hypothesis from the data presented here is that Mga2 could provide a link between the cellular membranes and cell size control. It could be envisaged that a size sensing mechanism acts to measure the amount of available membrane, perhaps the ER, and coordinate cell growth with cell division accordingly such that a cell is able to tightly control its cytoplasmic volume and hence its cell size. In the first instance it would be important to carry out time-lapse experiments with a membrane marker such as SPAC1B2.03c or Ole1 in order to investigate whether the variability in fluorescence seen in a population of *mga2*Δ cells (be this in overall membrane amount or in the amounts of a specific membrane component such as Ole1 itself) correlates with cell size at division. It would also be interesting to investigate whether Mga2 is a transcriptional regulator of Ole1 in fission yeast.

Another important link to make here is the coordination of cell size with nuclear size. Since fission yeast cells show a constant nucleocytoplasmic ratio of

8%, this suggests tight control between the pathway sensing cell size and that controlling the size of the nucleus (Neumann and Nurse, 2007). It is possible that membranes form a link between these two pathways since the outer nuclear membrane is continuous with the ER and therefore if the ER is somehow involved in a cell size sensing mechanism it could be envisaged that this could be tightly linked to nuclear size control.

5.5 Multinucleate cells as a tool to study the timing of mitosis

Throughout the work presented in this thesis, multinucleate cells of the temperature-sensitive *cdc11-119* strain have been used to study the timing of nuclear division in different genetic backgrounds. These cells have been an invaluable tool to study the control of mitotic entry in a single cytoplasmic environment and therefore in the absence of any cell to cell differences in factors such as nutrient availability, growth rate and absolute cell size and shape. Preliminary analysis, along with data from an earlier thesis published in the lab (Kiang, 2010), has suggested that a global control could act to synchronise the timing of nuclear divisions and that this may require Wee1 and Mga2.

One hypothesis put forward to test the roles of polar Pom1 and Nif1 proteins in the timing of the G2/M transition was to use multinucleate cells to investigate whether the inner nuclei (which should be sensing lower concentrations of these proteins) divide before the outer nuclei. In light of the results from the *mga2*Δ*cdc11-119* cells, which show asynchronous nuclear divisions within a common cytoplasm, it may be possible to disrupt a potential global signal synchronising the timing of nuclear division. Time-lapse studies could be used to then investigate whether in this situation the difference in the timing of mitosis is dependent on the relative positions of the nuclei within the elongated cell. Nuclear displacement experiments could also be carried out to position nuclei closer to the cell tips to observe whether position can directly influence the timing of mitosis.

5.6 Experimental measures used to study cell size control

An additional question that should be addressed here is whether it is time to move away from the traditional studies of cell length to more direct measures of cell size such as cell volume or cell surface area, or even cell mass or protein content.

Cell length has been an excellent tool until now to study cell size since in the rod-shaped cells of *S. pombe* cell length is proportional to cell volume and is also indicative of cell cycle stage (Mitchison, 1957). The major advantage of using cell length is that it is easy and quick to measure and requires only brightfield images of cells. However, in light of new technologies it should be assessed whether or not it might be beneficial to turn to a more direct analysis of cell size, which would leave room for size sensing models to be less focused on cell length.

For instance, a recent paper has suggested that cells are not measuring cell length or cell volume but cell surface area (Pan et al., 2014). By focusing so heavily on cell length to test our ideas it is possible that we may miss other possible mechanisms of size control. In addition to this, if we are to try and extend our idea to size sensing in other organisms this adds another reason to turn from cell length measures to cell volume or protein content analysis.

The data discussed here has also highlighted a need to not only focus on size control at entry into mitosis but to also look at other control points in the cell cycle, namely the G1/S transition. In order to form a wider picture of size control it will be useful to study the controls operating in G1, especially since it is here, at ‘Start’, when most other eukaryotic cells are shown to have size control.

5.7 Concluding remarks

Despite being such a long-studied and central question in cell biology, the mechanisms of cell size control have remained elusive. Understanding this problem has been made difficult by the complexities involved in unpicking the intricate control system. Cell size can be influenced by many different factors and for a long time experiments have been limited by technology.

The fission yeast *Schizosaccharomyces pombe* has served as an excellent model system for studying cell cycle transitions due to its regular geometry and

tractable genetics. Though it had been thought that the major size sensing system may have been identified in this organism, the situation has become once again more complicated by the data presented here which suggests that an alternative mechanism is likely to be operating either instead of or alongside this proposed model.

Cell size homeostasis studies have given us a new insight into this problem and have revealed additional information regarding the current components of the G2/M transition in addition to identifying potentially novel candidates which may be acting to coordinate cell growth with cell division.

Chapter 6. Materials and Methods

6.1 Yeast strains and growth conditions

6.1.1 Strains

Strains used are listed in Table 6.1. Strains were constructed by gene tagging or gene deletion performed by PCR and homologous recombination (outlined below and described in (Bahler et al., 1998)).

6.1.1.1 Gene fragment construction

Gene targeting oligos were designed using the 'Gene deletion' and 'C-terminal tagging' links on the Bähler lab website (Resources) and purchased from Sigma.

6.1.1.2 Yeast transformation

Cells were pelleted (around 3 x10^7 per transformation), washed in dH_2O and LiAc-TE and resuspended in 100 µl LiAc-TE. Added to this were 2 µl carrier DNA (12 mg/ml boiled sperm DNA, Sigma) and around 3 µg DNA fragment. Cells were incubated at room temperature for 10 minutes. 260 µl 40% PEG/LiAc-TE was added and cells were incubated for 1 hour at 29°C. Cells were heatshocked at 42°C for 5 minutes with 43 µl DMSO. After washing with dH_20 cells were resuspended in 150 µl dH_20 and plated onto either YE4S or nutrient selection plates, in duplicate.
LiAc-TE: 0.1 M lithium acetate, 10 mM Tris pH 7.5, 1 mM EDTA.
LiAc-TE-PEG: LiAc-TE, 40% (w/v) PEG4000 (Fisher Scientific).

6.1.1.3 Genetic crosses

Genotypes were combined by genetic crosses carried out on malt extract agar supplemented with L-Histidine, L-Leucine, Adenine and Uridine followed by either tetrad dissection or random spore analysis (cross product incubated with β-

glucuronidase from Helix pomatia (Invitrogen) at 29°C for >6 hours). Gene deletions and tags were verified by colony PCR.

6.1.2 Growth conditions

S.pombe media and methods used are described in Moreno *et al.* (Moreno et al., 1991). All cells were grown at 32°C in yeast extract complex media supplemented with 0.15 mg/ml L-Histidine, L-Leucine, Adenine and Uridine (YE4S), unless otherwise stated.

6.1.2.1 Generation of multinucleate cells

For the generation of multinucleate cells, strains with the temperature-sensitive *cdc11-119* allele were used. Incubation at the restrictive temperature, 36.5°C, results in cells undergoing rounds of nuclear division without cytokinesis.

6.1.2.2 Hydroxyurea treatment

For hydroxyurea treatment, cells were grown at 32°C in minimal media (EMM) supplemented with 0.15 mg/ml L-Histidine, L-Leucine, Adenine and Uridine (EMM4S). Hydroxyurea (Sigma) was added at a final concentration of 11 mM and cells were incubated for 4 hours and then washed three times with prewarmed EMM4S before being imaged or loaded into a microfluidic plate.

6.1.2.3 Nutrient shift-down

Precultures were grown in EMM + L-Glutamic acid (20 mM). For the nutrient shift, cells were washed three times with prewarmed EMM + L-Proline (10 mM) and resuspended in this media. From the time of the first wash, septation index was measured every 10 minutes for 2 hours and then every 15 minutes for a further hour. Septation index was calculated by taking the average number of septated cells in three groups of 100 cells. For nutrient shift experiments which included a

wee1-50 control, cells were grown at 25°C and shifted to the restrictive temperature (36.5°C) 5 hours before the nutrient shift.

6.1.2.4 Serial dilution assay

Serial dilution spot tests were carried out to compare the growth rates of different deletion mutants. Cells were grown to exponential log phase in YE4S liquid media and dilutions were prepared in a 96-well plate: cell concentration in 10 fold dilutions from $2x10^6$ to $2x10^2$ cells/ml. 5 µl of each cell concentration was spotted onto YE4S agar and incubated for 2 days at 32°C.

6.2 Imaging and cell length analysis

6.2.1 Protein localisation

For protein localisation, live cells were imaged in liquid media under a coverslip using a DeltaVision Elite (Applied Precision) comprised of an Olympus IX71 wide-field inverted fluorescence microscope, a PLAN APO 60x oil, 1.42 NA objective, and a Photometrics CoolSNAP HQ2 camera. The microscope was contained within an IMSOL 'imcubator' Environment Control System set at 32°C. Images were acquired in 0.2 or 0.4 µm Z-sections over 4.8-5.0 µm using SoftWoRx (Applied Precision) and processed using SoftWoRx and Huygens. Images are maximum intensity projections (or a 3D projection in the case of Figure 2.2B) of deconvolved images. Cell fixation for DAPI staining was carried out using formaldehyde (16%). For the visualisation of the growing end of the cell, Calcofluor (Sigma) was used to stain the cell wall.

6.2.2 Cell length analysis

Following cell culture as described in Moreno *et al*. (Moreno et al., 1991) cells were either measured in liquid culture on a glass slide or transferred to a Y04C microfluidic plate (CellASIC, see section 6.3.1). Images were acquired using the DeltaVision Elite (described above) or a Zeiss Axioskop 40 microscope

equipped with a 63x/1.4 NA objective and a Zeiss AxioCam MRm camera. Cell length was either measured from brightfield images or images of live cells stained with Calcofluor (Sigma). Measurements were taken using the PointPicker plug-in of ImageJ (National Institutes of Health) and septated cells were chosen as cells with a visible septum (Figure 6.1). Length in pixel number was converted to micrometres.

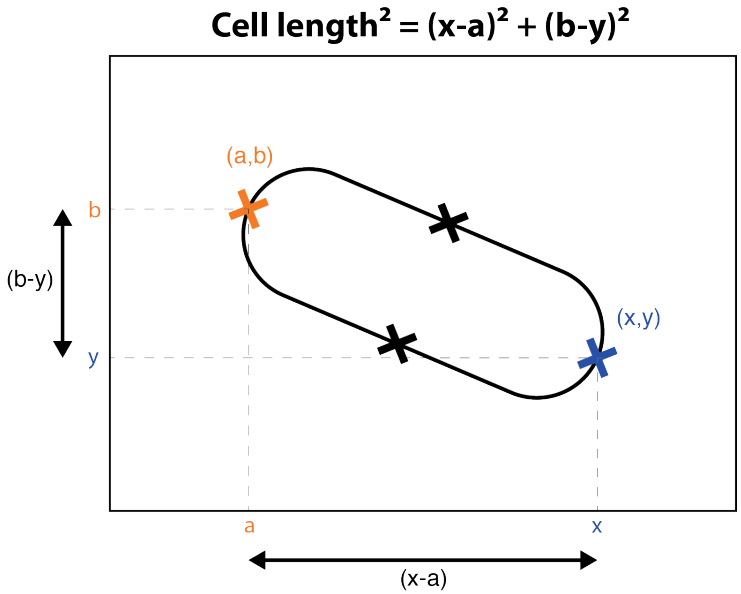

Figure 6.1|Method for measuring cell length and width

The ImageJ pointpicker plugin is used to 'pick' points on the cell perimeter. Two points are picked at the ends of the cell and then two opposite points are picked on each cell side (being careful to avoid areas of fission scarring where the cell width can increase slightly). The coordinate list is exported to Excel and Pythagoras' Theorum is used to calculate cell length (as shown) and cell width.

Comparison between strains was carried out using a two-tailed unpaired Student's *t*-test. In box-and-whisker plots boxes are delimited by the first quartile, median and third quartile, while whiskers mark maximum and minimum values within the 10-90% range. Values outside this range are shown as individual dots. In scatter dot plots, the line shows the mean and each dot corresponds to a single measurement.

6.2.3 Cell size variability screen

The viable set of a near genome-wide *S. pombe* haploid gene deletion collection was used (Kim et al., 2010, Spirek et al., 2010). The original screen involved screening the cell size phenotype of 2,969 different gene deletions (82% of fission yeast non-essential genes) (Navarro and Nurse, 2012).

Primary screening of microcolonies growing on YE4S agar was carried out using a Zeiss Axioskop 40 microscope equipped with a 20x/0.4 NA objective plus an additional 1.8x magnification. A Sony NEX-5N camera was used for image acquisition. For secondary screening, length measurements of candidates in liquid culture were carried out as detailed above. For Mga2 and Cid12, which were used for further analysis, the deletion strain was reconstructed using PCR and homologous recombination (see section 6.1.1) in order to ensure the full gene was deleted in a prototrophic background. The gene deletion was verified by colony PCR.

6.2.4 Cell length and variability analysis

Work included in this thesis, particularly the variability analysis, relied on length measurements taken from single cells to make predictions regarding the behaviour of the whole population. It was therefore important to check how reliable cell length at division and coefficient of variation measurements are for these populations to check that sufficient measurements were taken. In order to test this an *in silico* analysis was carried out using cell length at division measurements of 100 wild type and 100 *mga2*Δ cells (used as a representative of a variable population) (Figure 6.2). For the wild type population, cell length measurements ceased to fluctuate with sample sizes of over 50 cells and coefficient of variation values were stable above 60 cells. For the *mga2*Δ population this analysis indicated that samples of greater than 96 cells should be taken to make a reliable estimate of cell length and coefficient of variation for a variable population. This was used as a guideline for all length analyses in this part of the investigation.

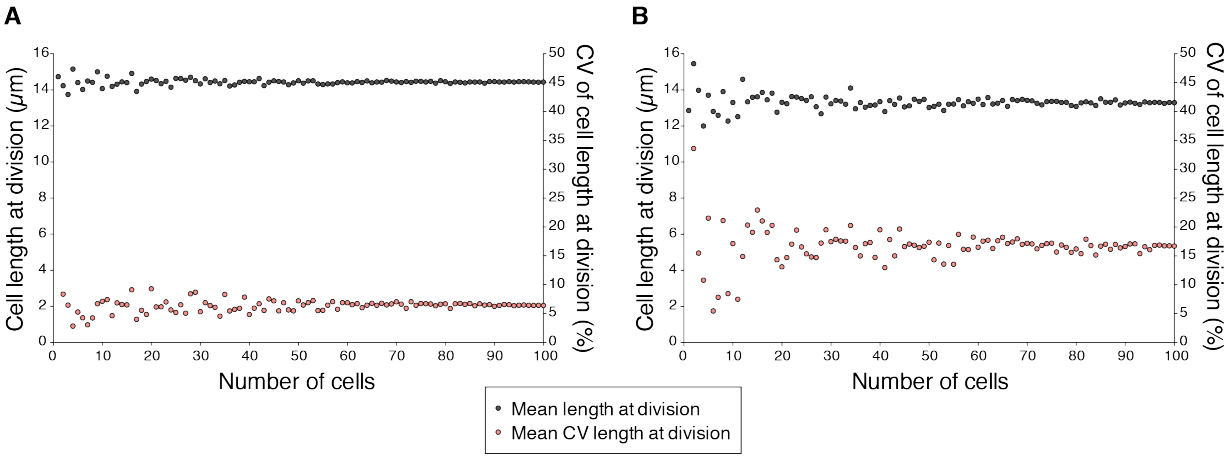

Figure 6.2|Cell length and variability analysis

An *in silico* analysis of mean cell length and coefficient of variation values for a wild type **(A)** and *mga2*Δ **(B)** population. The values of mean cell length and coefficient of variation were plotted incrementally for 1 to 100 cells, with the cell length measurements being reordered in a random fashion each time a measurement was added to the analysis.

6.3 Single cell studies

6.3.1 Microfluidic cell culture

The ONIX Microfluidic Perfusion System from CellASIC was used for single cell analysis. Microfluidic plates were set up as described here http://www.cellasic.com/ONIX_yeast.html. 50 µl of cell culture was loaded at a density of $1.26x10^6$ cells/ml and cells were imaged in the 3.5 µm and 4.5 µm chambers. YE4S medium was used and a flow rate of 3 psi was maintained throughout the experiment. Time-lapse imaging was started 1 hour after loading the plate and was carried out at 32°C or 36.5°C using the DeltaVision Elite system described above. For temperature-sensitive mutants, cells were shifted to the restrictive temperature in liquid culture for one generation before being loaded into a plate.

6.3.2 Size homeostasis analysis

For size homeostasis analysis, images were acquired at 10 minute intervals for 12 hours (of cells growing in a CellASIC plate, described above). Cells were

only measured during the first three generations after loading into the plate. Birth length was measured using the first frame in which two separate daughter cells were seen and single cells were tracked through the frames until a septum formed and this was taken as cell length at division. Cycle time was given as the time interval between these birth and division length measurements.

6.4 Protein extracts and Western blots

The levels of Cdc2 Tyr15 phosphorylation and Cdc13 protein were assessed by SDS-PAGE (NuPAGE Bis-Tris Precast Gels) and Western blotting procedure, according to manufacturers instructions (Life Technologies).

6.4.1 Total protein extraction

Cells were quenched with 10% trichloroacetic acid and kept on ice for 30 minutes. Cells were pelleted by centrifugation and washed with acetone. Cell pellets were washed and resuspended in 100 µl Lysis buffer. Cells were then disrupted in a FastPrep (FastPrep120) with acid-washed glass beads (0.4 mm, Sigma). The cell debris was pelleted and the supernatant was recovered as a protein extract.

Lysis Buffer
8 M urea
50 mM ammonium bicarbonate
cOmplete Mini EDTA-free protease inhibitor cocktail (Roche)
PhosSTOP phosphatase inhibitor cocktail (Roche)

6.4.2 Protein detection

The antibodies listed below were used for the detection of proteins by Western blotting. Signal was detected using SuperSignal West Femto Maximum Sensitivity Substrate (34095, Life Technologies) and imaged using ImageQuant LAS 4000. Quantification was done in ImageQuant TL software (GE Healthcare).

Primary antibodies

Cdc13: 1:6,000 SP4 (rabbit polyclonal, (Moreno et al., 1989))

Cdc2: 1:250 anti-PSTAIRE (rabbit polyclonal, Santa Cruz Biotech)

Cdc2-Y15P: 1:500 phospho-Cdc2 (Y15) (rabbit polyclonal, #9111 Cell Signalling Technology)

Alpha tubulin – 1:10,000 TAT1 (mouse monoclonal, (Woods et al., 1989))

Secondary antibodies

1:25,000 Horse radish peroxidase-conjugated donkey anti-rabbit (NA934V, GE Healthcare)

1:25,000 Horse radish peroxidase-conjugated goat anti-mouse (STAR120P, abD SeroTEC)

6.5 Fission yeast strains used in this study

A list of all strains used in this thesis is presented in Table 6.1. The table details the reference number of the strain, the full genotype, and the strain source, whether constructed here or requested from another lab.

Name	*Genotype*	Origin
PN1	*972 h-*	Lab collection
PN3141	*pom1-GFP::kanMX6 h-*	Bahler and Pringle, 1998
LW138	*nif1-GFP::hph h-*	This study
PN10503	*cdr2-GFP::kanMX6 ura4-D18 leu1-32 ade6-M21X h-*	Morrell et al., 2004
FR495	*pom1Δ::kanMX6 h+*	Navarro and Nurse, 2012
FR538	*nif1Δ::kanMX6 h+*	Navarro and Nurse, 2012
LW61	*pom1Δ::kanMX6 nif1Δ::kanMX6 h+*	This study
LW34	*pom1Δ::kanMX6 cut11-GFP-ura4+ ura4-D18? leu1-32?*	This study
LW64	*nif1Δ::kanMX6 cdr2-GFP::kanMX6 ura4-D18 leu+ ade6-M21X*	This study
DH1776-1A	*crn1:tdTomato:KanR KanR:P3:nmt1:GFP:atb2 h-*	Kume et al., 2011
LW123	*pom1Δ::kanMX6 nif1Δ::kanMX6 crn1:tdTomato:KanR KanR:P3:nmt1:GFP:atb2*	This study
FR405	*sty1Δ::clonNat h-*	Navarro and Nurse, 2012
FR551	*sty1Δ::natMX6 nif1Δ::kanMX6 h+*	Navarro and Nurse, 2012
FR443	*sty1Δ::natMX6 pom1Δ::kanMX6 h-*	Navarro and Nurse, 2012
FR364	*cdr1Δ::kanMX6 h+*	Navarro and Nurse, 2012
FR445	*cdr1Δ::natMX6 pom1Δ::kanMX6 h-*	Navarro and Nurse, 2012
FR553	*cdr1Δ::natMX6 nif1Δ::kanMX6 h+*	Navarro and Nurse, 2012
FR402	*cdr1Δ::kanMX6 sty1Δ::natMX6 h-*	Navarro and Nurse, 2012
FR1095	*cdr1Δ::NatR sty1Δ::NatR nif1Δ::KanR*	Navarro and Nurse, 2012
LW152	*cdc11-119 SPAC1B2.03c-mCherry::NatR leu1? ura4? pom1-GFP::kanMX6*	This study
LW184	*cdc11-119 SPAC1B2.03c-mCherry::NatR ura4-D18 nif1-GFP-hph*	This study
LW156	*cdc11-119 pom1-GFP::kanMX6 Cdr2-mCherry::hph*	This study
PN369	*wee1-50 h-*	Lab collection
DC235	*leu1ΔPcdc13::cdc13-L-cdc2::cdc13 3'UTR::ura4+ cdc2Δ::kanMX6 cdc13Δ::natMX6 cig1Δ::ura4+ cig2::ura4+ puc1Δ::ura4+ ura4-D18 h+*	Coudreuse and Nurse, 2010
DC276	*leu1ΔPcdc13::cdc13-L-cdc2(T14A Y15F)::cdc13 3'UTR::ura4+ cdc2Δ::kanMX6 cdc13Δ::natMX6 cig1Δ::ura4+ cig2::ura4+ puc1Δ::ura4+ ura4-D18 h+*	Coudreuse and Nurse, 2010
FN391	*cdc11-119 SPAC1B2.03c-mCherry::NatR leu1-32 ura4-D18 h+*	Lab collection
LW311	*cid12Δ::KanMX6 cdc11-119 SPAC1B2.03c-mCherry::NatR leu1? ura4?*	This study
LW314	*mga2Δ::KanMX6 cdc11-119 SPAC1B2.03c-mCherry::NatR leu1? ura4?*	This study
KM167	*ole1-GFP::KanR h-*	Lab collection
LW205	*mga2Δ::KanMX6 ole1-GFP::KanR*	This study
FR735	*leu1Δ::Pcdc13::cdc13-L-cdc2AF(as)::cdc13 3'UTR::ura4+ cdc2Δ::ScLEU2 cdc13Δ::natMX6 ura4-D18 h-*	Navarro and Nurse, 2012
PN5013	*leu1Δ::Pcdc13::cdc13-L-cdc2(as)::cdc13 3'UTR::ura4+ cdc2Δ::ScLEU2 cdc13Δ::natMX6 h+*	Lab collection
LW188	*mga2Δ::KanR leu1Δ::Pcdc13::cdc13-L-cdc2(T14A Y15F)as::cdc13 3'UTR::ura4+ ura4-D18 cdc2Δ::ScLEU2 cdc13Δ::natMX6 ade+*	This study
LW194	*mga2Δ::KanR leu1Δ::Pcdc13::cdc13-L-cdc2as::cdc13 3'UTR::ura4+ ura4-D18 cdc2Δ::ScLEU2 cdc13Δ::natMX6 ade+*	This study
LW216	*cid12Δ::KanMX6 h-*	This study
LW228	*mga2Δ::KanMX6 h-*	This study
LW321	*wee1Δ::hph leu1Δ::Pcdc13::cdc13-L-cdc2::cdc13 3'UTR::ura4+ cdc2Δ::kanMX6 cdc13Δ::natMX6 cig1Δ::ura4+ cig2Δ::ura4+ puc1Δ::ura4+ ura4-D18*	This study
LW334	*wee1Δ::hph leu1Δ::Pcdc13::cdc13-L-cdc2AF::cdc13 3'UTR::ura4+ cdc2Δ::kanMX6 cdc13Δ::natMX6 cig1Δ::ura4+ cig2Δ::ura4+ puc1Δ::ura4+ ura4-D18*	This study
FR1205	*wee1Δ::kanMX6 h+*	Navarro and Nurse, 2012
PN2341	*mik1Δ::LEU2 leu1-32 h-*	Lab collection
PN958	*rum1::ura4+ wee1-50 leu1-32 h? (sterile)*	Lab collection
PN2403	*ade6-M210/216 h-/h-*	Lab collection
LW166	*dph1Δ::KanMX6 ade6-M216 ura4-D18 leu1-32 h+*	Kim et al., 2010
LW167	*pek1Δ::KanMX6 ade6-M210 ura4-D18 leu1-32 h+*	Kim et al., 2010
LW168	*mms19Δ::KanMX6 ade6-M216 ura4-D18 leu1-32 h+*	Kim et al., 2010
LW169	*moe1Δ::KanMX6 ade6-M216 ura4-D18 leu1-32 h+*	Kim et al., 2010
LW170	*mga2Δ::KanMX6 ade6-M216 ura4-D18 leu1-32 h+*	Kim et al., 2010
LW171	*SPAC869.03cΔKanMX6 ade6-M210 ura4-D18 leu1-32 h+*	Kim et al., 2010
LW172	*cid12ΔKanMX6 ade6-M216 ura4-D18 leu1-32 h+*	Kim et al., 2010
LW173	*aps1Δ::KanMX6 ade6-M216 ura4-D18 leu1-32 h+*	Kim et al., 2010
LW174	*atd1Δ::KanMX6 ade6-M216 ura4-D18 leu1-32 h+*	Kim et al., 2010
LW175	*sft1Δ::KanMX6 ade6-M216 ura4-D18 leu1-32 h+*	Kim et al., 2010
LW176	*csn2Δ::KanMX6 ade6-M216 ura4-D18 leu1-32 h+*	Kim et al., 2010
LW177	*dad3Δ::KanMX6 ade6-M216 ura4-D18 leu1-32 h+*	Kim et al., 2010
LW178	*hpt1Δ::KanMX6 ade6-M216 ura4-D18 leu1-32 h+*	Kim et al., 2010
LW179	*med20Δ::KanMX6 ade6-M216 ura4-D18 leu1-32 h+*	Kim et al., 2010
LW181	*SPBC557.02cΔ::KanMX6 ade6-M216 ura4-D18 leu1-32 h+*	Kim et al., 2010
LW183	*trm112Δ::KanMX6 ade6-M216 ura4-D18 leu1-32 h+*	Kim et al., 2010

Table 6.1|Fission yeast strains used in this study

A list of all strains used in this thesis, including full genotype and strain origin.

Reference List

ANDERSON, C. A., ESER, U., KORNDORF, T., BORSUK, M. E., SKOTHEIM, J. M. & GLADFELTER, A. S. 2013. Nuclear repulsion enables division autonomy in a single cytoplasm. *Curr Biol,* 23**,** 1999-2010.

BAHLER, J. & PRINGLE, J. R. 1998. Pom1p, a fission yeast protein kinase that provides positional information for both polarized growth and cytokinesis. *Genes Dev,* 12**,** 1356-70.

BAHLER, J., WU, J. Q., LONGTINE, M. S., SHAH, N. G., MCKENZIE, A., 3RD, STEEVER, A. B., WACH, A., PHILIPPSEN, P. & PRINGLE, J. R. 1998. Heterologous modules for efficient and versatile PCR-based gene targeting in Schizosaccharomyces pombe. *Yeast,* 14**,** 943-51.

BAKER, J. R. 1952. The Cell-Theory: A Restatement, History, and Critique. Part III. The Cell as a Morphological Unit. *Quarterly Journal of Microscopical Science,* 93**,** 157-90.

BASERGA, R. 1984. Growth in size and cell DNA replication. *Exp Cell Res,* 151**,** 1-5.

BAUMGARTNER, S. & TOLIC-NORRELYKKE, I. M. 2009. Growth pattern of single fission yeast cells is bilinear and depends on temperature and DNA synthesis. *Biophys J,* 96**,** 4336-47.

BHATIA, P., HACHET, O., HERSCH, M., RINCON, S. A., BERTHELOT-GROSJEAN, M., DALESSI, S., BASTERRA, L., BERGMANN, S., PAOLETTI, A. & MARTIN, S. G. 2014. Distinct levels in Pom1 gradients limit Cdr2 activity and localization to time and position division. *Cell Cycle,* 13**,** 538-52.

BLOOM, J. & CROSS, F. R. 2007. Multiple levels of cyclin specificity in cell-cycle control. *Nat Rev Mol Cell Biol,* 8**,** 149-60.

BREEDING, C. S., HUDSON, J., BALASUBRAMANIAN, M. K., HEMMINGSEN, S. M., YOUNG, P. G. & GOULD, K. L. 1998. The cdr2(+) gene encodes a regulator of G2/M progression and cytokinesis in Schizosaccharomyces pombe. *Molecular biology of the cell,* 9**,** 3399-415.

BROOKS, R. F. 1977. Continuous protein synthesis is required to maintain the probability of entry into S phase. *Cell,* 12**,** 311-7.

BROOKS, R. F. 1981. *The Cell Cycle*, Cambridge University Press.

BROOKS, R. F. & SHIELDS, R. 1985. Cell growth, cell division and cell size homeostasis in Swiss 3T3 cells. *Exp Cell Res,* 156**,** 1-6.

BRYAN, A. K., GORANOV, A., AMON, A. & MANALIS, S. R. 2010. Measurement of mass, density, and volume during the cell cycle of yeast. *Proc Natl Acad Sci U S A,* 107**,** 999-1004.

CAMPOS, M., SUROVTSEV, I. V., KATO, S., PAINTDAKHI, A., BELTRAN, B., EBMEIER, S. E. & JACOBS-WAGNER, C. 2014. A constant size extension drives bacterial cell size homeostasis. *Cell,* 159**,** 1433-46.

CELTON-MORIZUR, S., RACINE, V., SIBARITA, J. B. & PAOLETTI, A. 2006. Pom1 kinase links division plane position to cell polarity by regulating Mid1p cortical distribution. *J Cell Sci,* 119**,** 4710-8.

CHANG, F., WOOLLARD, A. & NURSE, P. 1996. Isolation and characterization of fission yeast mutants defective in the assembly and placement of the contractile actin ring. *J Cell Sci,* 109 (Pt 1)**,** 131-42.

CHELLAPPA, R., KANDASAMY, P., OH, C. S., JIANG, Y., VEMULA, M. & MARTIN, C. E. 2001. The membrane proteins, Spt23p and Mga2p, play distinct roles in the activation of Saccharomyces cerevisiae OLE1 gene expression. Fatty acid-mediated regulation of Mga2p activity is independent of its proteolytic processing into a soluble transcription activator. *J Biol Chem,* 276**,** 43548-56.

CONLON, I. & RAFF, M. 1999. Size control in animal development. *Cell,* 96**,** 235-44.
CONLON, I. & RAFF, M. 2003. Differences in the way a mammalian cell and yeast cells coordinate cell growth and cell-cycle progression. *J Biol,* 2**,** 7.
CONLON, I. J., DUNN, G. A., MUDGE, A. W. & RAFF, M. C. 2001. Extracellular control of cell size. *Nat Cell Biol,* 3**,** 918-21.
COUDREUSE, D. & NURSE, P. 2010. Driving the cell cycle with a minimal CDK control network. *Nature,* 468**,** 1074-9.
CREANOR, J. & MITCHISON, J. M. 1982. Patterns of protein synthesis during the cell cycle of the fission yeast Schizosaccharomyces pombe. *J Cell Sci,* 58**,** 263-85.
CROSS, F. R. 1988. DAF1, a mutant gene affecting size control, pheromone arrest, and cell cycle kinetics of Saccharomyces cerevisiae. *Mol Cell Biol,* 8**,** 4675-84.
DARZYNKIEWICZ, Z., EVENSON, D. P., STAIANO-COICO, L., SHARPLESS, T. K. & MELAMED, M. L. 1979. Correlation between cell cycle duration and RNA content. *J Cell Physiol,* 100**,** 425-38.
DENG, L., BALDISSARD, S., KETTENBACH, A. N., GERBER, S. A. & MOSELEY, J. B. 2014. Dueling kinases regulate cell size at division through the SAD kinase Cdr2. *Curr Biol,* 24**,** 428-33.
DI TALIA, S., SKOTHEIM, J. M., BEAN, J. M., SIGGIA, E. D. & CROSS, F. R. 2007. The effects of molecular noise and size control on variability in the budding yeast cell cycle. *Nature,* 448**,** 947-51.
DOLZNIG, H., GREBIEN, F., SAUER, T., BEUG, H. & MULLNER, E. W. 2004. Evidence for a size-sensing mechanism in animal cells. *Nat Cell Biol,* 6**,** 899-905.
DONACHIE, W. D. 1968. Relationship between cell size and time of initiation of DNA replication. *Nature,* 219**,** 1077-9.
ELLIOTT, S. G. & MCLAUGHLIN, C. S. 1978. Rate of macromolecular synthesis through the cell cycle of the yeast Saccharomyces cerevisiae. *Proceedings of the National Academy of Sciences of the United States of America,* 75**,** 4384-8.
FANKHAUSER, G. 1952. Nucleo-Cytoplasmic Relations in Amphibian Development. *International Review of Cytology,* 1**,** 165-193.
FANTES, P. A. & NURSE, P. 1977. Control of cell size at division in fission yeast by a growth-modulated size control over nuclear division. *Experimental cell research,* 107**,** 377-86.
FANTES, P. A. 1977. Control of cell size and cycle time in Schizosaccharomyces pombe. *J Cell Sci,* 24**,** 51-67.
FANTES, P. A., GRANT, W. D., PRITCHARD, R. H., SUDBERY, P. E. & WHEALS, A. E. 1975. The regulation of cell size and the control of mitosis. *Journal of theoretical biology,* 50**,** 213-44.
FANTES, P. A. & NURSE, P. 1978. Control of the timing of cell division in fission yeast. Cell size mutants reveal a second control pathway. *Experimental cell research,* 115**,** 317-29.
FANTES, P. A. & NURSE, P. 1981. Division timing: controls, models and mechanisms. *In:* JOHN, P. C. L. (ed.) *The Cell Cycle.* Cambridge: Cambridge University Press.
FARRELL, J. A. & O'FARRELL, P. H. 2014. From egg to gastrula: how the cell cycle is remodeled during the Drosophila mid-blastula transition. *Annu Rev Genet,* 48**,** 269-94.
FISHER, D. L. & NURSE, P. 1996. A single fission yeast mitotic cyclin B p34cdc2 kinase promotes both S-phase and mitosis in the absence of G1 cyclins. *The EMBO journal,* 15**,** 850-60.
FOX, T. O. & PARDEE, A. B. 1970. Animal cells: noncorrelation of length of G1 phase with size after mitosis. *Science,* 167**,** 80-2.
FUTCHER, B. 1996. Cyclins and the wiring of the yeast cell cycle. *Yeast,* 12**,** 1635-46.

GAO, F. B. & RAFF, M. 1997. Cell size control and a cell-intrinsic maturation program in proliferating oligodendrocyte precursor cells. *J Cell Biol,* 138**,** 1367-77.
GENNIS, R. B. 1989. *Biomembranes: Molecular Structure and Function*, Springer.
GODIN, M., DELGADO, F. F., SON, S., GROVER, W. H., BRYAN, A. K., TZUR, A., JORGENSEN, P., PAYER, K., GROSSMAN, A. D., KIRSCHNER, M. W. & MANALIS, S. R. 2010. Using buoyant mass to measure the growth of single cells. *Nat Methods,* 7**,** 387-90.
GOULD, K. L. & NURSE, P. 1989. Tyrosine phosphorylation of the fission yeast cdc2+ protein kinase regulates entry into mitosis. *Nature,* 342**,** 39-45.
GREGORY, T. R. 2001. Coincidence, coevolution, or causation? DNA content, cell size, and the C-value enigma. *Biol Rev Camb Philos Soc,* 76**,** 65-101.
HACHET, O., BERTHELOT-GROSJEAN, M., KOKKORIS, K., VINCENZETTI, V., MOOSBRUGGER, J. & MARTIN, S. G. 2011. A phosphorylation cycle shapes gradients of the DYRK family kinase Pom1 at the plasma membrane. *Cell,* 145**,** 1116-28.
HAGAN, I. M. & HYAMS, J. S. 1988. The use of cell division cycle mutants to investigate the control of microtubule distribution in the fission yeast Schizosaccharomyces pombe. *J Cell Sci,* 89 (Pt 3)**,** 343-57.
HARA, Y. & KIMURA, A. 2009. Cell-size-dependent spindle elongation in the Caenorhabditis elegans early embryo. *Curr Biol,* 19**,** 1549-54.
HARRIS, H. 1999. *The Birth of the Cell*, Yale University Press.
HAYLES, J., FISHER, D., WOOLLARD, A. & NURSE, P. 1994. Temporal order of S phase and mitosis in fission yeast is determined by the state of the p34cdc2-mitotic B cyclin complex. *Cell,* 78**,** 813-22.
HAYLES, J., WOOD, V., JEFFERY, L., HOE, K. L., KIM, D. U., PARK, H. O., SALAS-PINO, S., HEICHINGER, C. & NURSE, P. 2013. A genome-wide resource of cell cycle and cell shape genes of fission yeast. *Open Biol,* 3**,** 130053.
HOOKE, R. 1665. *Micrographia: or, Some physiological descriptions of minute bodies made by magnifying glasses*, London: J. Martyn and J. Allestry.
JOHNSTON, G. C., PRINGLE, J. R. & HARTWELL, L. H. 1977. Coordination of growth with cell division in the yeast Saccharomyces cerevisiae. *Exp Cell Res,* 105**,** 79-98.
JORGENSEN, P., EDGINGTON, N. P., SCHNEIDER, B. L., RUPES, I., TYERS, M. & FUTCHER, B. 2007. The size of the nucleus increases as yeast cells grow. *Mol Biol Cell,* 18**,** 3523-32.
JORGENSEN, P. & TYERS, M. 2004. How cells coordinate growth and division. *Current biology : CB,* 14**,** R1014-27.
KAFRI, R., LEVY, J., GINZBERG, M. B., OH, S., LAHAV, G. & KIRSCHNER, M. W. 2013. Dynamics extracted from fixed cells reveal feedback linking cell growth to cell cycle. *Nature,* 494**,** 480-3.
KANDASAMY, P., VEMULA, M., OH, C. S., CHELLAPPA, R. & MARTIN, C. E. 2004. Regulation of unsaturated fatty acid biosynthesis in Saccharomyces: the endoplasmic reticulum membrane protein, Mga2p, a transcription activator of the OLE1 gene, regulates the stability of the OLE1 mRNA through exosome-mediated mechanisms. *J Biol Chem,* 279**,** 36586-92.
KANOH, J. & RUSSELL, P. 1998. The protein kinase Cdr2, related to Nim1/Cdr1 mitotic inducer, regulates the onset of mitosis in fission yeast. *Molecular biology of the cell,* 9**,** 3321-34.
KIANG, L. 2010. *Controls over S-phase and over nuclear sychrony.* Doctor of Philosophy, The Rockefeller University.
KILLANDER, D. & ZETTERBERG, A. 1965a. A quantitative cytochemical investigation of the relationship between cell mass and initiation of DNA synthesis in mouse fibroblasts in vitro. *Exp Cell Res,* 40**,** 12-20.

KILLANDER, D. & ZETTERBERG, A. 1965b. Quantitative Cytochemical Studies on Interphase Growth. I. Determination of DNA, Rna and Mass Content of Age Determined Mouse Fibroblasts in Vitro and of Intercellular Variation in Generation Time. *Exp Cell Res,* 38**,** 272-84.

KIM, D. U., HAYLES, J., KIM, D., WOOD, V., PARK, H. O., WON, M., YOO, H. S., DUHIG, T., NAM, M., PALMER, G., HAN, S., JEFFERY, L., BAEK, S. T., LEE, H., SHIM, Y. S., LEE, M., KIM, L., HEO, K. S., NOH, E. J., LEE, A. R., JANG, Y. J., CHUNG, K. S., CHOI, S. J., PARK, J. Y., PARK, Y., KIM, H. M., PARK, S. K., PARK, H. J., KANG, E. J., KIM, H. B., KANG, H. S., PARK, H. M., KIM, K., SONG, K., SONG, K. B., NURSE, P. & HOE, K. L. 2010. Analysis of a genome-wide set of gene deletions in the fission yeast Schizosaccharomyces pombe. *Nature biotechnology,* 28**,** 617-23.

KIM, S., LI, Q., DANG, C. V. & LEE, L. A. 2000. Induction of ribosomal genes and hepatocyte hypertrophy by adenovirus-mediated expression of c-Myc in vivo. *Proc Natl Acad Sci U S A,* 97**,** 11198-202.

KIMBALL, R. F., PERDUE, S. W., CHU, E. H. & ORTIZ, J. R. 1971. Microphotometric and autoradiographic studies on the cell cycle and cell size during growth and decline of Chinese hamster cell cultures. *Exp Cell Res,* 66**,** 17-32.

KRAPP, A., GULLI, M. & SIMANIS, V. 2004. SIN and the art of splitting the fission yeast cell. *Current biology : CB,* 14**,** R722-R730.

KUME, K., KOYANO, T., KANAI, M., TODA, T. & HIRATA, D. 2011. Calcineurin ensures a link between the DNA replication checkpoint and microtubule-dependent polarized growth. *Nat Cell Biol,* 13**,** 234-42.

LEE, C., ZHANG, H., BAKER, A. E., OCCHIPINTI, P., BORSUK, M. E. & GLADFELTER, A. S. 2013. Protein aggregation behavior regulates cyclin transcript localization and cell-cycle control. *Dev Cell,* 25**,** 572-84.

LEVY, D. L. & HEALD, R. 2010. Nuclear size is regulated by importin alpha and Ntf2 in Xenopus. *Cell,* 143**,** 288-98.

LLOYD, A. C. 2013. The regulation of cell size. *Cell,* 154**,** 1194-205.

LOOG, M. & MORGAN, D. O. 2005. Cyclin specificity in the phosphorylation of cyclin-dependent kinase substrates. *Nature,* 434**,** 104-8.

LUNDGREN, K., WALWORTH, N., BOOHER, R., DEMBSKI, M., KIRSCHNER, M. & BEACH, D. 1991. mik1 and wee1 cooperate in the inhibitory tyrosine phosphorylation of cdc2. *Cell,* 64**,** 1111-22.

MARKS, J., HAGAN, I. M. & HYAMS, J. S. 1986. Growth polarity and cytokinesis in fission yeast: the role of the cytoskeleton. *J Cell Sci Suppl.* 5**,** 229-41.

MARSHALL, W. F., YOUNG, K. D., SWAFFER, M., WOOD, E., NURSE, P., KIMURA, A., FRANKEL, J., WALLINGFORD, J., WALBOT, V., QU, X. & ROEDER, A. H. 2012. What determines cell size? *BMC Biol,* 10**,** 101.

MARTIN, S. G. & BERTHELOT-GROSJEAN, M. 2009. Polar gradients of the DYRK-family kinase Pom1 couple cell length with the cell cycle. *Nature,* 459**,** 852-6.

MARTIN-CASTELLANOS, C., BLANCO, M. A., DE PRADA, J. M. & MORENO, S. 2000. The puc1 cyclin regulates the G1 phase of the fission yeast cell cycle in response to cell size. *Molecular biology of the cell,* 11**,** 543-54.

MITCHISON, J. M. 1957. The growth of single cells. I. Schizosaccharomyces pombe. *Exp Cell Res,* 13**,** 244-62.

MITCHISON, J. M. 2003. Growth during the cell cycle. *Int Rev Cytol,* 226**,** 165-258.

MITCHISON, J. M. & CREANOR, J. 1971. Induction synchrony in the fission yeast. Schizosaccharomyces pombe. *Experimental cell research,* 67**,** 368-74.

MITCHISON, J. M. & NURSE, P. 1985. Growth in cell length in the fission yeast Schizosaccharomyces pombe. *Journal of cell science,* 75**,** 357-76.

MITCHISON, J. M., PASSANO, L. M. & SMITH, F. H. 1956. An Integration Method for the Inteference Microscope. *Quarterly Journal of Microscopical Science,* 97**,** 287-302.
MORENO, S., HAYLES, J. & NURSE, P. 1989. Regulation of p34cdc2 protein kinase during mitosis. *Cell,* 58**,** 361-72.
MORENO, S., KLAR, A. & NURSE, P. 1991. Molecular genetic analysis of fission yeast Schizosaccharomyces pombe. *Methods in enzymology,* 194**,** 795-823.
MORGAN, D. O. 1995. Principles of CDK regulation. *Nature,* 374**,** 131-4.
MORGAN, D. O. 1997. Cyclin-dependent kinases: engines, clocks, and microprocessors. *Annu Rev Cell Dev Biol,* 13**,** 261-91.
MORGAN, D. O. 2007. *The Cell Cycle: Principles of Control*, New Science Press.
MORRELL, J. L., NICHOLS, C. B. & GOULD, K. L. 2004. The GIN4 family kinase, Cdr2p, acts independently of septins in fission yeast. *J Cell Sci,* 117 (Pt 22)**,** 5293-302.
MORTIMER, R. K. 1958. Radiobiological and genetic studies on a polyploid series (haploid to hexaploid) of Saccharomyces cerevisiae. *Radiat Res,* 9**,** 312-26.
MOSELEY, J. B., MAYEUX, A., PAOLETTI, A. & NURSE, P. 2009. A spatial gradient coordinates cell size and mitotic entry in fission yeast. *Nature,* 459**,** 857-60.
MOSELEY, J. B. & NURSE, P. 2010. Cell division intersects with cell geometry. *Cell,* 142**,** 184-8.
MOSER, B. A. & RUSSELL, P. 2000. Cell cycle regulation in Schizosaccharomyces pombe. *Curr Opin Microbiol,* 3**,** 631-6.
MUNDKUR, B. D. 1953. Interphase nuclei and cell sizes in a polyploid series of Saccharomyces. *Experientia,* 9**,** 373-4.
NASH, R., TOKIWA, G., ANAND, S., ERICKSON, K. & FUTCHER, A. B. 1988. The WHI1+ gene of Saccharomyces cerevisiae tethers cell division to cell size and is a cyclin homolog. *EMBO J,* 7**,** 4335-46.
NAVARRO, F. J. & NURSE, P. 2012. A systematic screen reveals new elements acting at the G2/M cell cycle control. *Genome Biol,* 13**,** R36.
NEUMANN, F. R. & NURSE, P. 2007. Nuclear size control in fission yeast. *The Journal of cell biology,* 179**,** 593-600.
NURSE, P. 1975. Genetic control of cell size at cell division in yeast. *Nature,* 256**,** 547-51.
NURSE, P. 1985. The genetic control of cell volume. *The Evolution of Genome Size.* John Wiley and Sons.
NURSE, P. 1990. Universal control mechanism regulating onset of M-phase. *Nature,* 344**,** 503-8.
NURSE, P. 1997. Regulation of the eukaryotic cell cycle. *European journal of cancer,* 33**,** 1002-4.
NURSE, P. & BISSETT, Y. 1981. Gene required in G1 for commitment to cell cycle and in G2 for control of mitosis in fission yeast. *Nature,* 292**,** 558-60.
NURSE, P. & THURIAUX, P. 1977. Controls over the timing of DNA replication during the cell cycle of fission yeast. *Experimental cell research,* 107**,** 365-75.
NURSE, P. & THURIAUX, P. 1980. Regulatory genes controlling mitosis in the fission yeast Schizosaccharomyces pombe. *Genetics,* 96**,** 627-37.
NURSE, P., THURIAUX, P. & NASMYTH, K. 1976. Genetic control of the cell division cycle in the fission yeast Schizosaccharomyces pombe. *Molecular & general genetics : MGG,* 146**,** 167-78.
NURSE, P. & FANTES, P. A. 1981. Cell cycle controls in fission yeast: a genetic analysis. *In:* JOHN, P. C. L. (ed.) *The Cell Cycle.* Cambridge: Cambridge University Press.

PADTE, N. N., MARTIN, S. G., HOWARD, M. & CHANG, F. 2006. The cell-end factor pom1p inhibits mid1p in specification of the cell division plane in fission yeast. *Current biology : CB,* 16**,** 2480-7.
PAN, K. Z., SAUNDERS, T. E., FLOR-PARRA, I., HOWARD, M. & CHANG, F. 2014. Cortical regulation of cell size by a sizer cdr2p. *Elife (Cambridge),* 3**,** e02040.
PATTERSON, J. O., SWAFFER, M. & FILBY, A. 2015. An Imaging Flow Cytometry-based approach to analyse the fission yeast cell cycle in fixed cells. *Methods,* 82**,** 74-84.
PETERSEN, J. & HAGAN, I. M. 2005. Polo kinase links the stress pathway to cell cycle control and tip growth in fission yeast. *Nature,* 435**,** 507-12.
PETERSEN, J. & NURSE, P. 2007. TOR signalling regulates mitotic commitment through the stress MAP kinase pathway and the Polo and Cdc2 kinases. *Nature cell biology,* 9**,** 1263-72.
POMBASE. http://www.pombase.org [Online].
PURVES, D., SNIDER, W. D. & VOYVODIC, J. T. 1988. Trophic regulation of nerve cell morphology and innervation in the autonomic nervous system. *Nature,* 336**,** 123-8.
RAPPAZ, B., CANO, E., COLOMB, T., KUHN, J., DEPEURSINGE, C., SIMANIS, V., MAGISTRETTI, P. J. & MARQUET, P. 2009. Noninvasive characterization of the fission yeast cell cycle by monitoring dry mass with digital holographic microscopy. *J Biomed Opt,* 14**,** 034049.
RESOURCES, B. L. http://www.bahlerlab.info/resources/ [Online].
ROSSOW, P. W., RIDDLE, V. G. & PARDEE, A. B. 1979. Synthesis of labile, serum-dependent protein in early G1 controls animal cell growth. *Proc Natl Acad Sci U S A,* 76**,** 4446-50.
RUSSELL, P. & NURSE, P. 1986. cdc25+ functions as an inducer in the mitotic control of fission yeast. *Cell,* 45**,** 145-53.
RUSSELL, P. & NURSE, P. 1987a. The mitotic inducer nim1+ functions in a regulatory network of protein kinase homologs controlling the initiation of mitosis. *Cell,* 49**,** 569-76.
RUSSELL, P. & NURSE, P. 1987b. Negative regulation of mitosis by wee1+, a gene encoding a protein kinase homolog. *Cell,* 49**,** 559-67.
SAUCEDO, L. J. & EDGAR, B. A. 2002. Why size matters: altering cell size. *Curr Opin Genet Dev,* 12**,** 565-71.
SAUNDERS, T. E., PAN, K. Z., ANGEL, A., GUAN, Y., SHAH, J. V., HOWARD, M. & CHANG, F. 2012. Noise Reduction in the Intracellular Pom1p Gradient by a Dynamic Clustering Mechanism. *Dev Cell,* 22, 558-72.
SCHAECHTER, M., MAALOE, O. & KJELDGAARD, N. O. 1958. Dependency on medium and temperature of cell size and chemical composition during balanced grown of Salmonella typhimurium. *J Gen Microbiol,* 19**,** 592-606.
SCHAECHTER, M., WILLIAMSON, J. P., HOOD, J. R., JR. & KOCH, A. L. 1962. Growth, cell and nuclear divisions in some bacteria. *J Gen Microbiol,* 29**,** 421-34.
SHEHATA, T. E. & MARR, A. G. 1975. Effect of temperature on the size of Escherichia coli cells. *J Bacteriol,* 124**,** 857-62.
SHIELDS, R., BROOKS, R. F., RIDDLE, P. N., CAPELLARO, D. F. & DELIA, D. 1978. Cell size, cell cycle and transition probability in mouse fibroblasts. *Cell,* 15**,** 469-74.
SMITH, H. M. 1925. Cell Size and Metabolic Activity in Amphibia. *The Biological Bulletin,* 48**,** 347-378.
SOHRMANN, M., FANKHAUSER, C., BRODBECK, C. & SIMANIS, V. 1996. The dmf1/mid1 gene is essential for correct positioning of the division septum in fission yeast. *Genes Dev,* 10**,** 2707-19.

SOMPAYRAC, L. & MAALOE, O. 1973. Autorepressor model for control of DNA replication. *Nat New Biol,* 241**,** 133-5.
SON, S., TZUR, A., WENG, Y., JORGENSEN, P., KIM, J., KIRSCHNER, M. W. & MANALIS, S. R. 2012. Direct observation of mammalian cell growth and size regulation. *Nat Methods,* 9**,** 910-2.
SPIREK, M., BENKO, Z., CARNECKA, M., RUMPF, C., CIPAK, L., BATOVA, M., MAROVA, I., NAM, M., KIM, D. U., PARK, H. O., HAYLES, J., HOE, K. L., NURSE, P. & GREGAN, J. 2010. S. pombe genome deletion project: an update. *Cell cycle,* 9**,** 2399-402.
SVEICZER, A., NOVAK, B. & MITCHISON, J. M. 1996. The size control of fission yeast revisited. *J Cell Sci,* 109 (Pt 12)**,** 2947-57.
SVEICZER, A., NOVAK, B. & MITCHISON, J. M. 2004. Size control in growing yeast and mammalian cells. *Theor Biol Med Model,* 1**,** 12.
TAHERI-ARAGHI, S., BRADDE, S., SAULS, J. T., HILL, N. S., LEVIN, P. A., PAULSSON, J., VERGASSOLA, M. & JUN, S. 2015. Cell-size control and homeostasis in bacteria. *Curr Biol,* 25**,** 385-91.
THURIAUX, P., NURSE, P. & CARTER, B. 1978. Mutants altered in the control co-ordinating cell division with cell growth in the fission yeast Schizosaccharomyces pombe. *Molecular & general genetics : MGG,* 161**,** 215-20.
TURNER, J. J., EWALD, J. C. & SKOTHEIM, J. M. 2012. Cell size control in yeast. *Current biology : CB,* 22**,** R350-9.
TURNER, W. 1890. The Cell Theory, Past and Present. *J Anat Physiol,* 24**,** 253-87.
TYERS, M., TOKIWA, G. & FUTCHER, B. 1993. Comparison of the Saccharomyces cerevisiae G1 cyclins: Cln3 may be an upstream activator of Cln1, Cln2 and other cyclins. *EMBO J,* 12**,** 1955-68.
TYERS, M., TOKIWA, G., NASH, R. & FUTCHER, B. 1992. The Cln3-Cdc28 kinase complex of S. cerevisiae is regulated by proteolysis and phosphorylation. *EMBO J,* 11**,** 1773-84.
UNGER, M. W. & HARTWELL, L. H. 1976. Control of cell division in Saccharomyces cerevisiae by methionyl-tRNA. *Proc Natl Acad Sci U S A,* 73**,** 1664-8.
VAN MEER, G., VOELKER, D. R. & FEIGENSON, G. W. 2008. Membrane lipids: where they are and how they behave. *Nat Rev Mol Cell Biol,* 9**,** 112-24.
WANG, H., CAREY, L. B., CAI, Y., WIJNEN, H. & FUTCHER, B. 2009. Recruitment of Cln3 cyclin to promoters controls cell cycle entry via histone deacetylase and other targets. *PLoS Biol,* 7**,** e1000189.
WILSON, E. B. 1925. *The Cell in Development and Heredity*, Garland Publishing, Inc.
WOOD, E. & NURSE, P. 2013. Pom1 and cell size homeostasis in fission yeast. *Cell Cycle,* 12, 3228-3236.
WOOD, E & NURSE, P. 2015. Sizing up to divide: Mitotic cell size control in fission yeast. *Annu Rev Cell Dev Biol,* 31, 11-29.
WOODS, A., SHERWIN, T., SASSE, R., MACRAE, T. H., BAINES, A. J. & GULL, K. 1989. Definition of individual components within the cytoskeleton of Trypanosoma brucei by a library of monoclonal antibodies. *J Cell Sci,* 93 (Pt 3)**,** 491-500.
WU, L. & RUSSELL, P. 1997. Nif1, a novel mitotic inhibitor in Schizosaccharomyces pombe. *The EMBO journal,* 16**,** 1342-50.